Role of Peroxiredoxin 6 in human melanoma

Dissertation zur Erlangung des naturwissenschaftlichen Doktorgrades
der Bayerischen Julius-Maximilians-Universität Würzburg

vorgelegt von

Alexandra Schmitt

aus Würzburg

Würzburg 2015

Eingereicht am:_____

Mitglieder der Promotionskommission:

Vorsitzender:_____

Gutachter:_____

Gutachter:_____

Tag des Promotionskolloquiums:_____

Doktorurkunde ausgehändigt am:_____

Eidesstattliche Erklärung

Gemäß §4, Abs. 3, Ziff. 3, 5 und 8
der Promotionsordnung der
Fakultät für Biologie der
Bayerischen Julius-Maximilians-Universität Würzburg

Hiermit erkläre ich ehrenwörtlich, dass ich die vorliegende Dissertation selbständig angefertigt und keine anderen als die angegebenen Quellen und Hilfsmittel verwendet habe.

Ich erkläre weiterhin, dass die vorliegende Dissertation weder in gleicher, noch in ähnlicher Form bereits in einem anderen Prüfungsverfahren vorgelegen hat.

Weiterhin erkläre ich, dass ich außer den mit dem Zulassungsantrag urkundlich vorgelegten Graden keine weiteren akademischen Grade erworben oder zu erwerben versucht habe.

Würzburg, Januar 2015

_____

Alexandra Schmitt

Table of contents

1. Abstract

Peroxiredoxin 6 (PRDX6) is a bifunctional enzyme comprising a peroxidase and a Ca^{2+}-independent phospholipase ($iPLA_2$) activity. This renders the enzyme capable of detoxifying reactive oxygen species (ROS) and of catalyzing the liberation of arachidonic acid (AA) from cellular membranes. Released AA can be further metabolized to bioactive lipids including eicosanoids, which are involved in inflammation, cell growth, differentiation, invasion and proliferation. Human melanoma cells are often characterized by imbalances in both ROS and lipid levels, which can be generated by oncogenic signaling, altered metabolism or UV irradiation.

In previous studies, a comparative proteome analysis of the *Xiphophorus* fish melanoma model revealed a strong upregulation of Prdx6 in benign and malignant lesions compared to healthy skin. As the *Xiphophorus* melanoma model displays in many respects molecular characteristics that are similar to human melanoma, I investigated the functional role of PRDX6 in human melanoma cells.

The first part of the study deals with the regulation of PRDX6 in melanocytes and human melanoma cells. I could demonstrate that the protein level of PRDX6 was strongly enhanced by the induction of the EGFR orthologue Xmrk from the *Xiphophorus* fish as well as the human EGFR. The upregulation of PRDX6 was further shown to be mediated in a PI3K-dependent and ROS-independent manner.

The main part of the thesis comprises the investigation of the functional role of PRDX6 in human melanoma cells as well as the analysis of the underlying mechanism. I could show that knockdown of *PRDX6* enhanced the oxidative stress response and led to decreased proliferation of melanoma cells. This cell growth effect was mainly mediated by the $iPLA_2$ activity of PRDX6. Under conditions of strongly enhanced oxidative stress, the peroxidase activity became also important for cellular proliferation. Furthermore, the anti-proliferative effect in cells with lowered PRDX6 levels was the result of reduced cellular AA content and the decrease in the activation of SRC family proteins. Similarly, supplementation with AA led to regeneration of SRC family kinase activity and to an improvement in the reduced proliferation after knockdown of *PRDX6*. Since AA can be further processed into the prostaglandin PGE_2, which has a pro-tumorigenic function in some cancer types, I further examined whether this eicosanoid is involved in the proliferative function of PRDX6. In contrast to AA, PGE_2 was not consistently required for melanoma proliferation.

In summary, I could demonstrate that PRDX6 plays a major role in AA-dependent lipid signaling in melanoma cells and thereby regulates proliferation. Interestingly, the proliferation relevant $iPLA_2$ activity can be pharmacologically targeted, and melanoma cell growth was

clearly blocked by the inhibitor BEL. Thus, I could identify the phospholipase activity of PRDX6 as a new therapeutically interesting target for melanoma treatment.

2. Zusammenfassung

Peroxiredoxin 6 (PRDX6) ist ein bifunktionales Enzym, welches neben seiner Peroxidase-Aktivität auch eine Ca^{2+}-unabhängige Phospholipase-Aktivität besitzt. Aufgrund dieser beiden Aktivitäten ist das Enzym in der Lage, sowohl oxidativen Stress zu bekämpfen als auch die Freisetzung von Arachidonsäure aus zellulären Membranen zu katalysieren. Freie Arachidonsäure (AA) dient der Generierung von bioaktiven Lipiden wie zum Beispiel Eicosanoiden, welche an Entzündungsreaktionen, Zellwachstum, Differenzierung, Invasion und Proliferation beteiligt sind. Humane Melanomzellen zeichnen sich oft durch ein gestörtes Gleichgewicht reaktiver Sauerstoffspezies und zellulärer Lipide aus. Dieses Ungleichgewicht kann durch onkogene Signalgebung, einen veränderten Metabolismus oder UV-Bestrahlung hervorgerufen werden.

Eine vorangegangene Proteomanalyse des *Xiphophorus*-Fisch-Melanommodells zeigte, dass im Vergleich zur gesunden Haut die Menge an PRDX6 in benignen und malignen Läsionen stark erhöht ist. Da das *Xiphophorus*-Melanommodell in vielerlei Hinsicht die molekulare Situation des humanen Melanoms wiederspiegelt, habe ich die funktionale Rolle von PRDX6 in humanen Melanomzellen untersucht.

Der erste Teil der Studie beschäftigt sich mit der Regulierung von PRDX6 in Melanozyten und humanen Melanomzellen. Ich konnte nachweisen, dass die Menge an PRDX6 Protein durch die Induktion des EGFR Orthologs Xmrk aus *Xiphophorus* Fischen, sowie des humanen EGFR stark erhöht wurde. Auch konnte ich zeigen, dass die Heraufregulierung von PRDX6 von der Signalgebung der PI3 Kinase, aber nicht von reaktiven Sauerstoffspezies abhängig war.

Der Hauptteil der vorliegenden Forschungsarbeit befasst sich mit der Ermittlung der funktionalen Rolle von PRDX6 in humanen Melanomzellen und der Analyse des zugrundeliegenden Mechanismus. Ich konnte nachweisen, dass ein Knockdown von *PRDX6* die oxidative Stress-Antwort verstärkte und die Proliferation von Melanomzellen reduzierte. Der Effekt auf das zelluläre Wachstum wurde hierbei hauptsächlich durch die $iPLA_2$-Aktivität von PRDX6 verursacht. Bei stark erhöhtem oxidativem Stress konnte auch eine Relevanz der Peroxidase-Aktivität für die zelluläre Proliferation nachgewiesen werden. Auch ging der anti-proliferative Effekt mit einer Abnahme zellulärer AA und der Reduktion aktiver Kinasen der SRC-Familie einher. Die Zugabe von AA zu Zellen mit *PRDX6*-Knockdown führte zur Regeneration der SRC-Kinase-Aktivität und konnte die Proliferation wieder verbessern. Da AA zum Prostaglandin PGE_2 prozessiert werden kann, welches in einigen Krebsarten pro-tumorigene Funktionen erfüllt, untersuchte ich, ob dieses Eicosanoid auch für die proliferative Funktion von PRDX6 relevant ist. Im Gegensatz zu AA wies PGE_2 jedoch keine kontinuierliche pro-proliferative Funktion auf.

Zusammenfassend konnte ich zeigen, dass PRDX6 eine entscheidende Rolle im AA-Stoffwechsel von Melanomzellen spielt und hierdurch die Proliferation reguliert. Interessanterweise ist die proliferationsrelevante $iPLA_2$-Aktivität pharmakologisch hemmbar, und auch das Wachstum der Melanomzellen wurde durch den Inhibitor BEL deutlich inhibiert. Mit der Phospholipase-Aktivität von PRDX6 konnte ich somit einen neuen therapeutisch nutzbaren Angriffspunkt für das Melanom identifizieren.

3. Introduction

3.1 Melanoma

Melanoma is a malignant tumor of melanocytes that usually occurs in the skin, but can also develop in any other part of the body containing melanocytes, such as the eye or mucous membranes (Das et al. 2010). Melanoma accounts for less than 2% of skin cancer but causes the majority of skin cancer related deaths. Since the last 30 years melanoma incidence is continuously rising. The current American Cancer Society report estimates that around 76,100 new cases of melanoma will be diagnosed in the United States and around 9,710 patients will have died of the disease in 2014. Patients containing early-stage melanoma can be treated successfully by surgery, but patients with IV stage melanoma show poor prognosis with a 5-year survival rate that is only about 15% to 20%. The risk of developing melanoma increases with age and is about 0.1% for black people, 0.5% for Hispanics and about 2% for white people. Melanoma also represents the most common cancer in young adults, especially in young women ("American Cancer Society. Melanoma Skin Cancer Overview."; http://www.cancer.org/index).

Melanocytes differentiate from neural crest progenitors and are mainly located in the basal layer of the epidermis and in the hair follicles (Gray-Schopfer et al. 2007). Their physiological function is the production and transport of the pigment melanin to surrounding keratinocytes. Two types of melanin, responsible for the color of hair and skin, are synthesized within special membrane-bounded organelles called melanosomes. The melanosomes are transferred to neighbouring keratinocytes, where they form a cap above the nucleus to protect the DNA from UV light-induced damage (Costin & Hearing 2007). The brown/black eumelanin displays an important photoprotective function, whereas the orange/yellow pigment pheomelanin contains only low photoprotective properties (Rouzaud et al. 2005; Tsatmali et al. 2002). By absorbing and dissipating ultraviolet radiation (UVR), melanin protects the skin from UVR which would otherwise cause DNA damage as well as ROS and lipid peroxidation (Hoogduijn et al. 2004). Increased melanin pigment synthesis via UVR is mediated by direct effects of UV light on melanocytes (Friedmann & Gilchrest 1987) or through the activation of melanocortin-1 receptor (MC1R) by α-melanocyte stimulating hormone (αMSH). MC1R signaling enhances the level of MITF, a transcription factor required for the production of melanin-synthetizing enzymes (Liu & Fisher 2010). Reduction of its activity leads to reduced melanin synthesis and pigmentation (Gaggioli et al. 2003). MITF is the master regulator of melanocytes and was also found to be amplified in malignant melanoma (Garraway et al. 2005). Besides enhancing the expression of melanin synthesis enzymes tyrosinase and tyrosinase related protein 1 and 2 (TRP-1/-2)

(Bertolotto et al. 1998) and the transfer of melanosomes (Chiaverini et al. 2008), MITF is involved in the regulation of genes mediating proliferation, survival, differentiation, DNA replication and repair, mitosis and invasion (Hocker et al. 2008; Javelaud et al. 2011; Strub et al. 2011; Cheli et al. 2011).

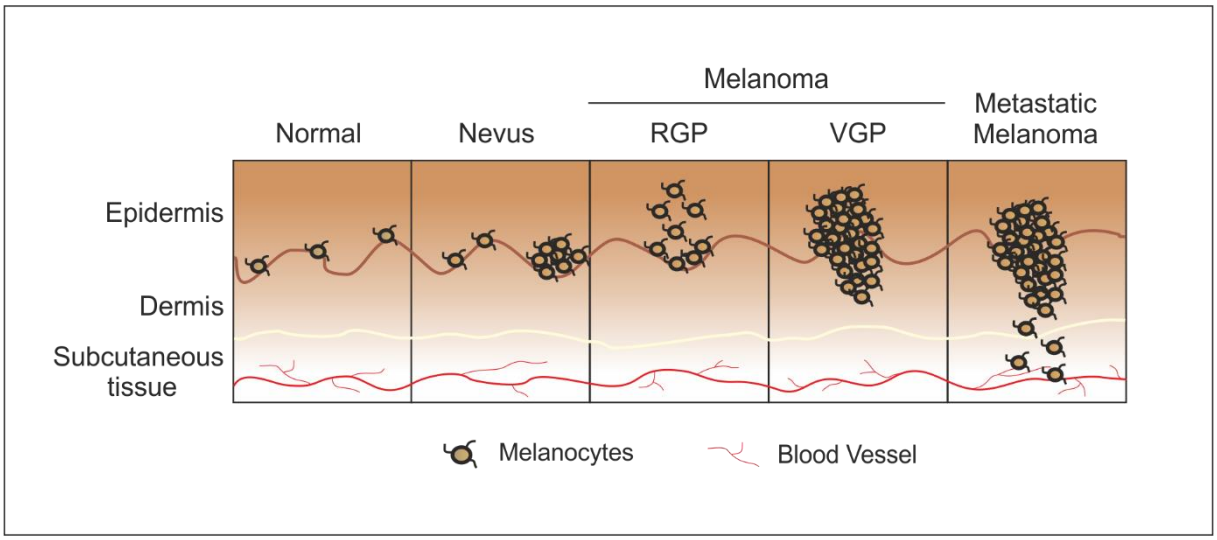

Figure 1: Stages of the transformation of normal melanocytes to melanoma. RGP: Radial Growth Phase; **VGP:** Vertical Growth Phase. (adopted from Gray-Schopfer et al. 2007; Lomas et al. 2008)

The transformation of normal melanocytes to malignant melanoma occurs in several distinct steps. The presumed development of melanoma from a pre-existing nevus is graphically represented in Fig. 1. Disruption of signaling pathways that are involved in cell growth control leads to hyper-proliferation and spreading of melanocytes. This incidence, which may result in the development of benign nevi, is mainly caused by mutations in the RAS/RAF signaling pathway leading to activation of ERK1/2 signaling. Nevi display many features of oncogene-induced senescence. They remain arrested in growth and rarely progress to melanoma (Michaloglou et al. 2005). It is, however, assumed that through additional loss of tumor suppressors, nevi can progress into the radial growth phase (RGP). During this first progressive stage, melanoma cells tend to proliferate intra-epidermally without metastasizing. The next step of melanoma progression is the vertical growth phase (VGP). Now the melanoma cells begin to penetrate the skin vertically and infiltrate the dermis and other tissues. This progress finally initiates the metastatic form of the disease. However, not all melanomas develop by passing through each of these different stages. Single melanocytes or nevi can also directly enter RGP or VGP, and each of the phases can directly progress into the metastatic stage (Miller & Mihm 2006).

3.1.1 Common melanoma signaling pathways

Two major pathways, the RAS/RAF/MEK/ERK (Mitogen-activated protein kinase; MAPK) and phosphatidylinositol 3-kinase (PI3K) pathways, play a central role in the development and progression of melanoma. Both signaling pathways are simultaneously activated by NRAS, which was the first identified human melanoma oncogene (Padua et al. 1984).
Together with HRAS and two splice variants of KRAS, NRAS belongs to the family of small GTP binding proteins (Giehl 2005). In response to cellular stimuli, including the activation of receptor tyrosine kinases by growth factors, the membrane-bound wildtypic RAS protein is transformed into an activated GTP-bound state. This activation leads to recruitment of serine/threonine kinase RAF to the cell membrane where it becomes activated. Among the different RAF isoforms, CRAF and BRAF are important in melanoma. Stimulated RAF mediates phosphorylation and activation of the MAP kinases MEK1 and MEK2 which in turn phosphorylate and activate the extracellular signal-regulated kinases ERK1/ERK2. Activated ERK proteins translocate to the nucleus and phosphorylate different transcription factors which are involved in the regulation of genes controlling cellular differentiation, migration, proliferation and survival (Katz et al. 2007). Oncogenic mutations in RAS family members affect the function of their intrinsic GTPase domain and lead to impaired GTP hydrolysis. Consequently, the proteins remain in a constitutively active state leading to enhancement of the downstream ERK1/2 signaling (Dahl & Guldberg 2007). In malignant melanoma, NRAS is the prevalently mutated *RAS* gene. 20-30% of malignant human melanoma samples exhibit NRAS mutations, mostly presented by amino acid substitutions at position 61. The most common substitutions are Q61K, Q61R and Q61L. Contrary to the incidence of NRAS mutations, KRAS and HRAS mutations are very rare in melanoma (Fernández-Medarde & Santos 2011).

Besides MAPK pathway activation, oncogenic RAS can also bind to and activate PI3K, leading to enhanced AKT activity (Sekulic et al. 2008) . The lipid kinase domain of activated PI3K phosphorylates phosphatidylinositol-4.5-biphosphate (PIP2) to generate phosphatidylinositol-3.4.5-triphosphate (PIP3). This second messenger stimulates 3-phosphoinositide-dependent protein kinase-1 (PDK1) which in turn phosphorylates the serine/threonine kinase AKT. Via membrane sequestering, phosphorylated AKT gets activated (Carnero, 2010; reviewed in Robertson, 2005). An additional phosphorylation event that can be mediated by mTORC2 (Guertin et al. 2006) or also AKT auto-phosphorylation at Ser473 (Toker 2000), is necessary for complete activation. Activated AKT phosphorylates a variety of downstream cellular proteins involved in proliferation, migration, cell cycle control and survival (Carnero 2010). Therefore increased activated AKT promotes the vertical growth phenotype in melanoma (Govindarajan et al. 2007) and is associated with shorter survival of melanoma patients (Dai et al. 2005).

Another downstream effector of RAS signaling is the Ral guanine exchange factor (RalGEF). Activated RalGEFs mediate the conversion of the small GTPases RalA and RalB to the active GTP-bound state, which promotes their function in different cellular processes (Feig 2003). Both Ral proteins are involved in the tumorigenic growth of human melanoma cell lines subcutaneously injected into the flanks of immunocompromised mice (Zipfel et al. 2010).
However, mutations in NRAS alone are not sufficient for tumorigenesis. In cutaneous melanoma, NRAS mutations were shown to co-occur with inactivation of the tumor suppressor $p16^{INK4A}$ (Jonsson et al. 2010) and 9% of NRAS mutant melanomas were also reported to contain PI3K pathway abnormalities such as mutations in PIK3R1 (PI3K regulatory subunit alpha) or PIK3R4 (PI3K regulatory subunit 4) (Shull et al. 2012).

Irrespective of NRAS mutations, the elevation of PI3K signaling is a common event in melanoma. In addition to the mentioned PIK3R mutations, loss of PTEN (phosphatase and tensin homolog) (Goel et al. 2006) or AKT3 amplification (Stahl et al. 2004) were found to promote hyper-activation of PI3K-AKT signaling (Chin et al. 2006). PTEN functions as tumor suppressor which negatively regulates the PI3K-AKT signaling cascade via dephosphorylation of PIP3 (Hennessy et al. 2005). Epigenetic silencing of PTEN, like promoter methylation, has been observed in up to 62% of patients with metastatic melanoma (Mirmohammadsadegh et al. 2006) and in some melanoma cases also an activating mutation of AKT3 (E17K) could be detected (Davies et al. 2008). Missense mutations in the PI3K catalytic subunit PIK3CA lead also to strong AKT activation but are only found in less than 3% of melanomas (Omholt et al. 2006; Curtin et al. 2006).

The most prevalent mutated gene in human melanoma is the RAF isoform *BRAF* which is most commonly mutated at codon 600, with an amino acid substitution of valine by glutamic acid (V600E). Around 60% of melanomas harbor this activating $BRAF^{V600E}$ mutation (Davies et al. 2002; Libra et al. 2005). $BRAF^{V600E}$ induces hyper-stimulation of the MAPK pathway and thereby promotes tumor development (Davies et al. 2002; Tuveson et al. 2003). Other activating BRAF mutations like V600K, V600D or V600R are also occasionally found in melanoma (Heinzerling et al. 2013). BRAF mutations play an important role in the initiation of melanocytic neoplasia and they are essential for melanoma growth and maintenance. Still, mutant BRAF alone is not sufficient to drive melanocyte transformation. Additional genetic alterations are required to induce melanoma (Pollock et al. 2003; Hoeflich et al. 2006; Dhomen et al. 2009). In murine melanocytes expressing $BRAF^{V600E}$, malignant transformation can e.g. be accelerated upon PTEN loss (Dankort et al. 2009). Inactivating PTEN and activating BRAF mutations are also observed to occur cooperatively in human melanoma cells, thus supporting a cooperation between RAS/RAF/MEK/ERK and PI3K-AKT signaling (Tsao et al. 2004).

MAPK and PI3K signaling are also triggered by receptor tyrosine kinases (RTKs) which are important upstream components of many different signaling cascades. Copy number alterations of MET and also the human epidermal growth factor receptor (EGFR) have been found but seem to be very late events in melanomagenesis (Chin et al. 2006). Expression of EGFR seems to play a relevant role in melanoma progression and metastasis (Boone et al. 2011) as well as BRAF inhibitor resistance (Sun et al. 2014). c-KIT represents another oncogenic RTK. 2% of all skin melanomas, 18% of mucosal melanomas and 21% of acral melanomas contain KIT mutations (Carvajal et al. 2011), the most common being KIT^{L576P} which displays constitutive activity (Willmore-Payne et al. 2005). Activation of KIT tyrosine kinase enhances cellular proliferation and survival via induction of MAPK and PI3K pathways (Flaherty et al. 2012). In conclusion, multiple oncogenes contribute to melanoma development via hyper-activation of MAPK and PI3K-AKT signaling.

Another pathway that is very often deregulated in melanoma is the $p16^{INK4A}$/CDK4/pRb pathway. The $p16^{INK4A}$ protein is encoded by the cyclin-dependent kinase inhibitor 2A *(CDKN2A)* locus and functions as tumor suppressor which normally plays a major role in the cell cycle control of melanocytes. Via binding to cyclin-dependent kinase 4 (CDK4) and/or cyclin-dependent kinase 6 (CDK6), $p16^{INK4A}$ suppresses the phosphorylation of retinoblastoma (Rb) protein and thereby causes cell cycle arrest by blocking the G1 to S phase transition (Sekulic et al. 2008; Hirai et al. 1995). The function of this tumor suppressor can be affected by germ line mutations in the *CDKN2A* gene. In 50% of melanoma cases, the $p16^{INK4A}$ gene is lost and in about 10% of melanoma the gene is inactivated by promoter methylation (Bennett 2008). Familial deficiency of $p16^{Ink4A}$ leads to accumulation of nevi and increased melanoma risk (Hussussian et al. 1994). In vertical growth phase melanomas it could be observed that loss of nuclear $p16^{INK4A}$ protein expression is associated with aggressive tumor cell proliferation and poor prognosis (Straume et al. 2000). Furthermore, $p16^{INK4A}$ was also shown to be involved in regulating intracellular oxidative stress (Jenkins et al. 2011).

Other interesting proteins that contain oncogenic mutations affecting their GTPase domain are the guanine nucleotide binding protein Q polypeptide (GNAQ) and the paralogue of GNAQ (GNA11). In contrast to RAS, GNAQ and GNA11 represent the α subunits of trimeric G proteins. Both proteins transfer G protein coupled receptor signals to phospholipase C-beta (PLC-beta) isoforms and thereby activate protein kinase C (PKC) signaling (reviewed in Hubbard & Hepler, 2006). The mutated versions have been discovered in uveal melanomas and blue nevi but do not play a role in cutaneous melanoma. Approximately 50% of uveal melanoma and up to 83% of blue nevi contain GNAQ mutations whereas mutations in GNA11 are detected in 32% of uveal melanomas and 6.5% of blue nevi. Oncogenic GNAQ contains

the mutation within a RAS-like domain at position Q209L. Similar to the mutant version of GNA11, $GNAQ^{Q209L}$ is constitutively active and enhances MAPK signaling (Van Raamsdonk et al. 2009; Van Raamsdonk et al. 2010).

3.1.2 Oxidative stress in melanoma

ROS are involved in the initiation and metastatic progression of melanoma. They cause DNA mutations and potentially stimulate survival, proliferation, invasion and angiogenesis (reviewed in Joosse et al., 2010). The role of ROS in the development of UV-induced melanoma has been demonstrated, as prevention of UV-induced ROS via N-acetylcysteine treatment could retard the onset of melanocytic tumors in mice (Cotter et al. 2007).

The generation of ROS in melanoma can be strongly induced through AKT mediated activation of the NADPH oxidases (Hoyal et al. 2003; Edderkaoui et al. 2011). ROS produced via this pathway was shown to activate NF-κB signaling which enhances melanoma cell proliferation (Brar et al. 2001) and promotes survival, resistance to apoptosis and metastasis (Madonna et al. 2012). It could be observed that the ROS-mediated activation of NF-κB leads to angiogenesis in the Xmrk melanoma animal model and is accompanied by a strong secretion of angiogenin (Schaafhausen et al. 2013), a pro-angiogenic factor contributing to the metastatic potential of human melanoma (Hartmann et al. 1999). AKT signaling also leads to the inhibition of pro-apoptotic factors. This facilitates the survival of cells harbouring extensive mitochondrial damage, which also provokes the formation of ROS. Both ROS generating effects of AKT were demonstrated to be involved in malignant transformation (Govindarajan et al. 2007). Melanoma tumor cells also exhibit higher levels of neuronal nitric oxide synthase (nNOS) and thereby an increased level of nitric oxide (NO), which correlates with the melanoma disease stage (Z. Yang et al. 2013). NO was shown to function as anti-apoptotic factor supporting melanoma cell growth (Salvucci et al. 2001; Grimm et al. 2008). However, to profit from the tumor-promoting effects of upregulated ROS levels, melanoma cells have to maintain their oxidative stress at a controlled and tolerable level. Consequently melanoma cells are characterized by anti-oxidative measures like the expression of superoxide dismutase (MnSOD), peroxiredoxins or cystathionase (CTH) (Meierjohann 2014). Disruption of the balanced oxidative stress load can prevent melanoma onset and progression. For example, inhibition of CTH was shown to decrease melanoma proliferation, soft agar growth, resistance to H_2O_2, and induces melanoma senescence (Leikam et al. 2014).

3.2 The Xmrk and HERmrk melanoma models

One of the oldest animal models for cancer research is represented by the *Xiphophorus* fish melanoma model, which was already described in the 1920s (C.Kosswig 1928; Gordon 1927). Crossing of two different *Xiphophorus* species, platyfish (*X. maculatus*) and swordtails (*X. hellerii*), leads to hybrids expressing high levels of the melanoma inducing oncogene *Xmrk* (*Xiphophorus* melanoma receptor kinase), which is the fish ortholog of the human *EGFR*. In these hybrids, melanoma develop with an incidence of almost 100% (Meierjohann & Schartl 2006).

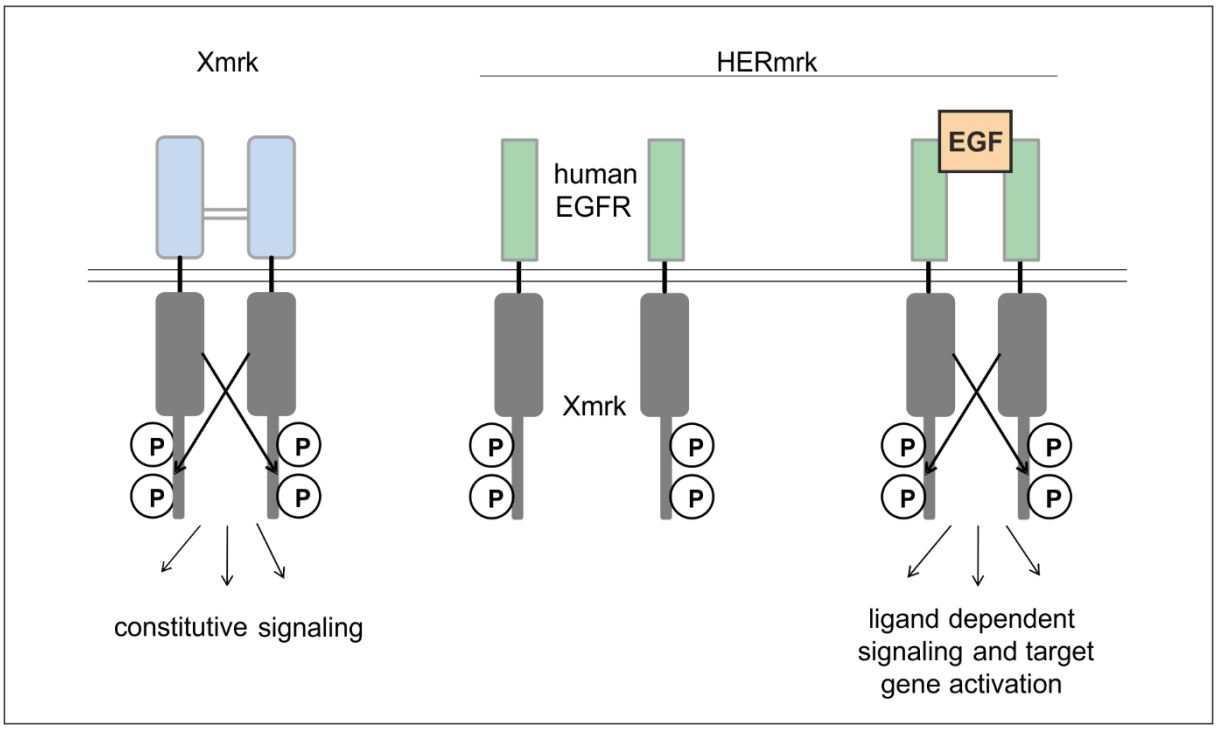

Figure 2: HERmrk receptor. The chimeric HERmrk receptor (middle) consists of the extracellular domain of the human EGFR and the intracellular part of Xmrk (left). Stimulation with EGF leads to ligand dependent signaling and target gene activation (right).

To analyze the Xmrk signaling network and its implications for melanoma development and progression, a murine melanocyte cell line expressing the HERmrk receptor was generated. HERmrk is a chimeric receptor tyrosine kinase, consisting of the intracellular domain of Xmrk and the extracellular domain of the human EGFR. Thus, stimulation of HERmrk cells with human epidermal growth factor (EGF) specifically triggers Xmrk signaling (Fig. 2) and allows the analysis of the Xmrk signal transduction pathways. Clonal cell lines expressing high (HERmrk^{hi}), intermediate (HERmrk^{me}) and low (HERmrk^{low}) levels of HERmrk were generated in previous works to analyze the effect of different RTK signaling strengths (Leikam et al. 2008).

In the present study, HERmrk^{me} and HERmrk^{hi} cells were used to investigate the regulation of PRDX6, as this enzyme was found to be upregulated in benign and malignant Xmrk-bearing tumors of the *Xiphophorus* melanoma model. PRDX6 belonged to the second largest functional group of regulated proteins identified by a comparative proteome analysis of this fish melanoma model and was found to be highly induced compared to normal skin (Lokaj et al. 2009).

3.3 Peroxiredoxin 6

Peroxiredoxin 6 (PRDX6) is a bifunctional enzyme containing a glutathione (GSH) peroxidase activity as well as a Ca^{2+}-independent phospholipase ($iPLA_2$) activity (Chen et al. 2000; Manevich & Fisher 2005). The protein belongs to the mammalian family of six nonseleno peroxidases (peroxiredoxin 1-6) and was first isolated from the ciliary body of the bovine eye (Shichi & Demar 1990). In contrast to PRDX1-5 this enzyme has only a single conserved catalytic cysteine residue (C47) and is therefore called 1-Cys PRDX. The other members containing two cysteine residues are classified as 2-Cys (PRDX1-4) or atypical 2-Cys (PRDX5) peroxiredoxins (Kang et al. 1998; Rhee et al. 2001). PRDX6 exhibits a wide-spread tissue distribution with high expression levels in lung, liver, testis, kidney and also the brain (Kim et al. 1998; Fujii et al. 2001; Rhee et al. 2001; Mo et al. 2003). Strong expression of the enzyme can also be detected in wounded and psoriatic skin (Kümin et al. 2006) as well as in the epidermis and blood vessels of normal human skin (Rolfs et al. 2013). Wang and colleagues demonstrated that *Prdx6*$^{-/-}$ mice develop normally, but under oxidative stress they have more severe tissue damage and show a higher mortality rate than wildtype mice (Wang et al. 2003).

3.3.1 Peroxidase activity of PRDX6

Like the other PRDXs, PRDX6 catalyzes the reduction of H_2O_2 and organic peroxides. In contrast to the other family members, PRDX6 can also bind to oxidized lipid substrates which enables the enzyme to reduce phospholipid hydroperoxides (Fisher et al. 1999; Manevich et al. 2009).This enzymatic activity of PRDX6 plays an important role in antioxidant defense, as lipid peroxidation can induce damage to cell plasma and organellar membranes. Therefore, reduction of phospholipid hydroperoxides is essential for cell survival. Knockdown of *Prdx6* in rat lung epithelial cells, for example, led to lipid peroxidation, membrane damage and apoptosis (Pak et al. 2002). Furthermore, by analysis of lung homogenates of *Prdx6* null mice exposed to hyperoxic stress, PRDX6 was indicated to have a major role in reducing phospholipid

hydroperoxides in the lung (Wang et al. 2003). Overexpression of the enzyme in different cell types was shown to protect from ROS-induced cytotoxicity (Manevich et al. 2002; Wang et al. 2004). In line with these observations, PRDX6 serves the protection of UVA- and UVB-induced ROS in the epidermis of mice (Kümin et al. 2006). The peroxidase activity of PRDX6 depends on the catalytically active cysteine residue C47 (Chen et al. 2000). Data derived from the PRDX6 crystal structure showed that C47 is hydrogen bonded to H39 and can be electrostatically activated by R132. As a result, C47, H39 and R132 form a catalytic triad for peroxidase activity (reviewed in Fisher 2011; Hofmann et al. 2002).

The use of glutathione instead of thioredoxin as the physiological reductant also demonstrates a special characteristic of PRDX6 that distinguishes its catalytic cycle from that of 2-Cys family members (Kang et al. 1998). Oxidation of the catalytic cysteine C47 to sulfenic acid (-SOH) is the initial step in the antioxidative function of PRDX6 (Peshenko & Shichi 2001) and is also required for the interaction of the enzyme with the π isoform of the glutathione S transferase (GST) (Zhou et al. 2013). Through this interaction, the sulfenic acid of PRDX6 forms a heterodimeric disulfide which is reduced back to the sulfhydryl by GSH. This catalytic process leads to regeneration of the PRDX6-peroxidase activity (Ralat et al. 2006; Ralat et al. 2008; Zhou et al. 2013). Another reducing agent that was reported to be used by PRDX6 for supporting peroxidase activity is ascorbate (Monteiro et al. 2007). The sulfenic cysteine (Cys-SOH) can also be hyperoxidized to a sulfinic (Cys-SO_2H) or sulfonic state (Cys-SO_3H) (Peshenko & Shichi 2001). In contrast to 2-Cys PRDXs, hyperoxidation of PRDX6 was shown to be irreversible and to increase its $iPLA_2$ activity (Kim et al. 2008).

3.3.2 $iPLA_2$ activity of PRDX6

Another important feature distinguishing PRDX6 from the other family members is its additional Ca^{2+}-independent phospholipase ($iPLA_2$) activity, which was identified by isolation of the protein from rat lung (Kim et al. 1997). Based on crystal structure (Choi et al. 1998) and mutagenesis studies, it was shown that S32 is essential for this activity along with H26 and D140, which again constitute a catalytic triad (Manevich et al. 2007; Manevich et al. 2009; Chen et al. 2000). The $iPLA_2$ activity of PRDX6 hydrolyses phospholipids at the sn-2 position of phospholipids with preference for phosphatidylcholines. Via cleavage of phosphatidylcholines, PRDX6 leads to the release of arachidonic acid (AA) (Kim et al. 1997; Manevich & Fisher 2005), an omega-6 (n-6) polyunsaturated fatty acid, which plays a crucial role in phospholipid metabolism and cell signaling (reviewed in Hooks & Cummings, 2008).

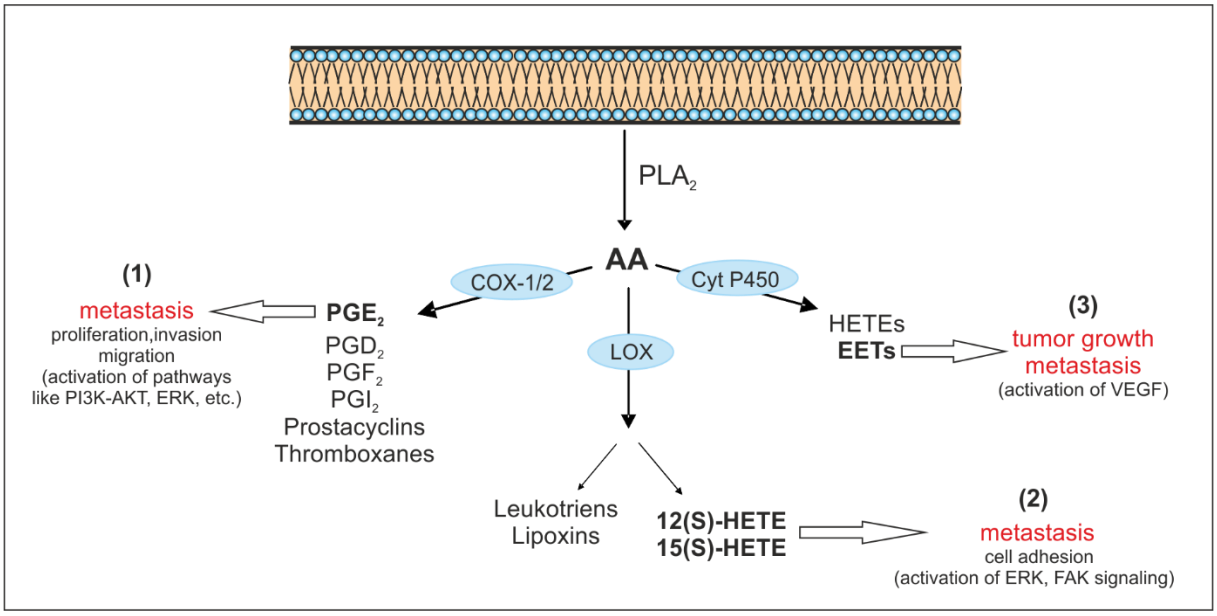

Figure 3: Overview of AA metabolism and its influence on melanoma. Phospholipase A_2 activity leads to the release of AA (arachidonic acid) from membrane lipids. Released AA is further processed by COX-1/2, LOX and Cyt P450 into different metabolites which can exert influence on melanoma. **1:** (Rundhaug et al. 2011; Singh & Katiyar 2011; Singh et al. 2011). **2:** (Kang et al. 2013). **3:** (Panigrahy et al. 2012)

Through the cyclooxygenase (COX), lipoxygenase (LOX) and cytochrome P450 epoxygenase pathways, released AA is converted into different bioactive eicosanoids, which can act as inflammatory mediators or participate in cellular signal transduction (reviewed in Harizi et al. 2008). The COX pathway facilitates the production of prostaglandins, thromboxanes (TXs) and prostacyclins (Smith et al. 1996) whereas LOXs mediates the formation of leukotriens, lipoxins and hydroxyeicosatetraenoic acids (HETEs) (Brash 1999). Via the cytochrome P450 epoxygenase pathway, AA is metabolized into HETEs and epoxyeicosatrienoic acids (EEts) (Zeldin 2001). All three enzymatic pathways have been shown to play a relevant role in different cancer types (Jiang et al. 2005; reviewed in Wang & Dubois 2010). A short overview of the AA metabolism and its major effects on melanoma is presented in Fig. 3.

In contrast to the peroxidase activity, which reaches its optimum at cytosolic pH, the pH optimum for the $iPLA_2$ activity of PRDX6 is in the acidic range (~ pH 4). The dependency of this low pH for $iPLA_2$ activity is consistent with the localization of PRDX6 to lamellar bodies and lysosomes in lung alveolar epithelium (Akiba et al. 1998; Kim et al. 1997; Wu et al. 2006). The compartmentalization of PRDX6-$iPLA_2$ in acidic organelles relies on a 10 amino acid sequence near the NH_2-terminus of the enzyme (Sorokina et al. 2009). The entry of PRDX6 into the secretory pathway and targeting to lysosomal compartments of lung epithelial cells is proposed to be afforded by the interaction of this sequence with MAP kinase activated 14-3-3ε chaperone protein (Sorokina et al. 2011). Furthermore, it could be shown that hyperoxidation of PRDX6 via H_2O_2 simultaneously increases its $iPLA_2$ activity (Kim et al. 2008).

Interestingly, phosphorylation of PRDX6 at T177 residue by MAPK in vitro enhances the $iPLA_2$ activity at pH 7.4 to a level which equals to the basal activity at pH 4 (Wu et al. 2009).
The $iPLA_2$ activity of PRDX6 plays an important role in the metabolism of lung surfactant phospholipids. Inhibition of $iPLA_2$ via inhibitor treatment or PRDX6 depletion leads to a significant reduction in the degradation as well as synthesis of mouse lung surfactant dipalmitoylphosphatidylcholin (DPPC), whereas overexpression of PRDX6 causes the opposite effect (Fisher et al. 2005; Fisher et al. 2006).

3.3.3 PRDX6 in cancer

Until now, most studies describing the function of PRDX6 in cancer were conducted in lung and breast cancer where PRDX6 promotes tumor growth and invasiveness. In lung cancer cells it was revealed that the PRDX6 mediated production of AA induces the activation of signaling pathways involving PI3K-AKT, p38 kinase and urokinase-type plasminogen activator (uPA). This effect finally enhances the invasive potential of the cancer cells whereas the peroxidase activity of PRDX6 was shown to facilitate the proliferation of lung cancer cells (Ho et al. 2010). Furthermore, it was observed that the growth of lung tumors in vivo can be promoted by both PRDX6 enzyme activities through upregulation of AP-1 and JNK (Jo et al. 2013).
In breast cancer cells, PRDX6 is suggested to promote cancer progression partially via upregulation of uPAR, ETS-1, RhoC and MMP9. Knockdown of *PRDX6* in breast cancer cells injected orthotopically into the exposed axillary mammary fat pad reduced tumor growth and the amount of pulmonary metastases in athymic mice. In comparison to parental mammary breast cells, PRDX6 is strongly upregulated in highly invasive and potentially metastatic breast cancer cells (Chang et al. 2007). Such upregulation of PRDX6 with increasing malignancy was also investigated by a quantitative proteome analysis of healthy, benign and malignant skin of the *Xiphophorus* melanoma model (Lokaj et al. 2009).
Another tumor-supportive feature of PRDX6 is its ability to mediate resistance to cancer therapeutic agents. It was shown that overexpression of PRDX6 prevents cisplatin-induced apoptotic cell death of human ovarian cancer cells (Pak et al. 2011) and, via binding to and modulation of DED caspases, PRDX6 impedes TRAIL induced cell death of HeLa cells (Choi et al. 2011).

In conclusion, PRDX6 seems to play an important role in the maintenance and progression of existing tumors of several solid cancer types.

3.4 Aim of the thesis

Melanoma models display a useful and important tool for achieving a better understanding of cellular processes which distinguish melanoma from its healthy counterpart. The use of different melanoma models allows the detection of important factors promoting melanoma formation and progression and which can serve as suitable targets for melanoma therapy.

Given that PRDX6 was shown to be one of the proteins that exhibited strikingly different expression profiles in benign, malignant and healthy skin of the *Xiphophorus* melanoma model, I was interested in the functional role of this enzyme in human melanoma.
The first aim of my thesis was to achieve insights into the expression and regulation of PRDX6 by using the HERmrk melanoma model as well as human melanocytes and melanoma cells.
The subsequent investigation of the functional role of PRDX6 in human melanoma cells displayed the second and most important part of the study. Here, the two enzymatic functions of PRDX6 were of particular interest. The assignment of the phenotypic effects of the enzyme to the peroxidase and $iPLA_2$ activity was therefore central to this work.

4. Material and methods

4.1 Material

4.1.1 Cell lines

Cell line	Supplier	Type
melan a HERmrk^{hi}	Meierjohann (Würzburg)	mouse melanocytes expressing medium levels of the HERmrk receptor
melan a HERmrk^{me}	Meierjohann (Würzburg)	mouse melanocytes expressing high levels of the HERmrk receptor
hEGFR transgenic melan a	Meierjohann (Würzburg)	mouse melanocytes expressing human EGFR
normal human epithelial melanocytes (NHEM)	ATCC	primary human melanocytes
Hermes3a	Cell Bank Holding	immortalized human melanocytes
A375	ATCC	human melanoma cell line
SK MEL28	ATCC	human melanoma cell line
MEL HO	A. Bosserhoff (Regensburg)	human melanoma cell line
SK MEL2	NCI/NIH	human melanoma cell line
UACC-62	NCI/NIH	human melanoma cell line
UACC-257	NCI/NIH	human melanoma cell line
M14	NCI/NIH	human melanoma cell line
MDA MB 435	NCI/NIH	human melanoma cell line
293T	M. Gessler (Würzburg)	human embryonic kidney cells (transformed with large T antigen)

4.1.2 Plasmids

Backbone	Insert	Source
pLKO-Tet-On	-	Addgene
pLKO-Tet-On	PRDX6 (human)-shRNA-1	this work
pLKO-Tet-On	PRDX6 (human)-shRNA-2	this work
pLKO-Tet-On	PRDX6 (human)-shRNA-3	this work
pBABE-hygro	PRDX6 (mouse)-S32A	this work

Backbone	Insert	Source
p201iEP	-	Prof. Manfred Gessler (Würzburg)
p201iEP	FLAG-PRDX6 (mouse)-WT	this work
p201iEP	FLAG-PRDX6 (mouse)-S32A	this work
p201iEP	FLAG-PRDX6 (mouse)-C47S	this work
PGL3-rNQO1 ARE+fn	ARE of *NQO1 gene*	Dr. Matthias Schäfer (Zürich)
pRL-CMV	-	Promega
pEGFP	-	Addgene
pPAX2	-	Prof. Manfred Gessler (Würzburg)
pCMV-VSVG	-	Prof. Manfred Gessler (Würzburg)

4.1.3 Oligonucleotides for cloning and real-time-PCR

Oligos for cloning		
Oligo	**Sequence (5`→3`)**	**Purpose**
induc.shPRDX6-1H3	CCGGCCCATCATCGATGATAGGAATCTCGAGATTCCTATCATCGATGATGGGTTTTT	inducible PRDX6 shRNA-1
induc.shPRDX6-1H5	AATTAAAAACCCATCATCGATGATAGGAATCTCGAGATTCCTATCATCGATGATGGG	
induc.shPRDX6-2H3	CCGGCGCATCCGTTTCCACGACTTTCTCGAGAAAGTCGTGGAAACGGATGCGTTTTT	inducible PRDX6 shRNA-2
induc.shPRDX6-2H5	AATTAAAAACGCATCCGTTTCCACGACTTTCTCGAGAAAGTCGTGGAAACGGATGCG	
induc.shPRDX6-3H3	CCGGTGGTCCTGATAAGAAGCTGAACTCGAGTTCAGCTTCTTATCAGGACCATTTTT	inducible PRDX6 shRNA-3
induc.shPRDX6-3H5	AATTAAAAATGGTCCTGATAAGAAGCTGAACTCGAGTTCAGCTTCTTATCAGGACCA	

Oligos for cloning		
Oligo	**Sequence (5`→3`)**	**Purpose**
mPRDX6Cys47-SerF	CTTTACCCCAGTGTCCACCA CAGAAC	murine PRDX6-C47S
mPRDX6Cys47-SerR	GTTCTGTGGTGGACACTGG GGTAAAG	
mPRDX6Ser32-AlaF	TCCTGGGAGATGCATGGGG CATTC	murine PRDX6-S32A
mPRDX6Ser32-AlaR	GAATGCCCCATGCATCTCC CAGGA	
mousePRDX6_EcoRI_up	GCGCGAATTCATGCCCGGA GGGTTGCTTC	wt murine PRDX6; murine PRDX6-S32A; murine PRDX6-C47S;
mousePRDX6_SalI_down	GCGCGTCGACTTAAGGCTG GGGTGTATAAC	
mPRDX6_FLAG_EcoRI_up	GCGCGAATTCATGGATTACA AGGATGACGACGATAAGCC CGGAGGGTTGCTTCTCG	FLAG-tagged wt murine PRDX6; FLAG-tagged murine PRDX6-C47S; FLAG-tagged murine PRDX6-S32A
mPRDX6_BstBI_down	GCGCTTCGAATTAAGGCTG GGGTGTATAAC	

PRDX6-specific sequences are underlined and point mutations are marked in red.

Oligos for real-time-PCR		
Oligo	**Sequence**	**ENSEMBL-IDs**
mPRDX6_up	TCATGGGGCATTCTCTTTTC	ENSMUSG00000026701
mPRDX6_down	GTCCCTGCCCTTATCATCAA	
Actin_up	GCTACAGCTTCACCACCACA	ENSMUSG00000029580
Actin_down	AAGGAAGGCTGGAAAAGAGC	
PRDX6_Hs_5	CGTGTGGTGTTTGTTTTTGG	ENSG00000117592
PRDX6_Hs_3	CCATCACACTATCCCCATCC	
Hu_RPS14_up	CTCAGGTGGCTGAAGGAGAG	ENSG00000164587
Hu_RPS14_down	GCAGCCAACATAGCAGCATA	
PLCD1F (forward)	GGTGTTGTGAGCATAAAACACTGG	ENSG00000187091
PLCD1R (reverse)	CGCCTGTAGATCCTCATCATCC	
MAPK12F (forward)	CTCCTTTGACGACGTTGACC	ENSG00000188130
MAPK12R (reverse)	TGAAGCTGAGCACCTCTTTGT	

Oligos for real-time-PCR		
Oligo	**Sequence**	**ENSEMBL-IDs**
PDPK1F (forward)	AACCAGAGAGCGGGATGTCA	ENSG00000140992
PDPK1R (reverse)	AGCAGACACAATCTCAGCCG	
TOB2F (forward)	ACGAAAAGGACTTCGGTCCC	ENSG00000183864
TOB2R (reverse)	AGAGAATCAGCACAGGGCAC	

Oligos for real-time-PCR were designed using NCBI Primer Blast (http://www.ncbi.nlm.nih.gov/tools/primer-blast/)

4.1.4 siRNAs

siRNA	Manufacturer	Catalog number	Sequence
ON-TARGET plus SMART Pool Human PRDX6	Thermo scientific	L-010173-00-0005	- CGAAAGGAGUCUUCACCAA - CCAAGAGGAAUGUUAAGUU - GAAAUACCUCCGCUACACA - GGACGUGGCUCCCAACUUU
ON-TARGET plus siRNA Human PRDX6	Thermo scientific	J-019173-08-0010	GGACGUGGCUCCCAACUUU
ON-TARGET plus Non-Targeting Pool	Thermo scientific	D-001810-10-20	n.a.

4.1.5 Antibodies

Primary Antibodies		
Antibody	**Manufacturer**	**Catalog number**
Actin β	Santa Cruz	Sc-47778
Prdx6	Abcam	ab92322
Prdx6-SO_3	Acris Antibodies	LF-PA0005
Lamp1	Abcam	Ab25630
P-Akt (Ser473)	Cell Signaling	4051
P-Mapk p42/44 (Thr202/Tyr204)	Cell Signaling	9101
P-Src (Tyr416)	Cell Signaling	2101
P-Rb (Ser780)	Cell Signaling	9307

Primary Antibodies		
Antibody	**Manufacturer**	**Catalog number**
EGFR	Cell Signaling	4267P
P-c-Raf (Ser338)	Cell Signaling	9427
P-PKC (βII Ser660)	Cell Signaling	9371
cleaved PARP	Cell Signaling	5625
Secondary Antibodies		
Antibody	**Manufacturer**	**Catalog number**
Goat anti-mouse IgG+IgM (H+L) (POD)	Thermo Scientific	31444
Goat anti-rabbit IgG (H+L) (POD)	Bio-Rad	170-6515
Alexa Fluor 594 goat anti-rabbit IgG (H+L)	Invitrogen	A11037
Alexa Fluor 488 goat anti-mouse IgG (H+L)	Invitrogen	A11001

4.1.6 Inhibitors, drugs and compounds

Compound	Manufacturer	Catalog number
LY294002	LC Labs	L7962
GÖ-6983	Calbiochem	365251
U0126	LC Labs	U-6770
ERK Inhibitor	Calbiochem	328006
AG1478	Calbiochem	658548
Erlotinib	Selleckchem	S1023
bromoenol lactone	Cayman Chem.	70700
Src Kinase Inhibitor I	Calbiochem	567805
COX-2 Inhibitor V, FK3311	Calbiochem	236015
PLX 4032	Axon Medchem	1624
DMEM	PAN	P04-03550
fetal calf serum (FCS)	PAN	1506-P131304
dialysed fetal calf serum	PAN	1506-P131304
penicillin streptomycin (PenStrep)	PAA	L11003
cholera toxin (CT)	Calbiochem	227035
Ham`s F10 Nutrient Mix	Gibco	41550-021
ITS™ Premix	Corning	354351

Compound	Manufacturer	Catalog number
3-Isobutyl-1-methylxanthine (IBMX)	Sigma	I5879
puromycin	Calbiochem	540222
12-*0*-tetradecanoyl phorbol acetate (TPA)	Calbiochem	524400
10x trypsin-EDTA	Sigma-Aldrich	P0781
DMSO	ROTH	47201
Cryo-SFM	PromoCell	C-29910
polybrene	Sigma-Aldrich	107689
sodium butyrate	Sigma-Aldrich	B5887
doxycycline	Calbiochem	324385
human epidermal growth factor (EGF)	PeproTech	AF-100-15
endothelin 1	Calbiochem	05-23-3800
human stem cell factor (hSCF)	Prospec	CYT-255
tiron	Fluka-Sigma	89460
vitamin E	Sigma-Aldrich	258024
NAC (n-acetylcysteine)	Sigma-Aldrich	A9165
apocynin	Calbiochem	178385
prostaglandin E2 (PGE_2)	Tocris bioscience	2296
arachidonic acid	Sigma-Aldrich	A3555
Hoechst 34580	Invitrogen	H21486
Mowiol® 4-88	Roth	0713.1
Immobilized protein A	Thermo scientific	20334
ampicillin	Roth	HP62.2
deoxynucleotid triphosphates (dNTPs)	Sigma-Aldrich	DNTPCA10-1KT
SYBR Green	life technologies	S7563

4.1.7 Enzymes

Enzyme	Manufacturer	Catalog number
glucose oxidase (GOx)	Sigma-Aldrich	G0543
T4 DNA Ligase	Fermentas	EL0014
AgeI	New England Biolabs	R0552S
EcoR	Fermentas	ER0271

Enzyme	Manufacturer	Catalog number
SalI	Fermentas	ER0641
BstBI	Fermentas	ER0121
His-Taq polymerase	Prof. Manfred Gessler (Würzburg)	-
Velocity DNA Polymerase	Bioline	BIO-21098

4.1.8 Transfection reagents

Transfection reagent	Manufacturer	Catalog number
Fugene HD	Roche	04709691001
Polyethylenimine (PEI)	Eurogentec Belgium	no more available
X-tremeGene siRNA Transfection Reagent	Roche	04476093001

4.1.9 Kits

Kit	Manufacturer	Catalog number
Pure Yield™ Plasmid Midiprep System	Promega	A2495
Pure Yield™ Plasmid Miniprep System	Promega	A1223
Wizard SV Gel & PCR Clean-Up System	Promega	A9282
GenElute PCR Clean-Up Kit	Sigma-Aldrich	NA1020-1KT
peqGOLD TriFast	PEQLAB	30210
RevertAid First Strand cDNA Kit	Fermentas	K1622
Bradford Reagent	Sigma-Aldrich	B6916
SuperSignal West Pico Chemiluminescent Su.	Fermentas	K1622
Dual-Luciferase Reporter Assay system	Promega	E1910
Cell proliferation ELISA BrdU	Roche	11647229001
PGE_2 high sensitivity ELISA Kit	Enzo Life Sciences	ADI-903-001

4.1.10 Technical equipment

Hera Cell 150i Incubator (Thermo Scientific)

Mini-PROTEAN Tetra Electrophoresis System (Biorad)

Trans Blot Cell (Biorad)

Photo Image Station 4000MM (Kodak)

Cary 50 Spectrophotometer (Varian)

Luminometer (Lumat LB 9501; Berthold)

Confocal microscope (Nikon)

Mastercycler ep Realplex (eppendorf)

NanoDrop ND-1000 Spectrophotometer (NanoDrop Technologies)

Microplate Reader (Tecan)

4.1.11 Buffer and media

4.1.11.1 Standard buffer

Buffer	Ingredients
ReproFast PCR buffer	100 mM $(NH_4)_2SO_4$; 200 mM Tris pH 8.8; 100 mM KCl; 20 mM $MgSO_4$; 1% Triton; 1% BSA
10x Annealing buffer	1 M NaCl, 100 mM Tris-HCL pH 7.4
PBS	137 mM NaCl; 2.7 mM KCl; 4.3 mM Na_2HPO_4; 1.47 mM KH_2PO_4. Adjusted to pH 7.4
TBST	10 mM Tris pH 7.9; 150 mM NaCl; 0,1% Tween
Lysis buffer	20 mM HEPES pH 7.8; 500 mM NaCl, 5 mM $MgCl_2$, 5 mM KCl; 0.1% deoxycholate, 0.5% Nonidet-P40; 10 µg/ml aprotinin; 10 µg/ml leupeptin; 200 µM Na_3VO_4; 1 mM phenylmethanesulphonyl- fluoride and 100 mM NaF
SDS Running buffer	250 mM Tris; 192 mM glycine; 0.5% SDS
Laemmli buffer	312.5 mM Tris pH 6.8; 10% SDS; 50% glycerine; 0,005% brome-phenol-blue; 25% β-mercapto-ethanol
Transfer buffer	25 mM Tris; 192 mM glycine; 20% methanole
HNTG buffer	20 mM HEPES pH 7.5; 150 mM NaCl; 10% glycerol; 0.1% Triton X-100

4.1.11.2 Cell culture media

Cell line	Culture medium
melanoma cells, 293T	DMEM containing 10% FCS and 1x PenStrep (“D10”)
murine melanocytes	DMEM,10% FCS, 200 nM TPA, 200 pM CT and 1x PenStrep
NHEM	HAM´s F10 Nutrient Mix with 20% FCS, 100 nM TPA, 200 nM CT, 1x PenStrep, 100 µM IBMX and ITS™ Premix (1:1000)
Cell line	**Culture medium**
Hermes3a	RPMI 1640 containing 10% FCS, 200 nM TPA, 200 pM CT, 100 ng/ml human stem cell factor, 10 nM endothelin 1
melanoma cells (during transfection)	Optimem (Gibco; 11058)
Cell line	**Starving medium**
murine melanocytes	DMEM containing 2,5% dialysed FCS and 1x PenStrep
Cell line	**Freezing medium**
melanoma cells, 293T, murine melanocytes,	DMEM containing 20% FCS and 10% DMSO
NHEM	Cryo-SFM (PromoCell; C-29910)

4.1.11.3 Cell culture buffer

1xPBS (pH 7.4)	
Ingredients	**Weight (g)**
NaCl	40.6
KCl	1
Na_2HPO_4 x H_2O	8.9
KH_2PO4 x H_2O	1.2
ddH_2O	ad 5 l

EDTA solution (pH 7.4)	
Ingredients	**Weight (g)**
EDTA	1
ddH_2O	ad 5 l

4.1.11.4 Bacterial culture media

Luria-Bertani-medium (LB) (pH 7.5)	
Ingredients	**Weight (g)**
trypton	10
yeast extract	5
sodium chloride	10
ddH_2O	ad 1 l
LB-Agar-medium (pH 7.5)	
Ingredients	**Weight (g)**
trypton	10
yeast extract	5
sodium chloride	10
agar	115
ddH_2O	ad 1 l

4.2 Methods

4.2.1 Cell culture methods

4.2.1.1 Maintenance of cell lines

All cell lines were cultured in tissue cell culture dishes (BD Falcon™) at 37 °C under 5% CO_2 in a Hera Cell 150i incubator. Before reaching confluence, the cells were passaged by washing once with EDTA solution followed by a 5 min incubation with 1x trypsin/EDTA. Afterwards, trypsin/EDTA was carefully removed. Medium was added to neutralize the trypsin and to suspend the detached cells, which were subsequently split for passaging. All cell lines were regularly tested for the presence of mycoplasma infection by PCR.

4.2.1.2 Cryopreservation of cell lines

For long term storage, cells were pelleted by centrifugation at 1000 rpm for 5 min at room temperature. The supernatant was discarded and the cells were resuspended in freezing medium. Cell suspensions were stored at -80 °C overnight in 1.5 ml cryo vials, which were placed in a freezing container. Afterwards, the vials were transferred to liquid nitrogen.

4.2.1.3 Thawing of cell lines

For thawing, cells were taken out of the liquid nitrogen, quickly thawed at 37 °C in a water bath and transferred to a 15 ml Falcon (BD Bioscience) containing 9 ml pre-warmed medium. Afterwards, cells were centrifuged once at 1000 rpm for 5 min, the supernatant was removed and cells were taken up in fresh medium.

4.2.1.4 Lentiviral infection and establishment of stable transgenic cell lines

shRNA targeting PRDX6 was expressed from the doxycycline-inducible lentiviral vector pLKOTeton. The FLAG tagged PRDX6 wt and mutation clones (S32A; C47S) were expressed from the lentiviral vector p201iEP.

For viral transduction, lentiviral expression vector (6 µg) and the helper plasmids pPAX2 (4.5 µg) and pCMV-VSVG (3 µg) were cotransfected into 293T cells using 1x PEI (100 mg/ml PEI diluted 1:100 in 150 mM NaCl) transfection reagent. The 293T cells were always transfected at 60 to 70% confluence in 10 cm dishes. The plasmids were mixed with DMEM to a final volume of 250 µl and 27 µl 1x PEI was added to 223 µl DMEM. The mixtures were incubated for 2 min at room temperature. Subsequently, the PEI mix was added to the DNA mix, followed by vortexing. The 500 µl transfection mix was then incubated at room temperature for 20 min. In the meantime, cell culture medium (D10) of the 293T cells was replaced by 5 ml fresh medium. Subsequently, the transfection mix was added dropwise to the 293T cells. 6 h later, medium change was performed and target cells were grown in 10 ml D10. For enhancement of viral transcription rate, cells were treated 24 h later with 200 µl sodium butyrate (500 mM) for 6 h. Medium was changed and after 48 h, in which virus accumulated in the supernatant, conditioned medium was harvested and filtered through 0.45 µm filters. For viral infection, target cells were incubated with the virus containing supernatant supplemented with 8 µg/ml polybrene, which was used to enhance the infection rate. After 6 h, the viral supernatant was replaced by fresh D10. Two days after viral infection, 1-2 µg/ml puromycin was added to select for stable transgenic cells. The selection was performed for around 6 days

4.2.1.5 siRNA Transfection

Cells were seeded into 6-well dishes and one day later, siRNA transfection was performed by using X-tremeGene siRNA transfection reagent. For one 6-well, 80 pmol siRNA was cautiously mixed, by pipetting, with Optimem medium up to a final volume of 100 µl. Without getting in contact with the wall of the tube, 5 µl X-tremeGene reagent was mixed with 95 µl Optimem, also by careful pipetting. Within 5 min, the X-tremeGene mixture was transferred to the siRNA mixture. This transfection mixture was incubated for 20 min at room temperature. During this time, the cell culture medium (D10) of the target cells containing a confluence of around 50% was replaced by 600 µl DMEM (without FCS and Pen/Strep). Afterwards, the 200 µl transfection mix was added dropwise to the cells into the 600 µl DMEM. 6 h later, 1 ml D10 was additionally given to the transfected cells. After 24 h, medium was changed and cells were used for subsequent experiments.

For the transfection of a 12-well, 40 pmol siRNA in a final volume of 50 µl Optimem was cautiously mixed with 50 µl x-tremeGene mixture containing 2.5 µl of the transfection reagent. The D10 medium was replaced by 300 µl DMEM (without FCS and Pen/Strep) and the 100 µl transfection mixture was given drop by drop to the cells after 20 min incubation time.

4.2.1.6 Proliferation and cell growth assays

Different methods were performed to analyze the proliferation rate or viability of cell lines.

4.2.1.6.1 Cell growth assay performed by manual cell counting

Cells were counted using a Neubauer hemacytometer. Cells were seeded at similar density in triplicates and allowed to grow for three to seven days. For manual counting, they were harvested by trypsinisation and were resuspended in an adequate amount of PBS (50-3000 µl) to sustain a countable cell dilution.

4.2.1.6.2 Analysis of BrdU incorporation

Analysis of BrdU incorporation was carried out using the Cell Proliferation ELISA BrdU Kit (Roche). During cell proliferation, the pyrimidine analog 5-bromo-2`-deoxyuridine (BrdU) is incorporated into the newly synthesized DNA instead of thymidine. The detection of incorporated BrdU is mediated by an anti-BrdU antibody conjungated with peroxidase (POD). These immune complexes are detected by a substrate reaction and then quantified by measuring the absorbance at the appropriate wavelength. The quantity of BrdU incorporation serves as indication of cells in S phase and represents an indirect measurement of cell proliferation.

Cells were cultured for 6 to 8 h in medium containing 10 µM BrdU and the incorporation was analyzed by using a microplate reader (Tecan). Measurement was done at 450 nm and all experiments were performed in triplicates.

4.2.1.6.3 xCELLigence assay

The xCELLigence system (Roche) was used to investigate proliferation rates indirectly by monitoring cell viability. For this system, cells were seeded into 96-well plates containing gold microelectrodes to monitor cell density by detecting electrical impedance over the well surface. The impedance gives information about the cellular coverage of each 96-well (high cell coverage is indicated by high impedance). This method allows the live analysis of cell growth at a high time resolution and over a long time period.

The cellular impedance was normalized to empty wells containing only 100 µl D10. Data were measured and illustrated with the xCELLigence RTCA software 1.2 from Roche and cell growth curves were performed by using Excel. All experiments were performed in triplicates or duplicates.

4.2.1.7 Luciferase assay

Cells were cotransfected with 0.5 µg firefly luciferase reporter plasmid (PGL3-rNQO1 ARE+fn), 0.2 µg renilla luciferase reporter vector (pRL-CMV) and 0.3 µg pEGFP vector by using Fugene HD transfection reagent. For one 12-well, the DNA was carefully mixed with 3 µl Fugene HD and filled up with Optimem to a final volume of 100 µl. Fugene HD was added without getting in contact with the wall of the tube. The transfection mixture was incubated for 20 min at room temperature and given dropwise to the cells into 1 ml culture medium per 12-well. Cotransfection of the pEGFP plasmid was performed as transfection control. 16 h later, culture medium was changed and around 48 h after transfection, luciferase activity was measured using the Dual-Luciferase Reporter Assay system (Promega) according to the manufacturer`s protocol for a single injector luminometer. Upon substrate conversion, the luciferase activity leads to emission of visible light. The intensity of this emitted light was measured to quantify the expression level of the luciferase reporter gene, which served as indicator for antioxidant response element (ARE) activity of the *NADPH dehydrogenase quinone 1* (*NQO1*) gene. Luciferase activity was measured by the use of a Luminometer (Lumat LB 9501; Berthold).

4.2.1.8 Immunofluorescence

Cells were cultured on glass cover slips in 6-well plates. After cells had reached a confluence of around 60 to 70%, glass cover slips were washed twice with PBS and were then fixed for 10 min in 2% paraformaldehyde. Cells were washed three times with PBS and were subsequently permeabilized for 5 min in PBS/1% Triton. Afterwards, samples were washed again three times with PBS and subsequently blocked for 30 min with PBS containing 1% BSA. Cells were then incubated with primary antibody (α-Lamp1 antibody) diluted 1:500 in PBS/1% BSA solution over night at 4 °C. After three washing steps with PBS, the coverslips were incubated at room temperature (RT) with the second antibody Alexa Fluor 488 goat anti-mouse IgG (1:1000 in PBS) for 1 h. Three washing steps with PBS, each for 5 min, followed and the samples were incubated with the next primary antibody (α-PRDX6 antibody or α-PRDX6-SO_3 antibody) over night at 4 °C. Both antibodies were diluted 1:200 in PBS/1% BSA.

Samples were then washed again three times with PBS and incubated for 1 h at RT with the second antibody Alexa Fluor 594 goat anti-rabbit IgG diluted 1:1000 in PBS. After at least three washing steps with PBS, nuclear staining was performed via incubation with 1 µg/ml Hoechst 34580 (diluted in PBS) for 5 min. Afterwards, samples were washed five times with PBS and the cover slips were embedded with Mowiol® 4-88 on object slides. Samples were then kept in the dark at 4 °C until confocal microscopy was performed by using the confocal microscope from Nikon. Fluorescence figures were processed via ImageJ.

4.2.1.9 Gas chromatography analysis

Stable transgenic MEL-HO and UACC-62 cells containing a doxycycline inducible shRNA against PRDX6 were cultured in 15 cm dishes and were treated with 100 ng/ml doxycycline. To keep the cells at a subconfluent level, they were split the third day after seeding and administration of doxycycline was repeated. At day five, medium was replaced and cells were again treated with doxycycline. 24 h later, cells were harvested by the use of a silicon rubber and pelleted by centrifugation at 13000 rpm for 2 min. Supernatant was discarded and the weight of the cell pellets was determined. Further experimental procedure and gas chromatography were performed by Dr. Werner Schmitz from the Department of Biochemistry and Molecular Biology at the University of Würzburg. For the sake of completeness, the method is described in the following.

For the quantification of arachidonic acid and other unsaturated and saturated eicosanoic acids 50 mg cell pellet was mixed with 10 µl standard (2.5 mM nonadecanoic acid methylester in methanol/chloroform (1/1, v/v)) and extracted with 3.55 ml chloroform/methanol/H_2O (10/60/1, v/v/v). Afterwards sample extract was mixed with 1 ml H_2O and 4 ml chloroform. After centrifugation, the lower phase was evaporated at 60 °C under a stream of nitrogen gas. The residue was dissolved in 2 ml methanol containing 1 M acetylchloride and incubated at 74 °C for 3 h. The developed methylesters were extracted twice with 2 ml hexane and the combined extracts were evaporated at 60 °C under nitrogen stream. The residue was dissolved in 100 µl hexane and spread on a silica gel TLC plate (Merck KGaA) which was evaluated in hexane/diethylether (7/3, v/v). Afterwards, the region containing fatty acid methylesters was scraped off and fatty acid methylesters were extracted from the silicia gel by 1 ml diethylether. The extract was evaporated at 40 °C under nitrogen stream and the residue was dissolved in 20 µl dichlorethane. 1 µl of the solution was applied on a GLC column (30 m Phenomenex Zebron ZB-1701 capillary GC-column with 0.32 mm ID) and fatty acid methylesters were separated by the following temperature program: 150 °C to 280 °C with 4° C/min and 280 °C to 281 °C with 0.1 °C/min; column head pressure: 100 kPa.

4.2.1.10 PGE_2-ELISA

To measure cellular PGE_2 content, subconfluent MEL-HO and UACC-62 cells were transfected with indicated siRNAs and were seeded into 6-well plates the next day. After 24 h, cell culture medium was replaced by 800 µl fresh D10. Secretion of PGE_2 into the culture medium was allowed for another 48 h, before the medium was harvested. At this time, cells exhibited a confluence of around 70 to 80%. The medium supernatant was centrifuged at 2000 rpm for 5 min and the thus gained supernatant was subsequently used in duplets for the PGE_2 high sensitivity ELISA Kit (Enzo Life Science). This competitive immunoassay allows the quantitative examination of PGE_2 in biological fluids like culture medium. The amount of PGE_2 was analyzed by using the Tecan microplate reader. Measurement was performed at 405 nm.

4.2.2 Protein methods

4.2.2.1 Cell lysate preparation

Cells were harvested by trypsinisation or with help of a silicon rubber and were pelleted by centrifugation at 13000 rpm for 2 min. The supernatant was discarded and, depending on the pellet size, the cells were lysed in 20-100 µl lysis buffer for 3 h. Centrifugation at 13000 rpm for 15 min separated cell debris from the cell lysate, whose protein concentration was measured via Bradford assay photometrically at 595 nm in a Cary 50 Spectrophotometer (Varian).

4.2.2.2 SDS-PAGE and western blot

Protein lysates containing the same amount of protein (20-50 µg) were denatured in Laemmli buffer at 95 °C for 5 min and were then separated on 8-12% polyacrylamide gels. Then the protein samples were transferred to nitrocellulose membranes (Hartenstein) in a wet blotting chamber (Biorad) at 4 °C. Both, SDS-polyacrylamide gel electrophoresis (SDS-PAGE) and immunoblotting was performed according to standard protocols (J. Sambrook, E.F. Fritsch 2001). Unspecific antibody binding was blocked with 5% BSA in TBST for 1 h. Incubation with primary antibodies, diluted in blocking solution according to the manufacturer`s recommended dilutions, was performed over night at 4 °C. After two washing steps with TBST for 10 min, the membranes were incubated with secondary antibodies diluted in 5% BSA in TBST for 1 h. Another three washing steps followed and the membranes were subsequently incubated with the SuperSignal West Pico Chemiluminescent Substrate (Thermo Scientific) for 1 min. The

substrate is highly sensitive for the detection of horseradish peroxidase (HRP) on immunoblots. As the used secondary antibodies are conjungated to HRP, the incubation of this substrate with the western blot membrane led to a chemical reaction whose emitted light was detected by the camera of a Photo Image Station 4000MM (Kodak).

4.2.2.3 Co-immunoprecipitation

40 µl protein A sepharose (immobilized protein A; Thermo Scientific) was centrifuged at 2000 rpm for 5 min at 4 °C. Supernatant was discarded and the sepharose beads were washed three times with ice cold HNTG buffer. All washing and centrifugation steps were performed at 4 °C and 2000 rpm, respectively. Under conditions of slow agitation and 4 °C, the protein A sepharose beads were incubated overnight with primary antibody (α-PCNA antibody or α-IgG antibody) diluted in 500 µl HNTG buffer according to the manufacturer`s recommended dilutions. Afterwards, beads were washed three times with HNTG buffer. 500 µg protein lysate was diluted 1:1 with HNTG buffer (containing 10 µg/ml aprotinin; 10 µg/ml leupeptin; 200 µM Na_3VO_4; 1 mM phenylmethanesulphonyl-fluoride) to a final volume of 500 µl and transferred to the washed protein A sepharose beads. The samples were incubated over night at 4 °C and were slowly agitated. After washing for five times with pure HNTG buffer, samples were denatured in 20 µl Laemmli buffer at 95 °C. Afterwards, samples were centrifuged 2 min at 2000 rpm and supernatant was analyzed by SDS PAGE and western blot.

4.2.3 DNA methods

4.2.3.1 Restriction enzyme digestion and ligation

DNA fragments and plasmids were digested by restriction enzymes for 1 h at 37 °C. Endonuclease enzymes and corresponding buffers were obtained from New England Biolabs or Fermentas.

Digestion protocol:

1 µg plasmid or 50 µl PCR product

1 µl enzyme

4 µl (for plasmid) or 6 µl (for PCR product) 10x enzyme buffer

filled up to 40 µl (for plasmid) or 60 µl (for PCR product) with H_2O

Via ligation, which was performed over night at 16 °C, DNA fragments were cloned into plasmids. T4 DNA-ligase and the corresponding buffer were obtained from Fermentas.

Protocol of ligase reaction mix for the ligation of insert DNA into vector DNA:

vector and insert were used at a ratio of 1:3

1 µl T4 DNA ligase

2 µl 10x ligase buffer

filled up to 20 µl with H_2O

4.2.3.2 Plasmid construction and site-directed mutagenesis

Cloning and construction of vectors followed standard protocols. Specifically, peroxiredoxin 6 shRNA sequences were derived from sequences published in the siRNA center (Thermo scientific: http://www.dharmacon.com/designcenter/designcenterpage.aspx) and cloned into the lentiviral pLKOTeton vector according to the manufacture`s protocol (https://www.addgene.org/static/data/32/66/1658e8f8-af64-11e0-90fe-003048dd6500.pdf).

For the establishment of FLAG-tagged murine wildtype (wt) Peroxiredoxin 6 and mutation clones (S32A and C47S), murine *Prdx6* cDNA was amplified by PCR after reverse transcription of RNA from mouse melanocytes using the RevertAid First Strand cDNA Kit (Fermentas). The oligonucleotides mousePRDX6_EcoRI up (GCGCGAATTCATGCCCGGAGGGTTGCTTC) and mousePRDX6_SalI_down (GCGCGTCGACTTAAGGCTGGGGTGTATAAC) were used for amplification and the PCR product was subcloned into the pBABE-hygro vector. For this purpose, the PCR product was gel purified by using Wizard SV Gel & PCR Clean-Up System (Promega) and was digested with EcoRI/SalI restriction enzymes. Afterwards, the PCR product was again purified using GenElute PCR Clean-Up Kit (Promega) and was ligated as EcoRI/SalI fragment into pBABE-hygro. The vector was then used as template for site directed mutagenesis performed by sewing PCR. For this purpose, two overlapping PCR products of each *Prdx6* mutation clone were first amplified by PCR using flanking oligonucleotides which harbor the required point mutation. For the establishment of PCR fragments containing complete *Prdx6* with introduced mutation, the respective amplified products were both used in the sewing PCR, and the outermost 5`and 3`primers were used for amplification. The complete experiment is described in the following:

Amplification of overlapping PCR products:

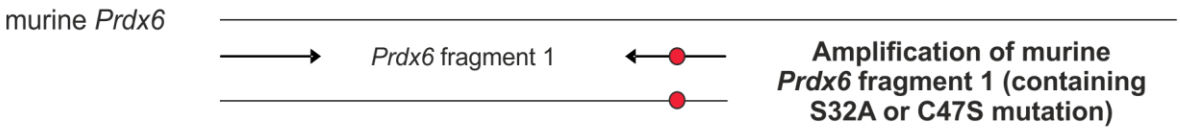

Used oligos for S32A: mousePRDX6_EcoRI_up and mPRDX6Ser32-AlaR
Used oligos for C47S: mousePRDX6_EcoRI_up and mPRDX6Cys47-SerR

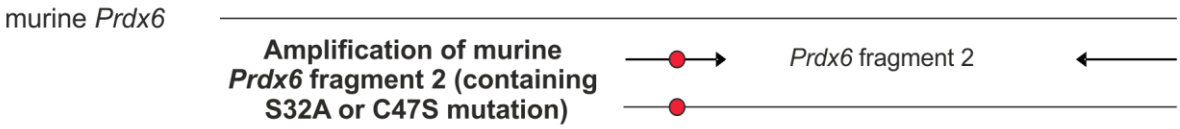

Used oligos for S32A: mPRDX6Ser32-AlaF and mousePRDX6_SalI_down
Used oligos for C47S: mousePRDX6Cys47-SerF and mousePRDX6_SalI_down

Sewing PCR:

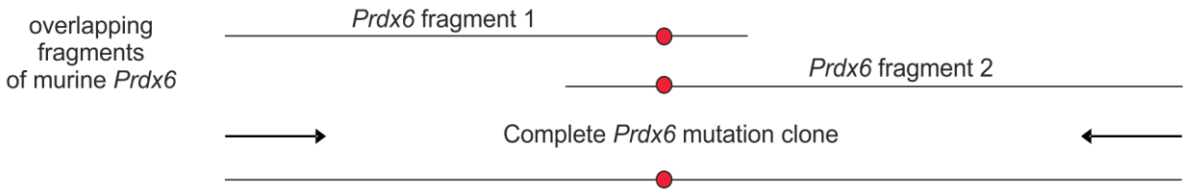

Both *Prdx6* overlapping fragments containing the same mutation were used in the sewing PCR for generation of the complete *Prdx6*-S32A or C47S version.

Used oligos: mousePRDX6_ECORI_up and mousePRDX6_SalI_down

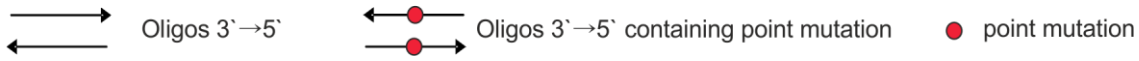

Sewing PCR reaction mix:

10 ng of each PRDX6 DNA fragment

5 µl 10X PCR-Buffer

0.7 µl dNTPs (10 mM)

0.75 µl 3`primer (10 pmol/µl)

0.75 µl 5`primer (10 pmol/µl)

1 µl polymerase (Velocity DNA Polymerase; Bioline)

filled up to 50 µl with H_2O

Sewing PCR program:

Step		Temp.	Time
1 preheating		95 °C	pause
2		95 °C	5`
3	4 repeats	95 °C	30``
4		60 °C	30``
5		72 °C	40``
6	35 repeats	95 °C	30``
7		57 °C	30``
8		72 °C	45``
9		72 °C	5`
10 storing		12 °C	pause

The PCR products were, similar to murine wildtypic *Prdx6*, ligated as EcoRI/SalI fragments into the pBABE-hygro vector, which was then used as template for *FLAG*-tag insertion. The murine *Prdx6* wt, C47S and S32A variants were amplified by PCR using the following oligos: mPRDX6_FLAG_EcoRI_up (GCGCGAATTCATGGATTACAAGGATGACGACGATAAGCCCGGAGGGTTGCTTCTCG) containing the *FLAG*-tag and mPRDX6_BstBI_down (GCGCTTCGAATTAAGGCTGGGGTGTATAAC).

The amplified, *FLAG*-tagged PCR products were gel-purified and digested with BstBI/SalI. After purification with the GenElute PCR Clean-Up Kit the PCR variants were ligated as BstBI/SalI fragments into the P201iEP plasmid. Digestion and ligation were performed as mentioned above.

4.2.3.3 Transformation, colony screen and plasmid preparation

The ligation reaction was mixed with 100 µl thawed competent DH5α bacteria and was incubated on ice for 30 min. To induce the DNA uptake, the bacterial suspension was then incubated at 42 °C for 90 seconds. Transformed bacteria were cooled on ice for 5 min, supplemented with 900 µl LB-medium and incubated on a shaker at 37 °C for 1 h. Afterwards the bacteria were centrifuged at 3000 rpm for 5 min. About 850 µl supernatant was discarded and the pellets were resuspended in the residual LB-supernatant before plated onto a LB-Amp-agar-dish which was then incubated upside-down at 37 °C overnight. Bacterial colonies were screened for successful insertion of the DNA fragment of interest by performing colony PCR. Positive clones were grown in LB-medium at 37 °C overnight and plasmid DNA was extracted

and isolated using the PureYield™ Plasmid Mini/Midiprep System from Promega according to the manufacturer`s protocol. Afterwards, plasmid DNA was sequenced by GATC Biotech (http://www.gatc-biotech.com/de/index.html) before used for transfection or further cloning procedure.

4.2.4 RNA and cDNA methods

4.2.4.1 RNA extraction and cDNA synthesis

Cells pellets were taken up in 1 ml pegGOLD TriFast Reagent and RNA was isolated according to the supplier`s instructions. For removal of residual contaminating genomic DNA, a 30 min DNaseI, RNase free (Fermentas) digestion was performed. RNA integrity was analyzed by using NanoDrop ND-1000 Spectrophotometer (NanoDrop Technologies). Reverse transcription was carried out using 1-4 µg total RNA exerting RevertAid First Strand cDNA Synthesis Kit (Fermentas) and random hexamer primers according to the manufacturer`s protocol.

4.2.4.2 Real-time-PCR

Real-time-PCR (RT-PCR) was performed on cDNA. cDNA amplification was monitored with Mastercycler ep realplex (Eppendorf) using SYBR Green reagent. mRNA abundance was analyzed using 2-ΔΔCT method (Livak & Schmittgen 2001) and normalized to expression levels of the housekeeping genes *Actin* (for murine cDNA) or *RPS14* (for human cDNA).

RT-PCR was performed as follows:

PCR reaction mix:

5 µl cDNA

2.5 µl 10X Buffer (Reprofast)

0.7 µl dNTPs (10 mM)

0.75 µl SYBR Green (1:2000)

0.75 µl 3`primer (10 pmol/µl)

0.75 µl 5`primer (10 pmol/µl)

0.3 µl His-Taq polymerase

14.25 µl H_2O

Standard PCR program:

Step		Temp.	Time
1 preheating		95 °C	pause
2		95 °C	5`
3	40 repeats	95 °C	15``
4		60 °C	15``
5		72 °C	15``
6		95 °C	5`
7		60 °C	15``
8		60 °C-95 °C gradient	15``
9		95 °C	15``

4.2.4.3 Microarray

RNA was isolated using the miRNeasy Kit (Quiagen) according to the manufacturers protocol, and microarray analysis was performed by Dr. Claus Jürgen Scholz (Microarray Core Unit; IZKF, University of Wuerzburg) using the Affymetrix® Human Gene 2.1 ST Array. All data were processed by Dr. Susanne Kneitz (Physiological Chemistry, University of Wuerzburg) using Bioconductor-preprocess Core software.

5. Results

5.1 Regulation of PRDX6

The first part of this study comprises the investigation of expression and regulation of PRDX6 in melanocytes and human melanoma cells. Involved signaling pathways as well as the role of oxidative stress were analyzed in more detail.

5.1.1 PRDX6 is a direct target of Xmrk and the human EGFR

Since PRDX6 is upregulated in *Xiphophorus* benign and malignant pigment cell tumors (Lokaj et al. 2009), transgenic melanocytes expressing an inducible version of the *Xiphophorus* melanoma oncogene Xmrk (melan a HERmrk^{hi} cells) were used to get an insight into the regulation of PRDX6. EGF mediated activation of HERmrk signaling did not affect the level of *PRDX6* mRNA transcripts (Fig. 4A), but strongly induced PRDX6 protein expression (Fig. 4B). A similar observation was made for murine melanocytes transgenic for the human EGF receptor (hEGFR), where an upregulation of PRDX6 protein levels was detected 24 h after EGF treatment (Fig. 4C). These results indicate that PRDX6 is a direct, post-transcriptional target of the EGFR orthologue Xmrk and the human EGFR.

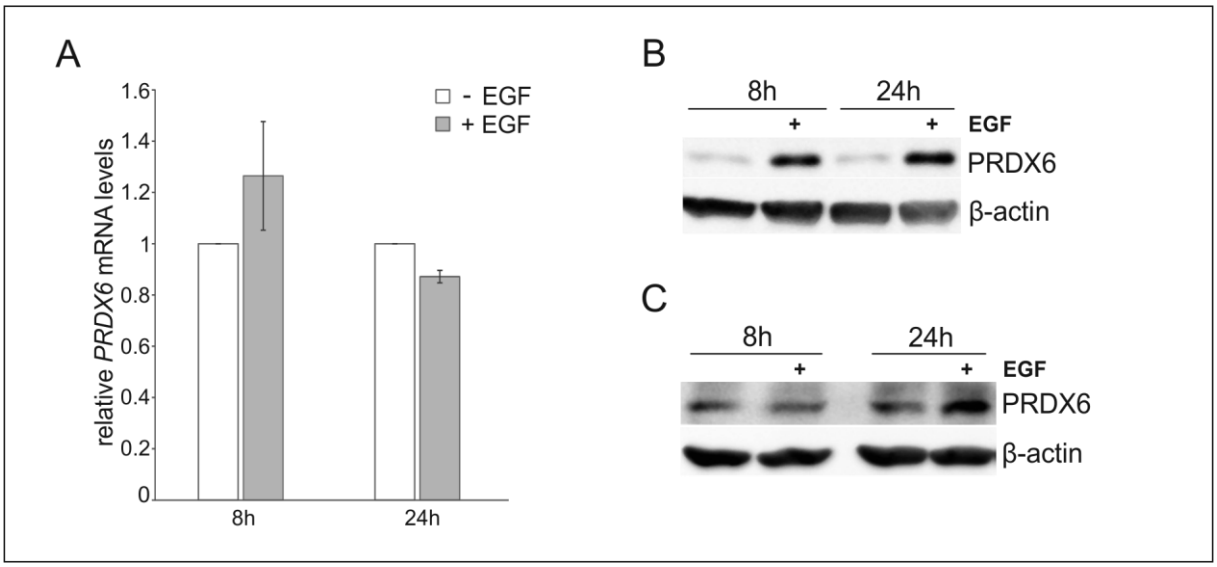

Figure 4: Regulation of PRDX6 in HERmrk^{hi} and hEGFR transgenic murine melanocytes. After starving in 2.5% HM for 72 h, cells were stimulated with human EGF (100 ng/ml). Expression of PRDX6 was analyzed by RT-PCR and western blot at the indicated time points. **A:** Relative *PRDX6* mRNA expression levels in melan a HERmrk^{hi} cells. Expression levels were normalized to *Actin*. Error bars indicate standard deviation (SD) of two independent experiments. **B, C:** Western blots showing PRDX6 levels of unstimulated and hEGF stimulated melan a HERmrk^{hi} cells (**B**) and hEGFR transgenic melanocytes (**C**). β-actin served as loading control.

Furthermore, PRDX6 expression was investigated in a panel of different human melanoma cell lines (Fig. 5A). On RNA level, *PRDX6* expression in melanoma cells was similar or higher in comparison to NHEM (primary neonatal human epidermal melanocytes). On protein level, A375, UACC-62 and MDA-MB-435 melanoma cells exhibited a very strong PRDX6 expression, whereas all other cell lines displayed PRDX6 levels which were comparable or even lower (SK-MEL-28) than that of NHEM.

Two cell lines with high PRDX6 expression (A375, UACC62) and two cell lines with low expression (MEL-HO, SK-MEL-28) were chosen to further confirm the regulation of PRDX6 by the human EGFR. The selected cell lines showed, similar to the PRDX6 level, a high (A375, UACC62) or low (MEL-HO, SK-MEL-28) EGFR level (Fig. 5B). Inhibition of EGFR signaling via treatment with the inhibitor erlotinib led to a clear decrease in the protein expression of PRDX6 in all cell lines except A375 (Fig. 5C). Furthermore, the decrease of PRDX6 correlated with the strength of inhibitor efficiency demonstrated by the downregulation of phosphorylated CRAF (P-CRAF).

In conclusion, these data demonstrate an EGFR-dependent regulation of PRDX6 in human melanoma cells.

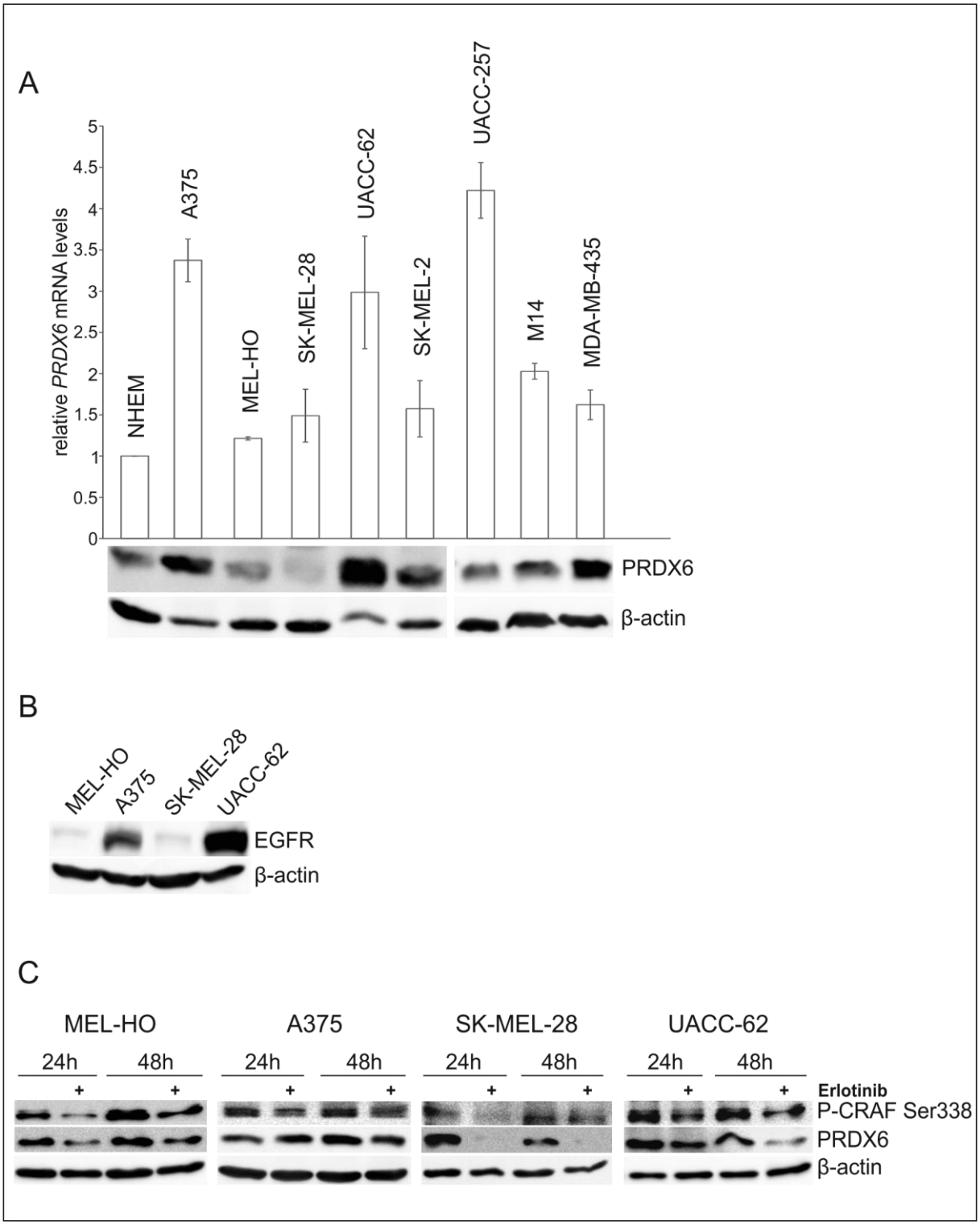

Figure 5: PRDX6 expression and EGFR-dependent regulation in human melanoma cells. A: Relative mRNA expression levels of *PRDX6* in different human melanoma cell lines compared to NHEM. Expression levels were normalized to *RSP14*. Error bars indicate SD of two independent experiments of the same RNA. Western blot shows the corresponding PRDX6 protein levels (lower panel). **B:** Western blot analysis of EGFR expression in melanoma cells containing low or high levels of PRDX6. **C:** Western blots representing EGFR-dependent expression of PRDX6. Subconfluent cells were treated with the EGFR inhibitor erlotinib (6 µM) for 24 h and 48 h. Efficiency of erlotinib was confirmed by reduced P-CRAF levels. β-actin served as loading control (**A, B and C**).

5.1.2 PRDX6 is regulated by the PI3K pathway

To investigate which downstream pathway is involved in EGFR-dependent regulation of PRDX6, starved HERmrk^{me} cells were treated with different inhibitors. The induced upregulation of PRDX6 protein expression after HERmrk stimulation was completely abolished by EGFR inhibitor AG1478, demonstrating again the EGFR-dependent regulation of PRDX6 (Fig. 6A). Inhibition of PI3K signaling by LY294002 prevented AKT activation and reduced the expression of PRDX6. Treatment with MEK inhibitor U0126 impeded HERmrk-induced ERK1/2 activation and led to a slight decrease in the PRDX6 level. However, ERK inhibitor showed, like the inhibition of PKC signaling by GÖ6983, no impact on PRDX6 induction.

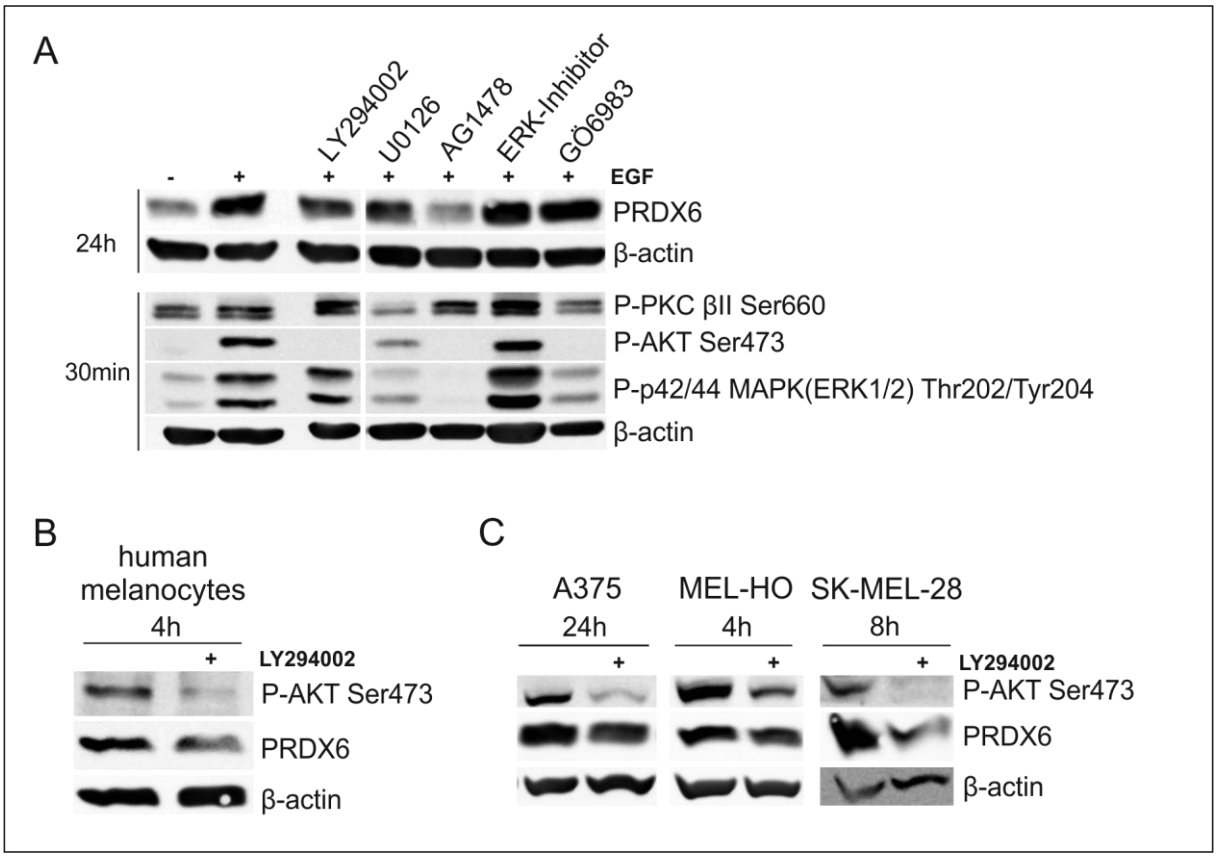

Figure 6: Identification of signaling pathways involved in the regulation of PRDX6. A: Western blot analysis of the PRDX6 level in HERmrk^{me} cells treated with the inhibitors: LY294002 (10 µM), U0126 (10 µM), AG1478 (10 µM), ERK-Inhibitor (10 µM) and GÖ6983 (1 µM). Of note, inhibition of ERK leads to an upregulation of phosphorylated ERK1/2 Thr202/Tyr204 which results from reduced feedback of the ERK1/2 pathway. Subconfluent cells were cultured for 72 h in 2.5% starving medium. 30 min after inhibitor administration cells were stimulated with hEGF (100 ng/ml). Inhibitor efficiency and PRDX6 expression were analyzed at the indicated time points. B, C: Western blots demonstrating PRDX6 levels of Hermes3a (**B**) as well as human melanoma cells (**C**) treated with LY294002 for 4 h, 8 h or 24 h. Inhibitor administration was performed on subconfluent cells and inhibitor efficiency was demonstrated by reduced activation of AKT. β-actin served as loading control (**A, B and C**).

As PI3K-AKT signaling had the strongest effect on PRDX6 regulation, its influence was also examined in Hermes3a cells (immortalized human melanocytes) and some human melanoma cell lines. Figures 6B and C show that PRDX6 levels were moderately decreased after

inhibition of PI3K for different time points which displayed the best inhibitory effect on the PI3K-AKT pathway in the respective cell line as judged by AKT activation.

Taken together, I could demonstrate that PI3K, e.g. downstream of the EGF receptor, is involved in the regulation of PRDX6.

5.1.3 Reactive oxygen species have no influence on PRDX6 level in melanoma cells and after HERmrk stimulation

HERmrk as well as PI3K signaling are potent inducers of reactive oxygen species (Leikam et al. 2014; Leikam et al. 2008; reviewed in Meierjohann 2014), and it is also known that melanomas of Xmrk-bearing *Xiphophorus* fish exhibit a ROS-dependent protein signature (Lokaj et al., 2009). Since I showed that the ROS-detoxifying enzyme PRDX6 is regulated by these kinases, I analyzed next whether its protein expression is a consequence of endogenous ROS.

Starved HERmrk^{me} cells were treated with the ROS scavengers tiron and vitamin E and the antioxidant N-acetylcysteine (NAC). To reduce the level of superoxide anion generated by NADPH oxidase, cells were treated with the NADPH oxidase inhibitor apocynin. In spite of ROS scavenging, PRDX6 levels were still upregulated after HERmrk stimulation (Fig. 7A).

Thus the results indicate that the EGFR-mediated regulation of PRDX6 is independent of ROS.

For additional examination in human melanoma cells, A375, MEL-HO and SK-MEL-28 cells were treated with different concentrations of the enzyme glucose oxidase (GOx). GOx generates oxidative stress via oxidation of glucose to hydrogen peroxide (H_2O_2). Under oxidative stress conditions, the catalytic C47 of PRDX6 can be oxidized to sulfenic acid (C-SOH), a process which is required for the antioxidative function of the enzyme (Peshenko & Shichi, 2001). When ROS levels are further enhanced, the sulfenic intermediate can be hyperoxidized to sulfonic acid (C-SO_3) (Kim et al. 2008), which is consequently indicative for a high level of oxidative stress as well as the peroxidase activity of PRDX6. Fig. 7B shows that administration of elevated GOx concentrations provoked an increase in the level of PRDX6-SO_3, whereas the overall PRDX6 protein level remained unaffected. Direct administration of H_2O_2 to A375 cells and NHEM also induced an increase in the PRDX6-SO_3 level, but did not influence the general PRDX6 protein abundance (Fig. 7C).

In conclusion, the data clearly demonstrate that oxidative stress leads to an upregulation of PRDX6-SO_3, but does not affect the overall PRDX6 level.

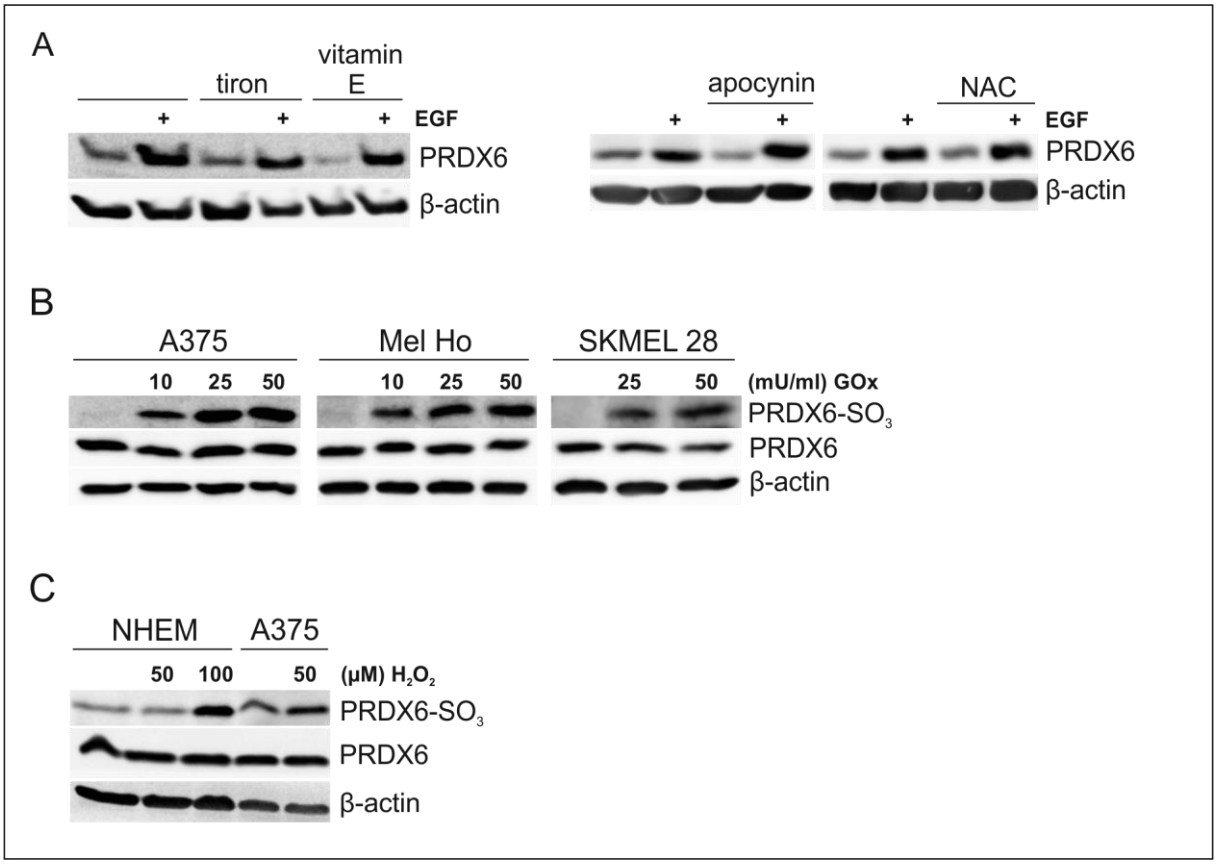

Figure 7: ROS-independent protein expression of PRDX6. A: After starving (in 2.5% starving medium for 72 h, HERmrk^{me} transgenic melanocytes were treated with tiron (80 µM), vitamin E (200 µM), apocynin (1 mM) and NAC (2 mM). 1 h later cells were stimulated with hEGF (100 ng/ml) for 24 h and PRDX6 level was determined by western blot. **B, C:** Western blots presenting the levels of PRDX6 and PRDX6-SO_3 in human melanoma cells treated with different concentrations of glucose oxidase (GOx; mU/ml) (**B**) as well as in NHEM and A375 melanoma cells treated with different concentrations of H_2O_2 (µM) (**C**) as indicated. Treatment with GOx was performed for 2 h, whereas H_2O_2 treatment was performed for 24 h. The different incubation times for the ROS inducers were chosen because of the different strengths of ROS increase by GOx and H_2O_2. β-actin served as loading control (**A, B and C**).

5.2 Localisation of PRDX6 and its interaction with PCNA

Both activities of PRDX6 can be regulated by the intracellular pH. The PRDX6-peroxidase activity reaches its optimum at cytosolic pH (pH 7-8), whereas the $iPLA_2$ activity requires an acidic pH (pH 4) (Chen et al. 2000). Accordingly, PRDX6 was shown to be localized to the cytosol as well as to lysosomes (Akiba et al. 1998; Kim et al. 1997). Therefore, immunofluorescence studies of NHEM and a melanoma cell line were performed to receive insights into the intracellular localization of PRDX6 in melanocytes and melanoma cells. Generally, PRDX6 was localized throughout the cell in both, NHEM and SK-MEL-28 cells (Fig. 8A). However, in SK-MEL-28 cells with particularly strong perinuclear lysosomal associated protein-1 (Lamp1) signal, which is indicative for lysosomes, total PRDX6 signal was excluded from the lysosomes. This was not observed for PRDX6-SO_3, which was evenly distributed in all cells and did not differ between NHEM and SK-MEL-28 cells (Fig. 8B). Most interestingly,

melanoma cells displayed a strong nuclear localization of total PRDX6, which was not observed in NHEM cells.

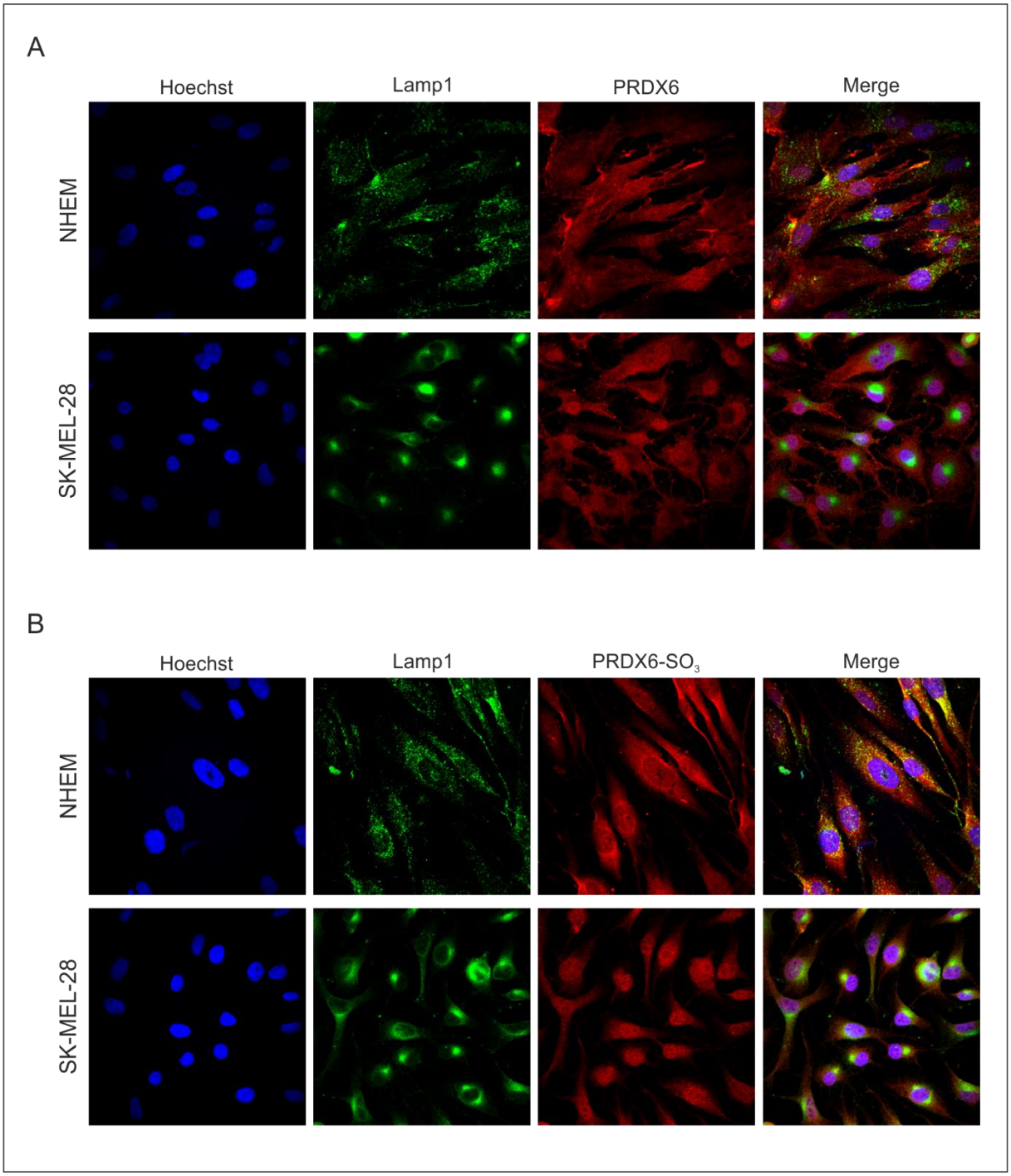

Figure 8: Localisation of PRDX6 in human melanocytes and melanoma cells. A, B: Immunofluorescence of NHEM and SK-MEL-28 cells presenting cellular localization of PRDX6 (total cellular PRDX6) (**A**) and PRDX6-SO_3 (only hyperoxidated PRDX6) (**B**). Cells were grown on glass slides and after reaching 60-70% confluence, double immunofluorescence staining was performed and evaluated by confocal laser microscopy (63x amplification). Nuclei were stained in blue via Hoechst-staining, PRDX6/PRDX6-SO_3 in red and Lamp-1 in green via secondary Alexa Flour 594 and Alexa Fluor 488 antibody, respectively. Fluorescence figures were processed via ImageJ.

Interestingly, in breast cancer cells PRDX6 was previously shown to interact with the proliferating cell nuclear antigen (PCNA) (Naryzhny & Lee 2010). Like PRDX6, PCNA is localized in the cellular nucleus, but substantial amounts can also be found in the cytoplasm (Naryzhny & Lee 2004). The protein facilitates the DNA replication by DNA polymerases (Mailand et al. 2013) and is highly expressed in proliferating cells, including cancer cells (reviewed in Stoimenov & Helleday 2009). Therefore, immunoprecipitation studies of SK-MEL-28 cells were performed with anti-PCNA antibody. The precipitate was blotted and incubated with antibodies recognizing PCNA, total PRDX6 and PRDX-SO_3 (Fig. 9A). To increase the level of the hyperoxidated version of PRDX6, PRDX6-SO_3, cells were additionally treated with H_2O_2 before the anti-PCNA immunoprecipitation was performed (Fig. 9B). An interaction with PCNA could be observed using the PRDX6 as well as the PRDX6-SO_3 antibody. These data demonstrate a clear interaction of PRDX6-SO_3 with PCNA. As the PRDX6 antibody also recognizes hyperoxidated PRDX6, it is not clear whether this interaction is PRDX6-SO_3 specific or not.

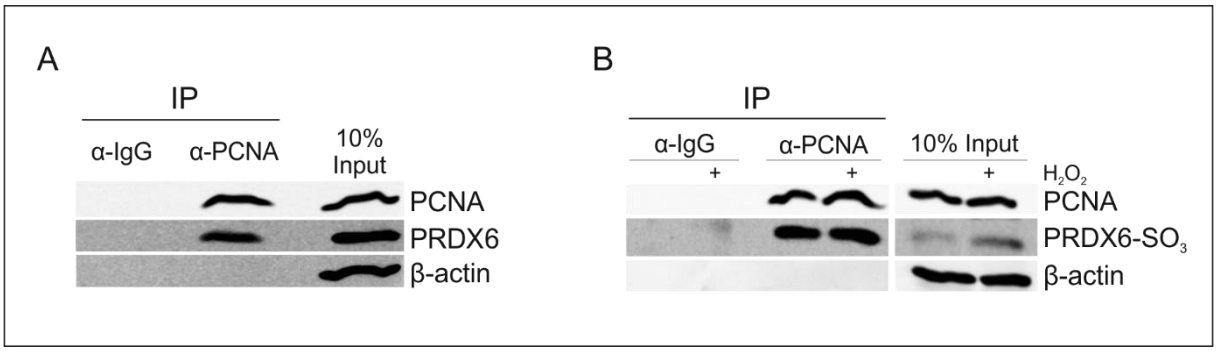

Figure 9: Co-immunoprecipitation (Co-IP) of PRDX6 and PCNA from SK-MEL-28 cells. PCNA-PRDX6 was immunoprecipitated from SK-MEL-28 cell lysate by using α-PCNA antibody coupled to sepharose A beads. α-IgG antibody was used as control. **A, B:** Western blots demonstrating the interaction of PRDX6 with PCNA. In **B**, cells were treated 24 h with 25 µM H_2O_2 before Co-IP was performed and western blot analysis shows the interaction of PRDX6-SO_3 with PCNA. 10% input displays 10% of the used protein lysate and β-actin served as loading control (**A and B**).

5.3 Function of PRDX6 in human melanoma cells

The next part of the study represents the analysis of the functional role of PRDX6 in human melanoma cells including the examination of the corresponding mechanism.

5.3.1 Knockdown of *PRDX6* reduces proliferation

To investigate the functional role of PRDX6 in human melanoma, knockdown experiments were performed and proliferation was monitored.

For longterm proliferation experiments, three specific *PRDX6* shRNA sequences were cloned into the lentiviral pLKO-Tet-On vector, which was subsequently used for the establishment of stable transgenic cell lines. Since shRNA-2 led to a clear decrease in the level of PRDX6 protein (Fig.10), transgenic cell lines expressing this doxycycline-inducible shRNA were used for the following experiments.

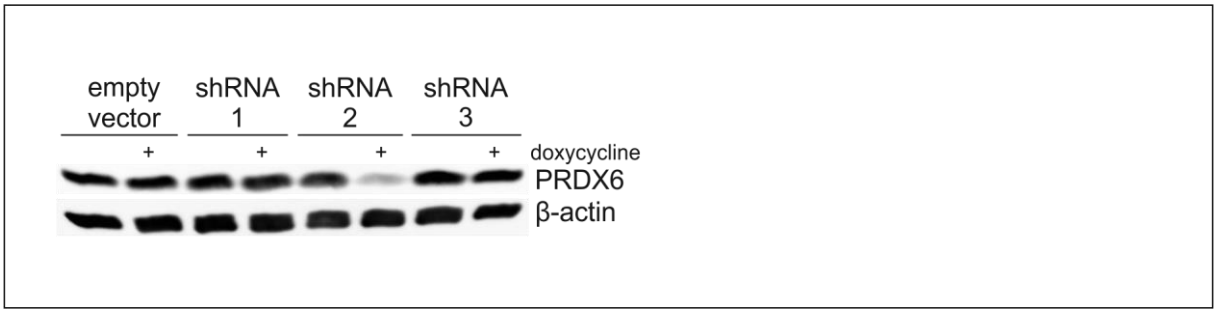

Figure 10: Examination of shRNA sequences targeting *PRDX6*. Subconfluent transgenic SK-MEL-28 cells containing pLKO-Tet-On empty vector or pLKO-Tet-On shRNA-1,-2 or -3 were treated with 100 ng/ml doxycycline. Three days later, cells were harvested and shRNA efficiency was analyzed by western blot. β-actin was used as loading control.

Fig.11 shows the analysis of cell proliferation rates of A375, MEL-HO and SK-MEL-28 cells stably transformed with pLKO-Tet-On-shRNA-2. Compared to empty vector (pLKO-Tet-On) infected cells, expression of *PRDX6* shRNA-2 led to a substantial decrease of PRDX6 levels as depicted by western blot analysis. Cell proliferation rate was determined by counting the cells manually at the indicated time points. MEL-HO as well as SK-MEL-28 cells exhibited a clear *PRDX6* knockdown induced decrease of proliferation at day 5 and 7. The MEL-HO cell line revealed the strongest effect on cell growth. Here, the *PRDX6*-specific shRNA construct seemed to be slightly leaky as reduced PRDX6 protein levels as well as decreased proliferation could also be observed in absence of doxycycline.

.

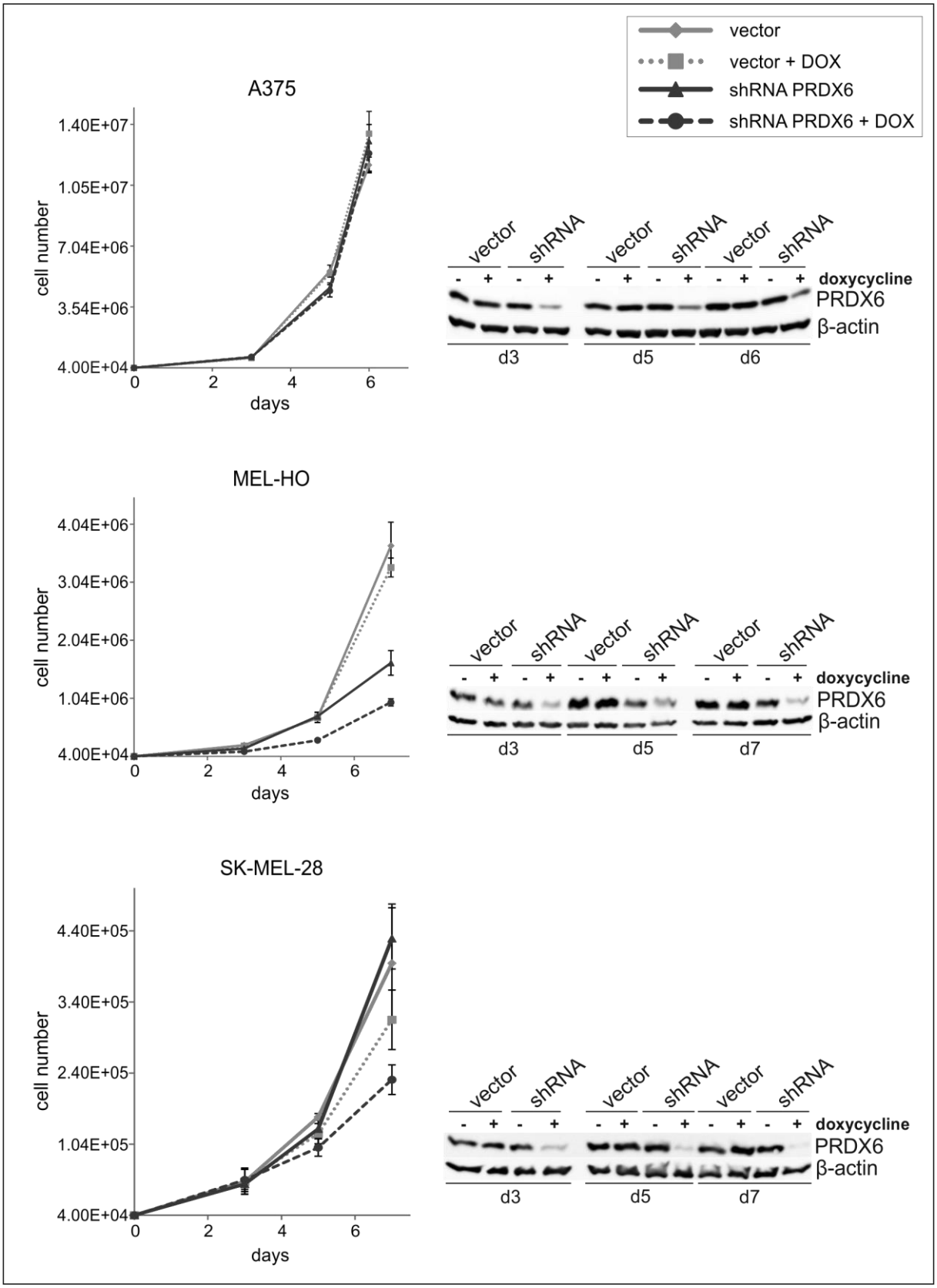

Figure 11: Influence of PRDX6 on melanoma cell proliferation. Transgenic cell lines, stably expressing a doxycycline (DOX)-inducible shRNA against *PRDX6* were seeded into 6-well dishes (A375: 3x 10^4 cells per well; MEL-HO and SK-MEL-28: 4x10^4 cells per well) and were treated with 100 ng/ml doxycycline 6 h later. Cells infected with empty vector served as control. Administration of doxycycline was repeated every third day. Graphs demonstrate cell growth curves obtained by manual cell counting at the indicated time points (**left panels**). For each cell line one example of three independent experiments is shown. Error bars indicate standard deviation (SD) of a

single experiment performed in triplicates. In parallel, cells were used for western blot analysis to confirm the doxycycline-induced downregulation of PRDX6 (**right panels**). β-actin served as loading control.

The proliferation of A375 cells remained unaffected. However, in this cell line, the knockdown was less efficient than in the other two melanoma cell lines, which might affect the proliferation results.

To confirm the effects of the shRNA-dependent knockdown, the proliferative role of PRDX6 was analyzed with *PRDX6*-specific small interfering RNAs (siRNAs). Control (non-target) and *PRDX6* siRNA were introduced into A375, MEL-HO, SK-MEL-28 and UACC-62 cells. Western blot analysis showed that siRNA-mediated knockdown clearly reduced the levels of PRDX6 protein (Fig.12A and B, lower panels). Measurement of BrdU incorporation also demonstrated growth inhibitory effects of *PRDX6* knockdown in MEL-HO and SKMEL-28 cells, but only slight effects in the A375 cell line (Fig. 12A, upper panel). The amount of incorporated BrdU was reduced by 47% and 37% in MEL-HO and SK-MEL-28 cells, respectively. In the A375 cell line, knockdown of *PRDX6* only led to a reduction of BrdU incorporation of 5%.

Since the xCELLigence system allows a higher time resolution and a continuous monitoring of cell growth over a longer time period, this indirect proliferation assay was also performed. xCELLigence impedance analysis displayed the same *PRDX6* knockdown-mediated impact on proliferation as observed before (Fig.12B, upper panels). Downregulation of *PRDX6* led to a clear decrease of cell impedance in MEL-HO as well as in SK-MEL-28 cells, but not in A375 cells. UACC-62 cells, which were added to the melanoma cell panel in this assay, revealed the strongest decrease in proliferation after siRNA-mediated knockdown of *PRDX6*.

Taken together, I could confirm a proliferative function of PRDX6 in three out of four investigated human melanoma cell lines.

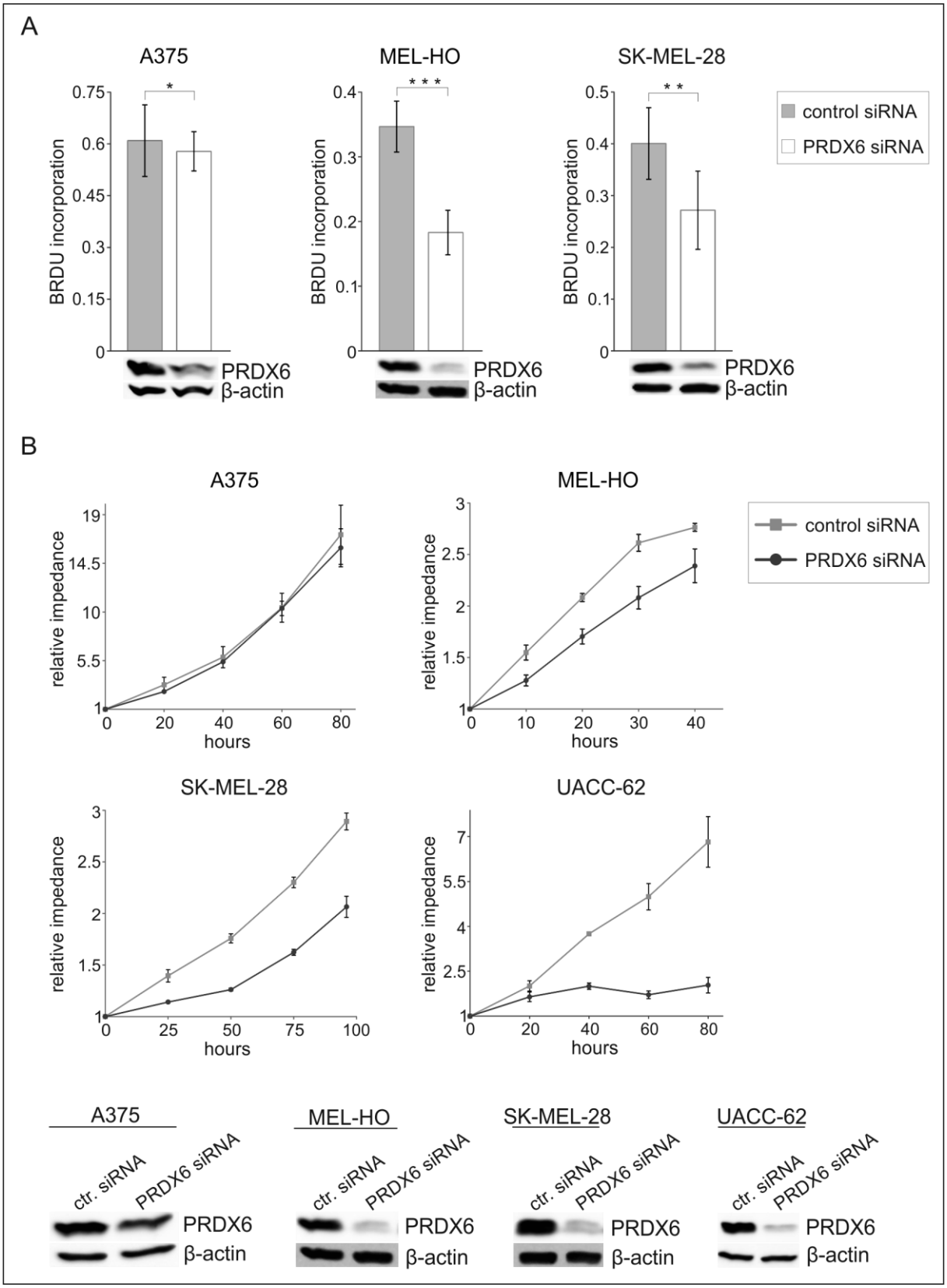

Figure 12: Influence of PRDX6 on melanoma cell proliferation. A: BrdU incorporation of proliferating human melanoma cells transfected with control or *PRDX6*-specific siRNA pools, respectively. 48 h after siRNA transfection, cells were seeded into 96-well plates (A375, SK-MEL-28: $3.5x10^3$; MEL-HO: $4x10^3$ cells per 96-well) and 48 h later they were treated with 10 µM BrdU for 6 (A375, MEL-HO) to 8 h (SK-MEL-28). Values expressed as mean +/- SD of three independent experiments (*: p<0.05; **: p<0.01; ***: p<0.001) performed in triplicates. For confirming siRNA-mediated knockdown of *PRDX6,* cells were in parallel seeded into 6-well plates and analyzed 4 days after siRNA transfection by western blot demonstrating the level of PRDX6 protein (**lower panels**). **B:** xCELLigence data

showing cellular impedance of human melanoma cells at the indicated time points. Cells were seeded into the xCELLigence 96-well plate ($2x10^3$ cells/96-well) 24 h after transfection with control or *PRDX6*-specific siRNA. Cellular impedance was monitored after cells had settled. Error bars indicate SD of a single experiment performed in triplicates. In parallel, cells were seeded into 6-well plates, harvested at day 5 after siRNA transfection and analyzed for PRDX6 expression by western blot (**lower panels**). β-actin served as loading control (**A and B**).

As the described proliferation assays cannot clearly distinguish between cell death and cell cycle inhibition, I also investigated the presence of apoptosis markers after knockdown of *PRDX6*. I chose exemplarily the cell lines UACC-62 and MEL-HO, which both show a robust growth inhibition by *PRDX6* siRNA.

A western blot analysis depicted in Fig. 13 shows that siRNA-mediated knockdown of *PRDX6* did not induce cleavage of the apoptosis marker PARP (Poly (ADP-ribose) polymerase). This observation suggests that PRDX6 influences cell growth by enhancing proliferation without affecting apoptosis.

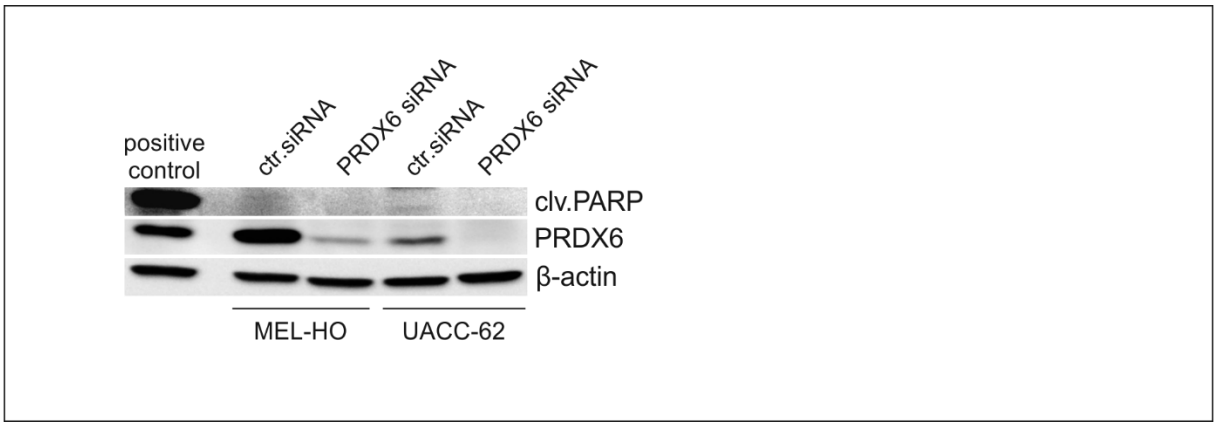

Figure 13: Cell death-independent action of PRDX6 on melanoma proliferation. Western blot analysis shows the level of cleaved PARP in response to siRNA-mediated knockdown of *PRDX6*. Protein levels were analyzed 72 h after siRNA transfection. MEL-HO cells treated for 24 h with doxorubicin (1 µM) were used as positive control. β-actin served as loading control.

5.3.2 Knockdown of *PRDX6* decreases P-Rb protein and P-SRC family kinase levels

To identify signaling pathways which are linked to the PRDX6-mediated effect on proliferation, the level of protein kinases regulating the cell cycle were examined by western blot analysis. MEL-HO and UACC-62 cells showed a clear decrease in the activation of SRC family kinases (Fig. 14A) and Rb protein (Fig.14B) after siRNA-mediated knockdown of *PRDX6*. This observation leads to the hypothesis that PRDX6 influences cellular proliferation through the regulation of P-SRC family kinase and P-Rb levels.

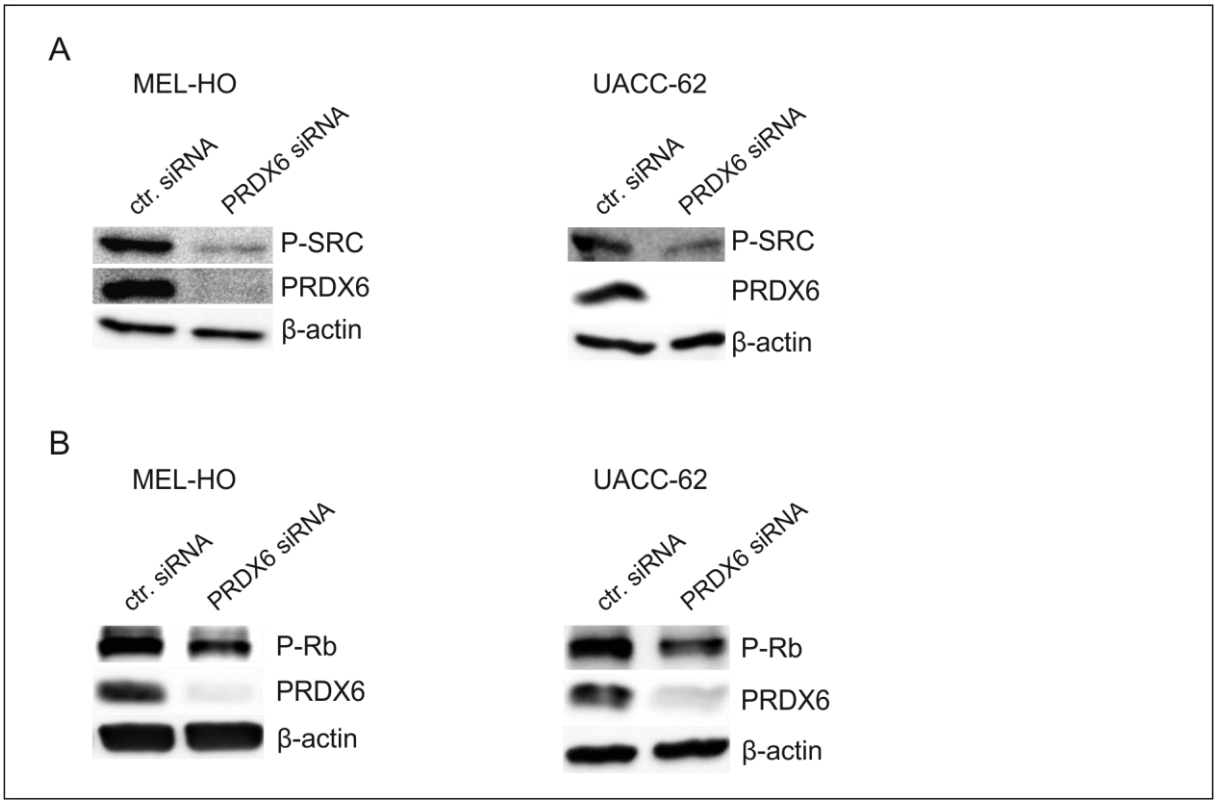

Figure 14: Influence of PRDX6 on Rb protein and SRC family kinase activation. A, B: MEL-HO and UACC-62 cells were transfected with control and *PRDX6*-specific siRNA. Four days after transfection, cells were harvested and protein levels were analyzed. Western blots demonstrate the level of P-SRC family kinases (**A**) and P-Rb protein (**B**) in response to siRNA-mediated knockdown of *PRDX6*. β-actin was used as loading control.

5.3.3 PRDX6 influences proliferation via its iPLA$_2$ activity

As PRDX6 harbors two enzymatic activities, I was interested in finding out which activity is involved in mediating the proliferative effect. S32 of PRDX6 is essential for the function of the iPLA$_2$ activity, and C47 is the catalytically active amino acid residue of the PRDX6-peroxidase. It was reported previously that point mutations at one of these residues disturb one enzymatic activity without affecting the other (Chen et al. 2000). To determine which enzymatic activity of PRDX6 is responsible for melanoma cell proliferation, I performed a complementation experiment. First, I generated PRDX6 expression plasmids of the wildtype enzyme or of point mutated PRDX6 constructs with a mutation of S32 to A (S32A) or C47 to S (C47S), respectively. Wildtype *Prdx6* was amplified from murine cDNA and subcloned into the pBABE-hygro vector, which was subsequently used as template for the establishment of FLAG-tagged murine *Prdx6* as well as for the generation of FLAG-tagged *Prdx6* mutants via sewing-PCR. The FLAG-tagged products were cloned into the p201iEP vector that was subsequently used for the establishment of stable transgenic UACC-62 cells. Control siRNA and siRNA targeting only endogenous human (h)*PRDX6* were introduced into the transgenic UACC-62 cells stably expressing the FLAG-tagged murine wildtype PRDX6 (mPRDX6-WT), PRDX6-S32A or

PRDX6-C47S. Using this system, the level of endogenous human PRDX6 could be decreased by specific siRNA without affecting the expression level of either wildtype mPRDX6 or the mutants. Fig.15 presents a schematic overview of the performed experiment.

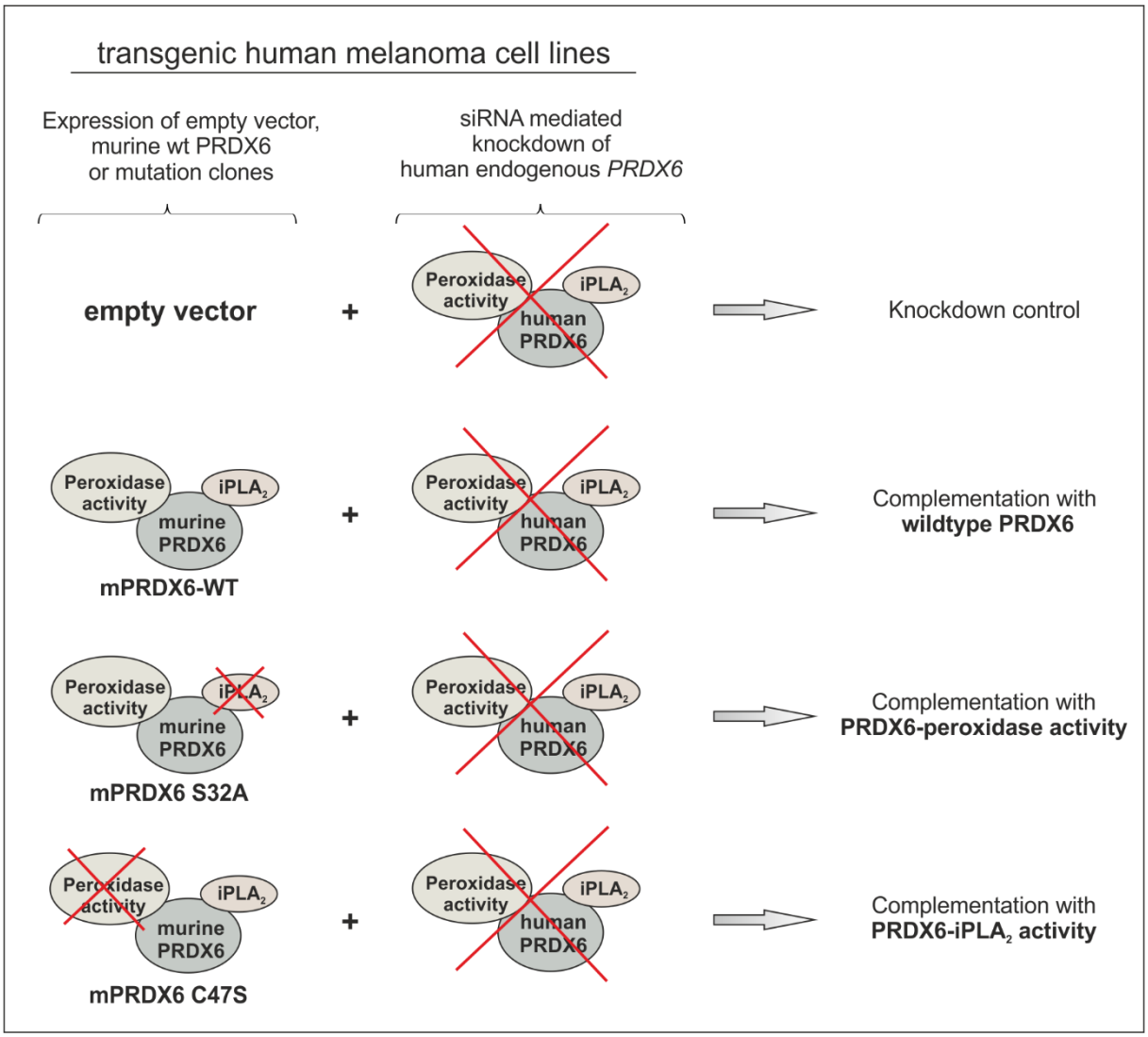

Figure 15: Schematic view of the performed complementation experiment for identification of the enzymatic PRDX6 activity responsible for the proliferative function. siRNA-mediated knockdown of human endogenous *PRDX6* along with the simultaneous expression of empty vector (serves as control), murine wildtype PRDX6, PRDX6-S32A or PRDX6-C47S.

The western blot analysis depicted in Fig.16A shows that the system worked well as the knockdown of the endogenous h*PRDX6* (lower bands) as well as the expression of the FLAG-tagged mPRDX6 clones (upper bands) were clearly visible, and the knockdown did not affect expression of the FLAG-tagged PRDX6 constructs.

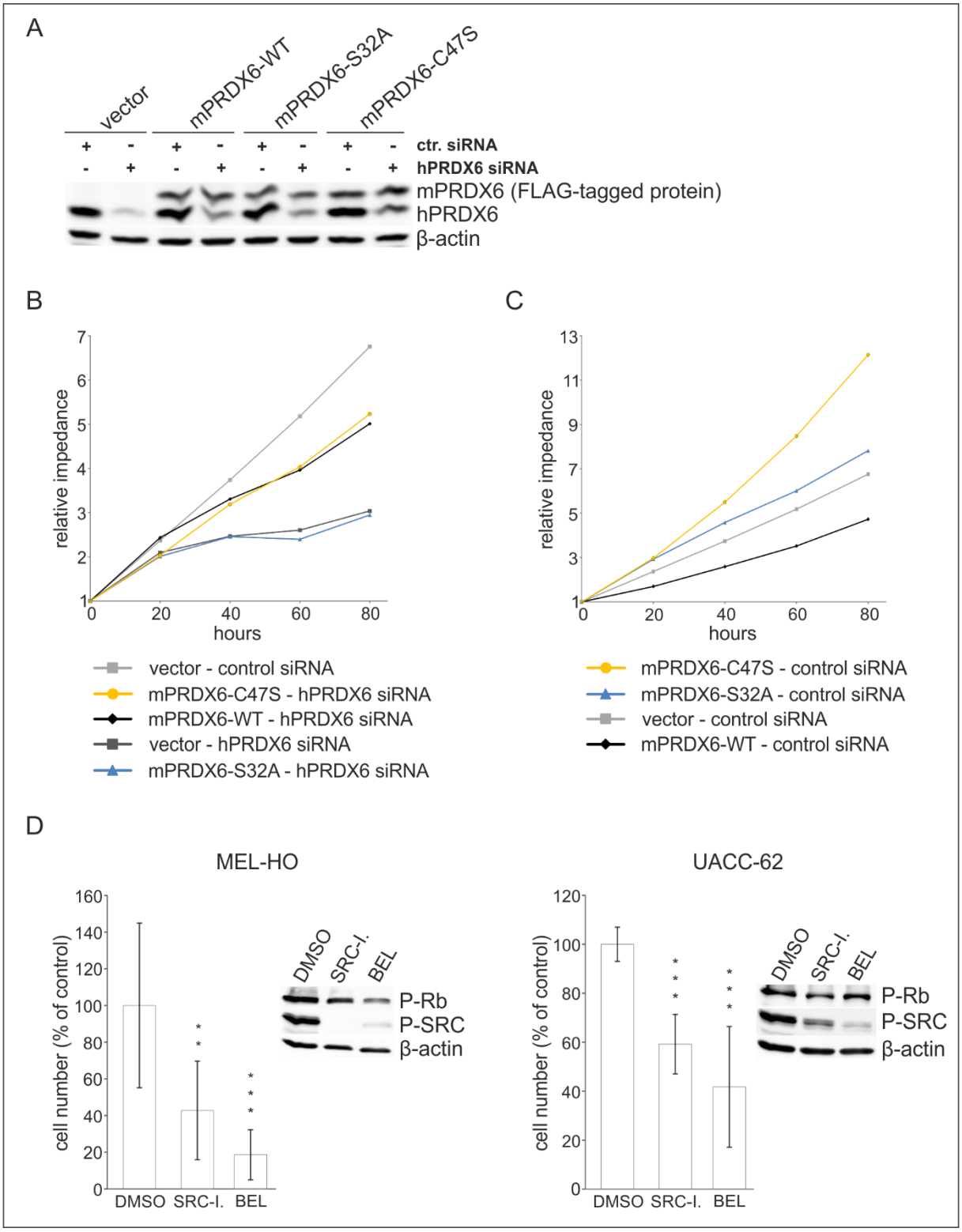

Figure 16: iPLA$_2$ dependent effect of PRDX6 on proliferation. A: 24 h after indicated siRNA transfection, control UACC-62 cells (transgenic for empty vector) or UACC-62 cells expressing FLAG-tagged wildtype mPRDX6, mPRDX6-S32A, or mPRDX6-C47S were seeded into 6-well plates (5x10^4 cells/well). PRDX6 protein level was analyzed at day 4 after transfection and western blot analysis shows reduced levels of endogenous human PRDX6 next to the expression of FLAG-tagged mPRDX6-WT and mutation clones. β-actin was used as loading control. **B, C:** For the xCELLigence assay, cells were seeded into the xCELLigence 96-well plate (2x10^3 cells/well) 24 h after siRNA transfection. Cellular impedance was monitored after cells had settled. xCELLigence data represent cellular impedance of transgenic UACC-62 cells, transfected with control siRNA or siRNA targeting human PRDX6, at the indicated time points. The mean values of duplicates of one single experiment are presented. Stable transgenic cells, infected with empty vector (p201-iEP) were used as control (**A, B and C**). **D:** Bar graphs presenting

the relative number of cells in response to SRC family kinase inhibition (SRC kinase inhibitor I; SRC-I.) and bromoenol lactone (BEL; inhibitor of $iPLA_2$) compared to DMSO (control) treatment, the latter being set as 100% (**left panels**). Western blots demonstrate inhibitor efficiency and $iPLA_2$ dependent activation of SRC family kinases and Rb protein. β-actin was used as loading control (**right panels**). Cells were seeded into 6-well dishes (MEL-HO: $6x10^4$ cells/well; UACC62 $8x10^4$ cells/well) and 6 h later treated with SRC kinase inhibitor I (10µM), BEL (15µM) or DMSO as control. 48 h later medium was changed and inhibitor administration was repeated. After additional 48 h, cells were harvested for manual counting and subsequent western blot analysis. Error bars represent SD of three independent experiments performed in triplicates (**: $p<0.01$; ***: $p<0.001$).

To investigate whether the exogenous PRDX6 constructs can compensate for the knockdown of endogenous *PRDX6*, xCELLigence impedance analyses were performed (Fig. 16B). Interestingly, the data revealed that the expression of the mPRDX6-S32A mutant was not able to rescue or attenuate the inhibitory effect of PRDX6-specific siRNA on proliferation, whereas UACC-62 cells expressing mPRDX6-WT or C47S mutant exhibited improved cell growth after knockdown of endogenous h*PRDX6*.

To test the effect of overexpressing the exogenous PRDX6 constructs in absence of endogenous *PRDX6* knockdown, xCELLigence assay was also performed with control siRNA transfected cells. Fig. 16C illustrates that an increase of the mPRDX6-C47S mutant, which contains only the $iPLA_2$ activity, strongly enhanced cellular proliferation. Expression of the peroxidase competent mPRDX6-S32A mutant led only to a negligible increase compared to control cells (empty vector cells). Interestingly, transgenic UACC-62 cells expressing additional wildtype PRDX6 exhibited a lower proliferation rate than the control cells.

In conclusion, the $iPLA_2$ activity acts growth-promoting on its own, but loses its effect in presence of additional peroxidase activity. The reasons for this are currently unclear. It is, however, possible that an increased antioxidative PRDX6 function might create a state of homeostatic imbalance of ROS in melanoma cells, which might impact proliferation.

To independently test the relevance of $iPLA_2$ phospholipases in melanoma, Mel-HO and UACC-62 cells were treated with BEL (Bromoenol lactone), a general inhibitor of Ca^{2+}-independent phospholipases, and the influence on proliferation was analyzed by manual cell counting. BEL significantly reduced cell growth by about 81% in Mel-Ho cells and by 58% in UACC-62 cells (Fig.16D; left panel of each cell line) and went along with a reduction of P-SRC family kinases in both cell lines and with a decrease of P-Rb in MEL-HO cells (Fig. 16D; right panels of each cell line). The cell growth supporting role of SRC family kinases was demonstrated by a strong reduction of cell proliferation in the presence of SRC family kinase inhibitor (Fig.16D).

In conclusion, the data verify that the $iPLA_2$ activity of PRDX6 plays a prominent role in melanoma cell proliferation, presumably by altering the activity state of SRC family kinases.

To further examine whether the peroxidase activity of PRDX6 is at least required under oxidizing conditions, control and *PRDX6*-specific siRNA were introduced into MEL-HO cells and cell growth was analyzed in presence of glucose oxidase or H_2O_2. Analysis of BrdU incorporation revealed that knockdown of *PRDX6* led to a stronger impact on proliferation compared to control in presence of GOx or H_2O_2 (Fig.17). Thus, under oxidative stress the peroxidase activity of PRDX6 seems also to be involved in cellular proliferation.

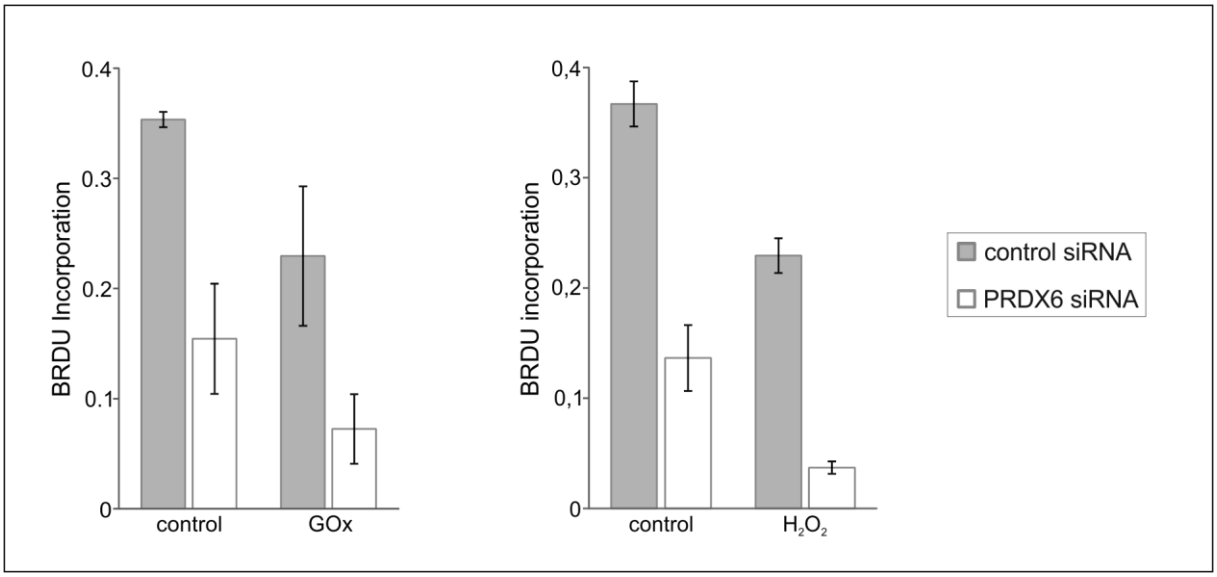

Figure 17: Role of the antioxidative function of PRDX6 activity in melanoma cell growth. Graphs represent measurement of BrdU incorporation of proliferating MEL-HO cells under control and stress-induced conditions. 48 h after transfection with control or *PRDX6*-specific siRNA, cells were seeded into a 96-well plate ($4x10^3$ cells/well). 24 h later, cells were treated with GOx (1 mU/ml) or H_2O_2 (25 µM) for 24 h. Administration of H_2O was used as control. Afterwards, BrdU (10 µM) incorporation was performed for 6 h. Error bars indicate SD of a single experiment performed in triplicates.

In addition, I performed a luciferase assay to test the effect of PRDX6 reduction on oxidative stress, using an Nrf2 reporter plasmid. In response to oxidative stress, the nuclear factor erythroid derived-related factor 2 (Nrf2) translocates to the nucleus and regulates, via binding to antioxidant response elements (AREs) in the promotor region of its target genes, the expression of proteins which control the cellular redox balance and protect the cell against oxidative damage. These proteins include for example the NADPH dehydrogenase quinone 1 (NQO1), glutathione S transferase (GST) or also PRDX1 and PRDX6 (Kaspar et al. 2009; Lieder et al. 2012). The ARE-binding activity of Nrf2 was previously used in a luciferase reporter system (see also Lieder et al., 2012) as indicator for oxidative stress. Control (non-target) or *PRDX6*-specific siRNA pools were introduced into A375 cells which were additionally transfected with a luciferase reporter plasmid containing the firefly luciferase under control of the ARE of the *NQO1* gene. Figure 18 demonstrates that the luciferase activity, which was increased upon GOx treatment, was upregulated after knockdown of *PRDX6*, thus indicating a role of PRDX6 in oxidative stress defence in melanoma cells.

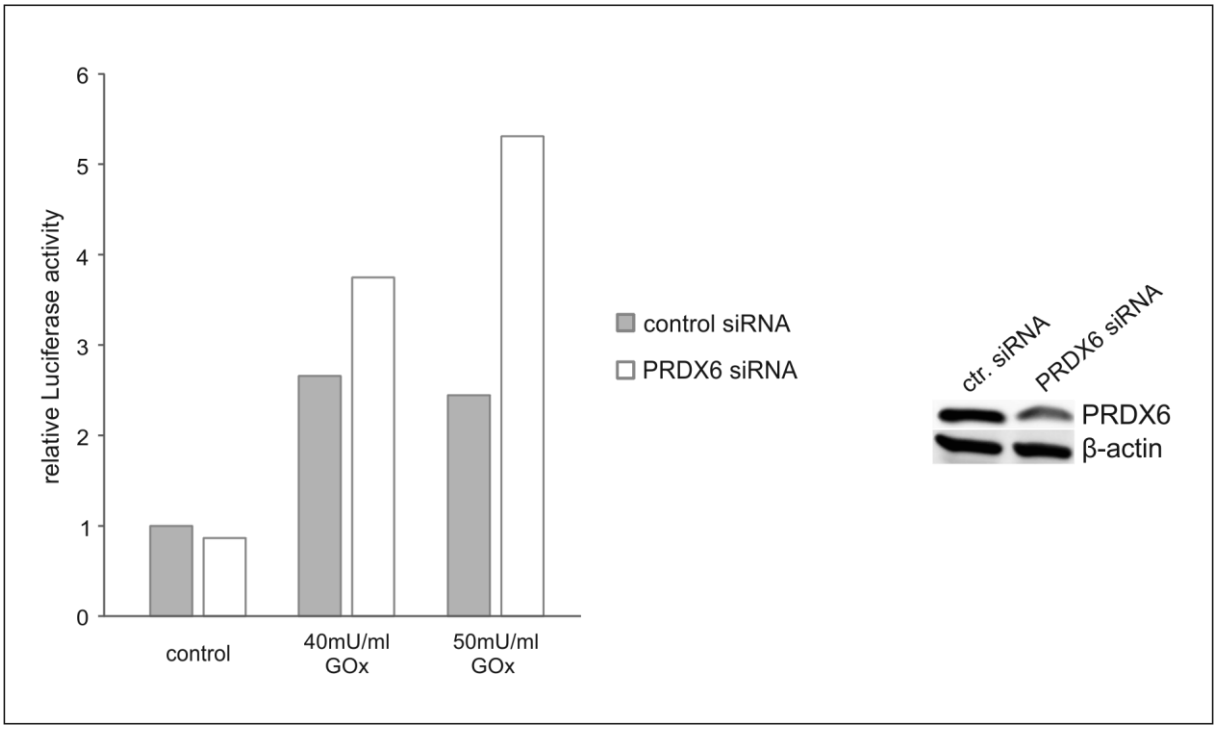

Figure 18: Influence of PRDX6 on Nrf2-mediated stress response. A375 cells were grown in 12-wells and transfected with control siRNA or *PRDX6*-specific siRNA pools, respectively. 24 h later, cells were co-transfected with firefly luciferase reporter plasmid (PGL3-rNQO1 ARE+fn) as well as renilla luciferase reporter vector (pRL-CMV). Around 46 h after co-transfection, cells were treated for 6 h with different GOx concentrations as indicated. Afterwards luciferase activity was measured. Graph represents firefly luciferase activity normalized to renilla luciferase activity under control and GOx treatment (**left panel**). The bars demonstrate one single experiment. Western blot analysis of the PRDX6 level confirms siRNA-mediated knockdown of *PRDX6* (**right panel**). β-actin served as loading control.

Taken together, the results indicate that the $iPLA_2$ activity of PRDX6 plays an important role under normal conditions, whereas the peroxidase activity becomes important when ROS levels are raised.

5.3.4 Knockdown of *PRDX6* lowers the amount of arachidonic acid and decreases the level of PGE_2 in UACC-62 cells

As the $iPLA_2$ activity of PRDX6 promotes the release of arachidonic acid (AA) by cleavage of phosphatidylcholines, I investigated the effect of PRDX6 on cellular lipids with specific emphasis on eicosanoids. For this purpose, gas chromatography was performed in collaboration with Werner Schmitz from the Department of Biochemistry and Molecular Biology (University of Würzburg).

Transgenic MEL-HO and UACC-62 cells stably expressing doxycycline-inducible shRNA against *PRDX6* were used in these experiments. Interestingly, a knockdown of *PRDX6* led to a decrease in total cellular amount of AA in both cell lines, with MEL-HO cells showing the

strongest effect (Fig. 19A, left panel). Western blot analysis confirmed strongly reduced PRDX6 and P-SRC family kinase levels after doxycycline-induced shRNA expression (Fig. 19A, right panel).

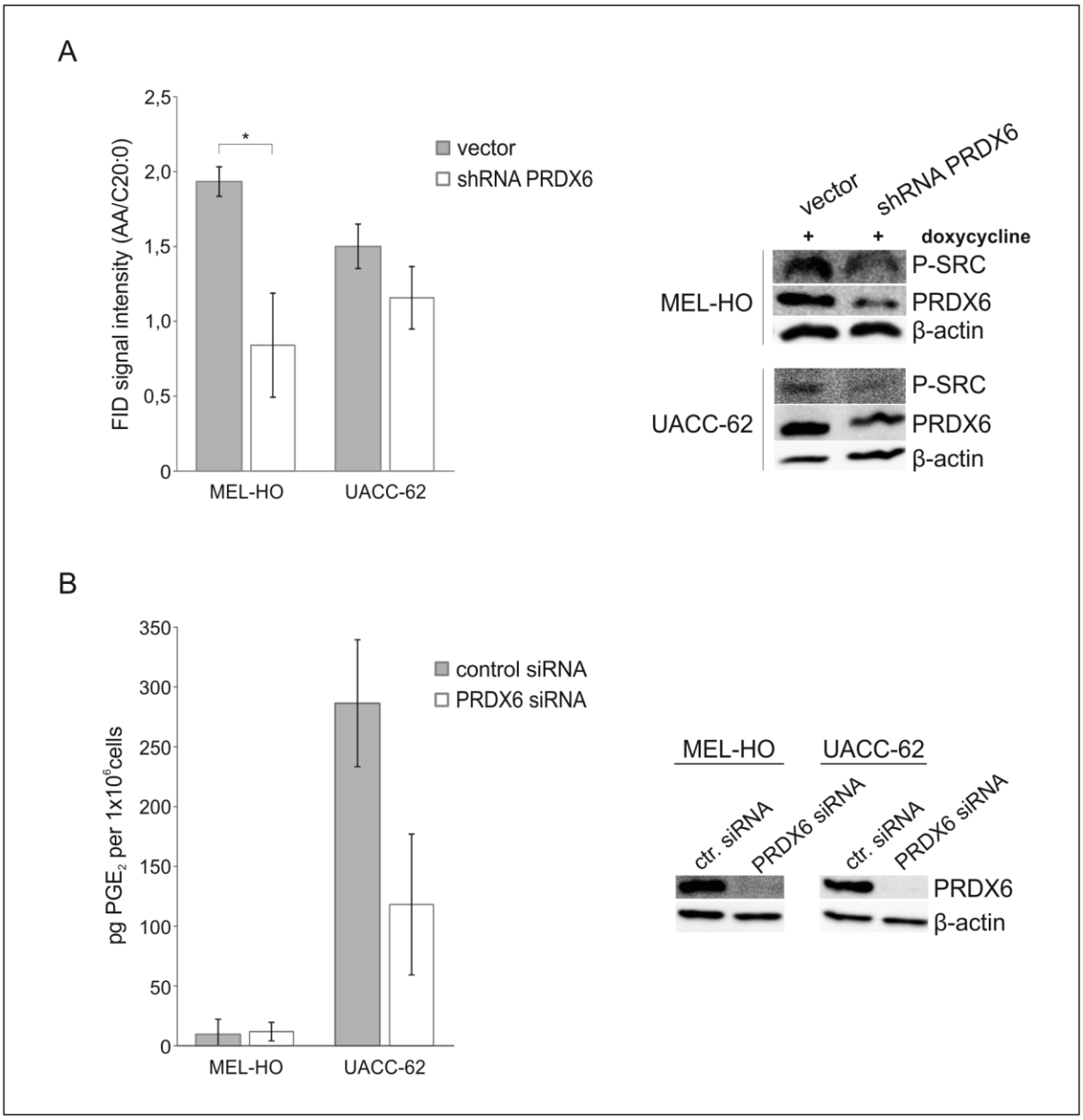

Fig.19: Influence of PRDX6 on arachidonic acid and PGE_2 levels in human melanoma cells. A: Gas chromatography analysis demonstrating AA (arachidonic acid) levels of stable transgenic cell lines containing an inducible shRNA against *PRDX6* (**left panel**). Subconfluent cells were grown in 15 cm dishes, treated three times with doxycycline (100 ng/ml) to induce shRNA expression and harvested at day 6 for gas chromatography and western blot analyses. Empty vector cells served as control. Data are shown as FID (flame ionization detector signal) intensity ration of AA/C20:0. The unaffected eicosanoid acid C20:0 was used as internal reference. Three (MEL-HO) and two (UACC-62) independent experiment are presented (*: $p<0.05$). Error bars represent the standard deviation. Corresponding protein blots confirm knockdown of PRDX6 as well as decreased P-SRC family kinase levels (**right panel**). **B:** PGE_2-ELISA showing the amount of PGE_2 in cells transfected with control or *PRDX6*-specific siRNA (**left panel**). Cells were grown in 6-well plates and culture medium was changed 48 h after transfection. 48 h later, when cells had reached a confluence of around 70% to 80%, culture medium was analyzed for PGE_2 level. Error bars represent SD of two independent experiments performed in duplicates. The cells were

analyzed by western blot to confirm siRNA-mediated decrease of PRDX6 (**right panel**). β-actin was used as loading control (**A,B**).

As AA is generally processed into different metabolites after its release from phospholipids, the next step was to examine whether PRDX6 can affect the levels of the tumor-relevant prostaglandin PGE_2 (Yamaki et al., 2004). Thus, MEL-HO and UACC-62 cells were transfected with siRNA targeting *PRDX6* (Fig. 19B right panel) and the amount of PGE_2 was examined using a PGE_2-ELISA. In comparison to control siRNA transfected cells, knockdown of *PRDX6* decreased the PGE_2 content in UACC-62 cells (Fig. 19B left panel). Mel-HO cells showed in general a relatively low level of PGE_2 and a difference between *PRDX6* knockdown and control siRNA could not be observed.

Taken together, the data demonstrate that PRDX6 participates in regulating total cellular AA content. Furthermore the enzyme was shown to influence the level of PGE_2 in UACC-62 cells.

5.3.5 The proliferative function of the $iPLA_2$ activity of PRDX6 is mediated via AA

To check whether AA or PGE_2 may be involved in the growth-promoting effect of the $iPLA_2$ activity of PRDX6, rescue experiments were performed with UACC-62 and MEL-HO cells in presence of *PRDX6*-specific siRNA. Cells were additionally treated with either AA or PGE_2 and proliferation was investigated via manual cell counting. Compared to control siRNA transfected cells, knockdown of *PRDX6* led to a decrease in the proliferation by 32% in MEL-HO and 36% in UACC-62 cells. Treatment with AA or PGE_2 could partially rescue this inhibitory effect in both cell lines, but also enhanced general growth under control conditions, particularly in MEL-HO cells (Fig. 20A). Here, AA as well as PGE_2 led to a significant increase in general cell growth. In case of UACC-62 cells, this effect was only observed by PGE_2 treatment.
AA administration could also rescue SRC family kinase activation in both cell lines (Fig. 20B), while PGE_2 showed this effect only in the MEL-HO cell line, which displays very low intrinsic PGE_2 levels (Fig.19B).

To get better insight into the general role of prostaglandins in melanoma proliferation, MEL-HO and UACC-62 cells were treated with an inhibitor of the cyclooxygenase 2 (COX-2), the enzyme which enables the formation of several prostaglandins (PGs), including PGE_2, from AA (Yamaki et al. 2004). Interestingly, COX-2 inhibition resulted in a significant increase in proliferation in both cell lines (Fig. 20C left panels of each cell line). Furthermore, western blot analysis revealed no change in the levels of activated SRC family kinases (Fig. 20C, right panels of each cell line).

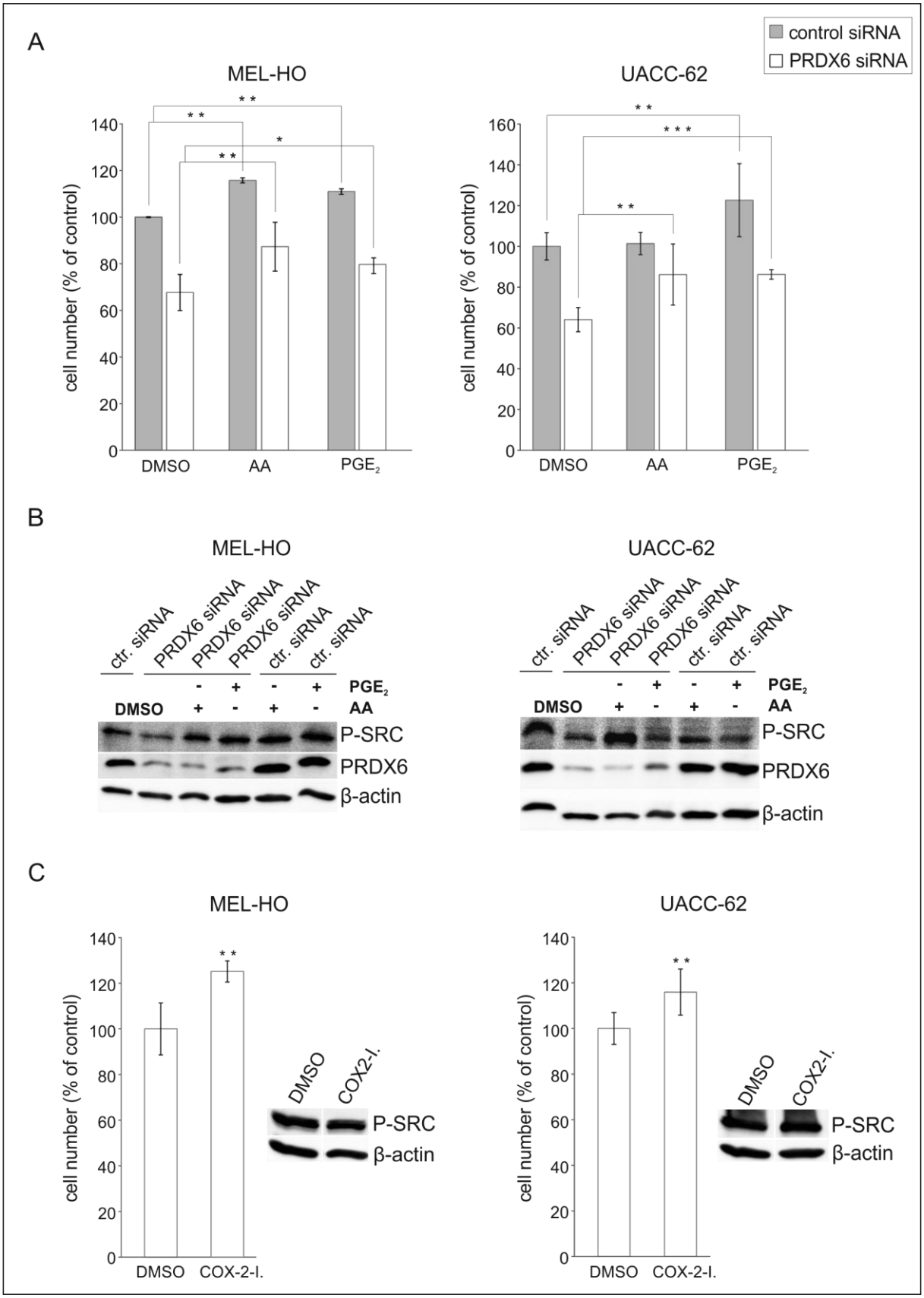

Figure 20: Effect of AA and PGE_2 on melanoma cell proliferation. A, B: MEL-HO and UACC-62 cells were transfected with control siRNA and siRNA targeting *PRDX6*. 24 h later, cells were seeded into 6-well dishes (MEL-HO: $5x10^4$ cells/well and UACC-62: $6.5x10^4$ cells/well). 6 h after seeding, cells were treated with AA (10 µM), PGE_2 (5 µM) or DMSO as control. 48 h later, medium was changed and the treatment was repeated. After additional 48 h, cells were harvested for manual counting and protein blot analysis. Bar diagrams demonstrate percentage of counted cells in response to AA and PGE_2 administration compared to control (set as 100%) (**A**). Error bars present

SD of two independent experiments (*: p<0.05; **: p<0.01; ***: p<0.001) performed in triplicates. Corresponding western blots show PRDX6 and P-SRC family kinase levels **(B). C:** MEL-HO and UACC-62 cells were seeded into 6-well dishes (MEL-HO: $6x10^4$ cells/well; UACC62 $8x10^4$ cells/well). After 6 h, cells were treated with COX-2 inhibitor (COX-2-I.; 80 µM). DMSO was used as control. 48 h later, the medium was replaced and inhibitor administration was repeated. Additional 48 h later, cells were counted manually and analyzed by protein blot. Bar graphs show the percentage of counted cells in response to COX-2 inhibition (**left panels**) compared to DMSO treatment (set as 100%). Error bars represent SD of three independent experiments (**: p<0.01) performed in triplicates. Western blot analyses demonstrate the levels of activated SRC family kinases (**right panels**). β-actin served as loading control (**B and C**).

These data indicate that in melanoma COX-2 has no effect on SRC family kinase activity and even displays an anti-proliferative function, probably due to other, PGE_2-independent effectors which are generated by the enzyme.

In summary, the results show that SRC family kinase activation and the pro-proliferative function of PRDX6 in melanoma cells is mainly mediated by AA.

6. Discussion

Research and understanding of cellular processes promoting melanoma formation and progression are indispensable steps for the development of effective therapies. Particularly, the ongoing detection of new proteins as useful melanoma targets is of great interest. In the present study, I demonstrated a pro-tumorigenic function of PRDX6 in human melanoma cells, mainly mediated via its $iPLA_2$ activity.

6.1 PRDX6 in other tumor entities

Until now, the function of PRDX6 in cancer is controversially discussed, and there are examples of pro- and anti-tumorigenic features of this protein. The serum from patients with lung squamous carcinoma (Zhang et al. 2009) as well as tissue and serum of breast cancer patients (F.-J. Liu et al. 2014) were shown to contain elevated levels of PRDX6 compared to the respective healthy subjects. In line with these observations, overexpression of the enzyme was shown to enhance the metastatic potential of breast and lung cancer cells (Chang et al. 2007; Lee et al. 2009). In contrast tumor size and lymph node metastasis of papillary thyroid carcinomas are inversely correlated with PRDX6 expression (Nicolussi et al. 2014). Therefore, a tumor-promoting function of PRDX6 seems to depend on both, the tumor type and the stage of tumor development. Depletion of PRDX6 from keratinocytes enhanced HPV-8- or chemically induced skin carcinogenesis in mice. Contrary, HPV-8 induced skin cancer in these animals could be prevented via PRDX6 overexpression in keratinocytes, an effect that was accompanied by decreased levels of oxidized lipids (Rolfs et al. 2013). This observation suggests that PRDX6 prevents the accumulation of oxidative damage and thereby impedes the early steps of tumorigenesis. However, overexpression of PRDX6 promoted the malignant conversion of existing tumors (Rolfs et al. 2013).

6.2 Analysis of PRDX6 levels and its regulation in melanocytes and melanoma cells

One goal of my study was to achieve insights into the regulation of PRDX6. There exist different mechanisms of PRDX6 regulation, and most publications describe the transcriptional regulation of the corresponding gene. In many cell types, oxidative stress is a potent inducer of PRDX6 expression. In rat lung epithelial cells treated with H_2O_2 as well as rat lungs exposed

to hyperoxia, PRDX6 mRNA and protein expression was strongly enhanced (Kim et al. 2003). Chowdhury and colleagues demonstrated that in human lung cancer cells, the ROS-stimulated gene expression of *PRDX6* is transcriptionally mediated trough an antioxidant response element (ARE), which is located in the promoter region of the enzyme. This ARE is also responsible for the regulation of basal *PRDX6* gene transcription (Chowdhury et al. 2009). In contrast, I found that in human melanocytes and melanoma cells, PRDX6 was mainly regulated on post-transcriptional level, and enhanced oxidative stress did not influence the level of PRDX6 protein.

I identified the EGFR as potent inducer of PRDX6 protein expression, with contribution of the PI3K pathway. In ovarian or epidermoid carcinoma cells, activation of EGFR results in the generation of H_2O_2 (Bae et al. 1997; Liu et al. 2006) and also HERmrk (Leikam et al. 2014; Leikam et al. 2008) or PI3K signaling (Meierjohann 2014) are potent inducers of oxidative stress. However, via studies with ROS scavengers in HERmrk cells, I could demonstrate that the EGF-mediated PRDX6 induction is independent of oxidative stress. Still, ROS can lead to activation of EGFR signaling (Takeyama et al. 2000). Thus, in melanoma cells which are prone to high levels of oxidative stress (Meierjohann 2014), an involvement of ROS in the regulation of PRDX6 expression cannot completely be excluded, even though additional oxidative stress did not alter the overall PRDX6 protein level. Instead, I observed an increase in the level of hyperoxidated PRDX6 in melanocytes and melanoma cells. This indicates a ROS-detoxifying activity, as hyperoxidation of PRDX6-C47 to a sulfonic state (C-SO_3H) is only possible when the peroxidase of PRDX6 is active (Peshenko & Shichi 2001).

Another growth factor described to be involved in the regulation of PRDX6 is the keratinocyte growth factor (KGF) (Gallagher & Phelan 2007). In dermal epithelium (Frank et al. 1997) as well as in mouse liver cells (Gallagher & Phelan 2007) KGF was shown to induce *Prdx6* transcription which seems to be mediated through protein kinase C (PKC) and/or mitogen-activated protein kinase ERK1/2 signaling. PKC can also be activated by PI3K signaling (Frey et al. 2006), and in the present study, I demonstrated that the PI3K is also involved in the protein expression of PRDX6. Furthermore, PI3K-AKT and MAPK signaling pathways are involved in the activation of different transcription factors like c-JUN and c-MYC. Binding sites for these two factors are located in the *Prdx6* promoter region (Lee et al. 1999).

6.3 The function of PRDX6 in human melanoma cells

In my study, I found that the PRDX6 protein is localized throughout the cell. Surprisingly, this also includes the nucleus. The precise reason for the nuclear localization is still not known. Kim and colleagues already demonstrated a predominant nuclear localization of hyperoxidated PRDX6 in HeLa cells (Kim et al. 2008). I made similar observations in human melanoma cells as well as NHEM cells. Hyperoxidation of PRDX6 is an irreversible process and can be used as indicator for hyperoxidative stress (Kim et al. 2008). Therefore, endogenous oxidative stress might have led to the observed generation of PRDX6-SO_3 under control conditions. There are various sources of ROS in pigment cells. In melanocytes, the synthesis of melanin is a biochemical process leading to the generation of H_2O_2 (Meyskens et al. 1999) and also melanoma cells have been reported to produce large amounts of hydrogen-peroxide (Ibañez et al. 2011)

In the present study, knockdown of PRDX6 enhanced the sensitivity towards H_2O_2 treatment and therefore demonstrated a functional role of PRDX6-peroxidase activity in melanoma cell proliferation under stressed conditions. However, under normal conditions, the peroxidase function of PRDX6 did not play a role in human melanoma cells. Contrary results were obtained from lung cancer cells. Here, the PRDX6-peroxidase is required for growth under normal conditions (Ho et al. 2010). In addition, *Prdx6* knockout mice revealed increased lung injury and mortality in response to hyperoxia (Wang et al. 2003). The conflicting results might be explained by a different ROS-dependent signaling in melanoma and lung cancer cells.

Instead of the peroxidase activity, I identified the $iPLA_2$ activity of PRDX6 as proliferation driver in melanoma cells. Phospholipases play an important role in the metabolism of phospholipids, and alterations of these enzymes are linked to metabolic diseases like diabetes, obesity and cancer (Hu et al. 2013). Metabolic alterations and adaptions of cancer cells have been extensively studied. The dysregulation of metabolic pathways enables cancer cells to achieve autonomous proliferation and survival (reviewed in Tennant et al. 2010). Oncogenes like EGFR, PI3K, MAPK, p53 and c-MYC are upstream of lipid metabolic pathways and their signals promote the expression and activity of enzymes playing a role in fatty acid synthesis (reviewed in Cairns et al. 2011). As an example, the expression of fatty acid synthase (FASN) is controlled via the PI3K-AKT and MAPK pathways and is mediated by the master regulator of fatty acid metabolism, SREBP-1 (sterol regulatory element-binding protein-1) (Krycer et al. 2010; Yang et al. 2002), which is suggested to be a promising target for cancer therapy (Guo et al. 2014). In glioblastoma nude mouse xenografts, SREBP-1 promoted cancer growth and survival (Griffiths et al. 2013). Interestingly, PRDX6 also contains a SREBP-1 binding element in its promoter region. As the $iPLA_2$ activity renders PRDX6 capable of releasing arachidonic

acid (AA) from phospholipids, the enzyme takes also part in lipid metabolism. Therefore, it would not be surprising if SREBP-1, which promotes also the transcription of the $iPLA_2\beta$ enzyme (Lei et al. 2010), is involved in the regulation of PRDX6.

Together with their downstream produced metabolites, PLA_2 have been shown to play important roles in the regulation of cell proliferation and migration as well as inflammation (reviewed in Scott et al. 2010; Wang & Dubois 2010). In human melanoma cells, a high level of $iPLA_2$ is associated with high proliferation (Scuderi et al. 2008). Consistent with this report, I could demonstrate that the inhibition of Ca^{2+}-independent phospholipases by bromoenol-lactone profoundly reduced the proliferation of melanoma cells. The finding that the $iPLA_2$ activity of PRDX6, among all other enzymes with $iPLA_2$ activity, has a major contribution on melanoma cell growth, was rather surprising. There exist several Ca^{2+}-independent phospholipases which belong to one main type of the PLA_2 superfamily (reviewed in Schaloske & Dennis 2006). For $iPLA_2\beta$, a role in breast cancer was reported previously. In studies with $iPLA_2\beta$-knockout mice, McHowat and colleagues demonstrated that depletion of endothelial cell $iPLA_2\beta$ prevents breast cancer metastasis to the lung (McHowat et al. 2011).

The $iPLA_2$ activity of PRDX6 was shown to promote invasion of lung cancer cells via the release of AA (Ho et al. 2010). In the present study, I identified AA as the main mediator of the PRDX6-growth-promoting function in human melanoma cells. I could demonstrate that the proliferative function of PRDX6-derived AA was mediated by SRC family kinases. A proliferative effect of AA in melanoma cells was also observed by He and colleagues. Via the use of B16 melanoma cells subcutaneously injected into C57BL6 mice, the group reported that inhibition of delta 6 desaturase, which is the rate limiting enzyme in the production of AA, suppresses melanoma growth as well as inflammation and angiogenesis (He et al. 2012).

Arachidonic acid is the major prerequisite for the development of prostaglandins, leukotriens and hydroxyeicosatetraenoic acids via the COX, LOX and EPOX pathway, respectively (reviewed in Harizi et al. 2008). The activity of COX-2 and 12/15-lipoxygenase (12/15-LOX) has been described to positively influence melanoma progression. COX-2 is strongly expressed in melanoma and the expression level was shown to correlate with tumor thickness (Becker et al. 2009; Minisini et al. 2013). Studies performed with human (Scuderi et al. 2008) and murine (Tabolacci et al. 2010) melanoma cells as well as human uveal melanoma cells (Marshall et al. 2007) demonstrated a proliferative function of COX-2 whereas others completely excluded a role of COX-2 in melanoma growth (Bachi et al. 2009). The enzyme mediates the production of several metabolites including PGE_2, which binds and activates four G-protein-coupled receptors, EP1 to EP4. Their stimulation leads to the activation of different

signaling pathways that are involved in survival, proliferation, angiogenesis and invasion (reviewed in Rundhaug et al. 2011). Inhibition of COX-2, PGE_2 and PGE_2 receptors via berberine, green tea catechin and grape seed proanthocyanidins provokes the suppression of melanoma cell invasion and migration (Singh et al. 2011; Singh & Katiyar 2011; Vaid et al. 2011), which confirms an important role of PGE_2 in melanoma metastasis. In squamous cell carcinoma and endometrial adenocarcinoma cells, PGE_2 was shown to transactivate the cancer growth-promoting EGFR signaling pathway via binding to the EP2 receptor (Donnini et al. 2007; Sales et al. 2004). This EGFR pathway stimulation seems to be dependent on c-SRC and protein kinase A (PKA) activity, as their inhibition prevents the PGE_2/EP2-mediated phosphorylation of EGFR (Donnini et al. 2007). Yamaki and colleagues also demonstrated a PGE_2 mediated activation of SRC kinase signaling, which promotes the growth of lung cancer cells (Yamaki et al. 2004).

In the present study, PGE_2 revealed a pro-proliferative effect and was able to partially rescue reduced melanoma cell growth of MEL-HO and UACC-62 cells as well as SRC family kinase activity of MEL-HO, but not UACC-62 cells after knockdown of *PRDX6*. However, rather than blocking proliferation, inhibition of COX-2 increased the proliferation in melanoma cells. This is most likely attributed to the fact that other, possibly anti-proliferative metabolites are produced by COX-2 in addition to PGE_2. It was reported that some pro-migratory effects can inhibit proliferation (Ampuja et al. 2013) and therefore, some products of COX-2 might have pro-tumorigenic effects in melanoma even if they suppress proliferation. However, irrespective of the observed PGE_2-effect, my data indicate that COX-2 is not involved in the growth-promoting function of PRDX6-$iPLA_2$ in melanoma cells.

The 12/15-LOX pathway mediates the production of 12(S)-HETE and 15(S)-HETE from AA. Both are able to increase melanoma cell adhesion or metastasis, e.g. via activation of ERK and focal adhesion kinase (FAK) signaling, as described in case of 12(S)-HETE (Kang et al. 2013). Like PGE_2, 12(S)-HETE also binds to a G protein coupled receptor, leading to the stimulation of various signaling molecules including SRC kinase (Guo et al. 2011; Reddy et al. 2009; Szekeres et al. 2000). A similar mechanism is probably responsible for PRDX6-dependent SRC family kinase activation in melanoma and might also be involved in the growth-promoting effect of the enzyme.

In the biology of melanoma, SRC family kinases play an important role as their activity is involved in proliferation, invasion and transendothelial migration (reviewed in Homsi et al. 2007). By the use of a SRC family kinase specific inhibitor, I could confirm their growth-promoting function in human melanoma cells. SRC family kinases enhance the

activation of ERK1/2, which is highly relevant for melanoma growth. Furthermore, they are also required for the expression of several transcriptional targets downstream of ERK1/2 (Teutschbein et al. 2010; Wellbrock et al. 2002).

Interestingly, a decline in the level of 12-HETE was reported to decrease the level of p-Rb-protein (Yang et al. 2007). The retinoblastoma protein (Rb) is an important tumor suppressor playing a central role in the regulation of cell proliferation. In the majority of human cancers, this protein is functionally inactivated (reviewed in Knudsen & Knudsen 2008). Rb binds to E2F transcription factors and represses their transcriptional activity. Phosphorylation of the tumor suppressor via the activity of cyclin-dependent kinase 4 (CDK4) and 6 (CDK6) impedes the target binding and enables E2F to activate the transcription of S phase promoting genes (reviewed in Chen et al. 2009 and Giacinti & Giordano 2006). Zhang and colleagues demonstrated that BEL-induced inhibition of $iPLA_2$ activity provokes inhibition of the cyclin-E/CDK2 activity, which results in the persistence of the Rb-E2F complex and a cell cycle arrest in the G1 phase (Zhang et al. 2006). In my studies, I similarly revealed an $iPLA_2$- as well as PRDX6-dependent phosphorylation of the Rb protein, assuming a comparable mechanism in melanoma cells.

6.4 PRDX6 - a target for melanoma therapy?

The current knowledge about melanoma has led to the development of various therapeutic strategies. Targeted as well as immunologic therapies have successfully found their way into the clinic (reviewed in Tronnier & Mitteldorf 2014; Lo & Fisher 2014). However, side effects and the development of melanoma resistance make it necessary to achieve better combined therapies and to find new effective anti-cancer targets.

The fact that inhibition of the PRDX6-$iPLA_2$ activity impairs melanoma cell growth poses an interesting therapeutic option. Due to their carcinogenic potential, PLA_2 isoforms are discussed as anticancer targets (Cummings 2007). Inhibition of $iPLA_2$ was already shown to decrease the growth of prostate cancer cells in vitro (Sun et al. 2008) and knockdown of group II secretory phospholipase A2 ($sPLA_2$) reduces lung cancer growth in vivo and in vitro (Yu et al. 2012). For the treatment of atherosclerosis, inhibitors of the PLA_2 family members soluble PLA_2 ($sPLA_2$) and lipoprotein-associated PLA_2 ($IpPLA_2$) have already been developed and are tested in clinical trials (reviewed in Rosenson & Hurt-Camejo 2012).

The involvement of PRDX6 in the activation of SRC family kinases also emphasizes its inhibition as possible strategy to treat cancer. In preclinical studies, SRC inhibitors were shown to execute promising anti-melanoma effects (Buettner et al. 2008; Ferguson et al. 2013) and also clinical studies have already shed a positive light on the inhibition of SRC kinases in cancer. A clinical phase II trial on non-small cell lung cancer (NSCLC) patients revealed that the SRC inhibitor dasatinib led to prolonged stable disease (Johnson et al. 2010). In a phase II trial with patients suffering from metastatic melanoma, the combined use of dasatinib with the chemotherapeutic drug dacarbazine, showed a clinical benefit rate of 59,2% (Puls et al. 2011).

SRC family kinase inhibition was furthermore shown to overcome BRAF inhibitor resistance in melanoma (Girotti et al. 2013; Vergani et al. 2011). Thus, through the regulation of SRC family kinase activity, PRDX6 might also contribute to resistance development. Preliminary data from the present study, obtained by the use of melanoma cells resistant to the BRAF inhibitor vemurafenib, gave first insights into this hypothesis. Data from Jhang Ho Pak and colleagues suggests that inhibition of PRDX6 also sensitizes cancer cells to ROS-producing therapeutic treatments. The authors showed that overexpression of PRDX6 diminished cisplatin-induced apoptosis in ovarian cancer cells (Pak et al. 2011).

6.5 Concluding remarks

In the present study, I clearly demonstrated a crucial role of $iPLA_2$ in the cell growth of human melanoma cells. In view of the fact that there exist a lot of different PLA_2 family members, which are able to mediate the release of AA, it is very interesting that the $iPLA_2$ activity of PRDX6 alone can display such a strong effect on AA release and cell proliferation. By the action of multiple enzymes, AA is processed into different metabolites, many of which are potent inducers of cancer cell growth and proliferation in vitro (Cummings 2007). Therefore, inhibition of PRDX6 might be a possible anti-cancer strategy.

Based on existing studies, the obtained data suggest that downstream of PRDX6-$iPLA_2$ activity, specific AA metabolites might mediate SRC family kinase activation and thereby influence the proliferation of melanoma cells. A possible model of the PRDX6 signaling cascade, which summarizes a part of the present results, is shown in Figure 21.

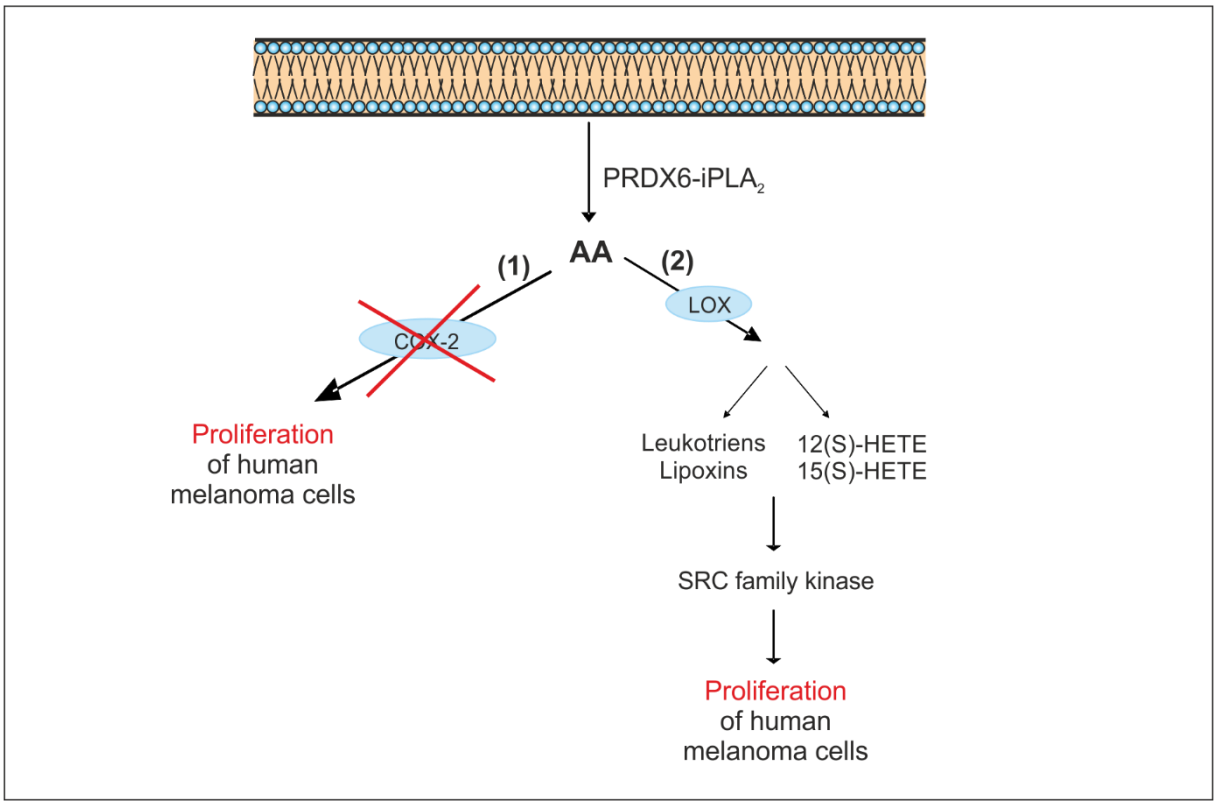

Figure 21: Model of PRDX6 signaling in human melanoma cells. The $iPLA_2$ activity of PRDX6 regulates the level of released AA and thereby the proliferation of human melanoma cells. **(1)** Processing of AA via COX-2 is not involved in the PRDX6-mediated effect on melanoma cell proliferation. **(2)** The activity of LOX mediates the production of AA-metabolites like HETEs. Downstream of PRDX6-$iPLA_2$ activity, some of these metabolites might activate SRC family kinases and thereby stimulate melanoma cell proliferation.

My data provide a rationale for future studies of the effect of PRDX6 inhibition on the metastatic potential of melanoma cells and tumor maintenance as well as the combination of PRDX6 inhibition with known anti-cancer drugs.

7. Appendix

7.1 Role of PRDX6 in manipulating melanoma resistance to vemurafenib

In addition to regulating proliferation of normal melanoma cells, SRC family kinases are involved in melanoma resistance to the BRAF inhibitor vemurafenib (PLX4032) (Girotti et al. 2013). Since knockdown of *PRDX6* leads to decreased levels of activated SRC family kinases, I was interested in testing whether PRDX6 can also influence melanoma resistance to PLX.

PLX-resistant 451Lu melanoma cells were transfected with siRNA against *PRDX6* and were treated with PLX4032. Western blot analysis determined that the activation of SRC family kinases was almost completely suppressed by knockdown of *PRDX6* (Fig. 22A). In contrast, cells transfected with control siRNA exhibited a very high level of P-SRC family kinases independent of DMSO or PLX4032 administration. With regard to the proliferation of PLX-resistant 451Lu cells, it could be noted that PLX4032 treatment increased the proliferation by 67% compared to DMSO control. This PLX4032-induced cell growth could be prevented by siRNA-mediated knockdown of *PRDX6*, which reduced the proliferation by 26% below control level (Fig. 22B).

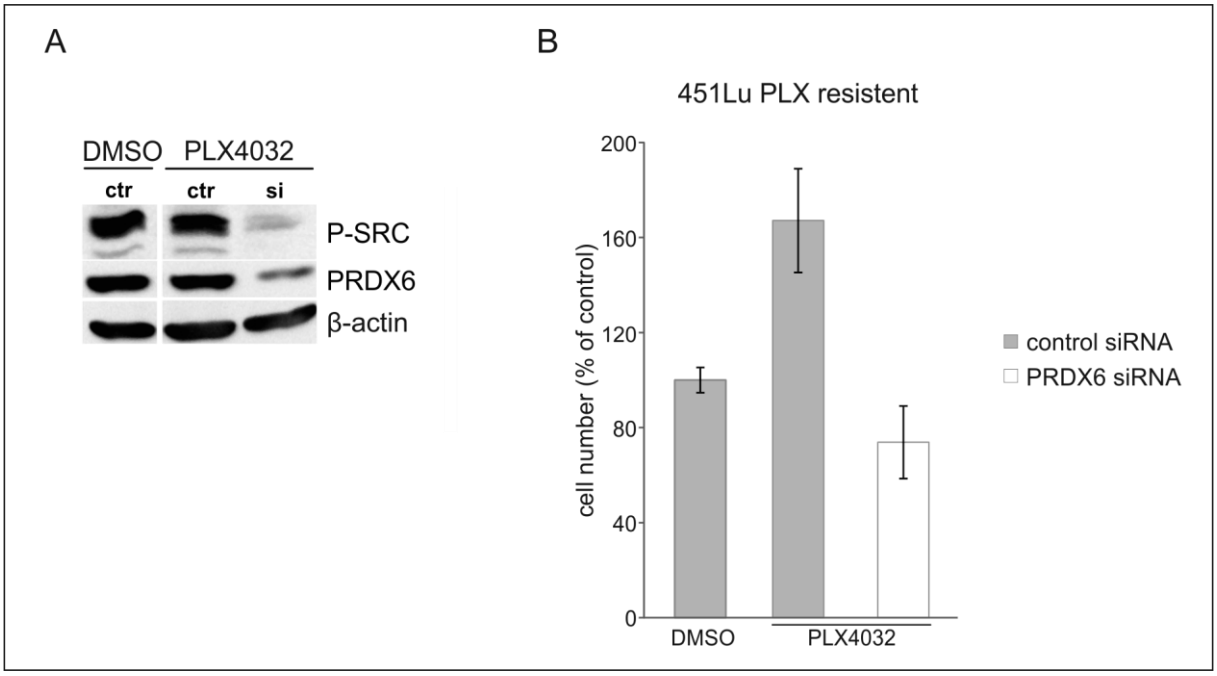

Figure 22: Effect of PRDX6 in PLX resistant 451Lu melanoma cells. 24 h after transfection with control and *PRDX6*-specific siRNA, 451Lu cells were seeded into 6-well dishes (6x10^4 cells/well). 6 h later they were treated with vemurafenib (=PLX4032) (0.5µM) or DMSO as control. The treatment was repeated 48 h later. After additional 48 h, cells were counted manually and analyzed by Western blot. **A:** Western blot showing PRDX6 and activated SRC family kinase levels. β-actin served as loading control. **B:** Proliferation analyzed via manual cell counting. Bar

graphs represent relative number of cells in response to PLX4032 compared to DMSO administration, the latter being set as 100%. Error bars represent SD of a single experiment performed in triplicates.

These data show that decreased PRDX6 protein levels reduce the growth advantage of melanoma cells resistant to vemurafenib. However, a strong sensitization to the BRAF inhibitor was not detected.

7.2 Microarray

To investigate whether PRDX6 is indirectly involved in the regulation of gene expression, control and *PRDX6*-specific siRNA were introduced into MEL-HO cells. Three days later, microarray analysis was performed by Dr. Claus Jürgen Scholz (Microarray Core Unit; IZKF, University of Würzburg) using Affymetrix® Human Gene 2.1 ST Array and data were processed by Dr. Susanne Kneitz (Physiological Chemistry, University of Würzburg). The following heat map shows the regulation of genes influenced via knockdown of PRDX6 (Fig. 23).

DDX46	1,237	USP6NL	0,768	CGB1	-0,832	NRP1	-1,007
KRTAP5-2	1,170	GABRG1	0,768	TEX13A	-0,839	TLE2	-1,014
PRDX6	1,093	OR5L2	0,766	C20orf173	-0,840	MST1	-1,018
PABPC1L2B	1,043	ORM2	0,764	ACTA1	-0,842	SRD5A2	-1,027
CDY2A	1,031	SLC38A2	0,763	CELA2A	-0,846	TREML5P	-1,030
MDC1	1,030	OR51G2	0,760	ZGPAT	-0,850	HBA1	-1,036
CD163L1	0,980	GOLGA8DP	0,756	EAF2	-0,853	SLC7A10	-1,043
TRBV5-4	0,898	FAM48B2	0,755	AZGP1P1	-0,853	BRWD1-IT1	-1,074
ANKRD36	0,897	OR56B1	-0,755	OR5A2	-0,854	RPS15AP10	-1,077
BCAT1	0,889	FCGR2B	-0,761	ACAT2	-0,856	IGHV3-72	-1,083
CCZ1B	0,889	ZNF525	-0,765	CRNN	-0,857	PAPPA	-1,120
CLEC4M	0,878	SIGLEC17P	-0,772	CGB7	-0,859	CIC	-1,131
TOB2	0,872	KIAA1199	-0,773	IRF9	-0,873	PLCD1	-1,139
IGBP1P1	0,869	HIST1H2BD	-0,774	LRRC37A4P	-0,874	OR2M5	-1,150
NT5DC1	0,866	SAMD15	-0,778	PTX3	-0,875	KRT75	-1,214
OR2L8	0,852	FCGR3A	-0,786	ADAM19	-0,881	ZNF280A	-1,280
RPL13A	0,839	IGLV3-10	-0,786	ANK3	-0,886	REP15	-1,280
ANKRD54	0,838	SERPINA3	-0,786	HIST2H4B	-0,887	TAS2R19	-1,280
DPY19L1P1	0,837	ZNF736	-0,787	FAM18B1	-0,889	OR2V1	-1,280
GOLT1A	0,837	SLC26A1	-0,787	PRB3	-0,901	PAEP	-1,294
ZNF461	0,831	ITGA11	-0,787	PCDHB14	-0,901	ZNF208	-1,299
CYP1A1	0,829	IL36G	-0,793	IL6	-0,902	ARRDC4	-1,354
IGKV1D-17	0,824	TIRAP	-0,811	MAPK12	-0,921	DEFB118	-1,502
PAQR4	0,822	PDPK1	-0,811	ZNF285	-0,939	SPANXN2	-1,535
ZNF737	0,821	TRBV3-1	-0,813	CCL11	-0,949	KRTAP9-7	-1,543
ZNF266	0,817	RACGAP1P	-0,818	PCDH11X	-0,978	CETN3	-1,577
OR2G6	0,801	SLC2A14	-0,821	PGM5	-0,989	PRAMEF23	-1,617
MTRNR2L2	0,799	ORM1	-0,822	NAPSB	-0,995	TARM1	-1,687
PCDHB12	0,782	DHRSX	-0,824	OR1F1	-0,997	SLC9A7	-1,903
RNF144B	0,773	MEOX2	-0,831	SCGN	-1,003	LGR5	-1,972

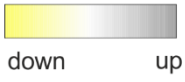

Figure 23: Heat map of gene regulation (log fold change ≥ 0,75). Data present individual values of gene regulation after siRNA-mediated knockdown of *PRDX6* in MEL-HO cells. In yellow-grey log fold changes are shown. Genes marked in red were chosen for validation.

The expression of the genes *PDPK1*, *MAPK12*; *PLCD1* and *TOB2*, described in the following, were chosen for validation.

The downregulated *PDPK1* gene encodes for the 3-phosphoinositide-dependent protein kinase-1 (PDK1) which promotes full activation of AKT, but is also involved in regulation of the MAPK pathway. In melanoma and colon cancer cells containing BRAF or NRAS mutations, knockdown of *PDK1* decreases proliferation and induces apoptosis (Lu et al. 2010). Genetic evidence for an important role of PDK1 in melanoma development and progression was provided by Scortegagna and colleagues. The authors demonstrated that genetic *Pdk1* inactivation strongly inhibited metastasis and prolonged the onset of melanoma in mouse melanoma models driven by melanocytic expression of $Braf^{V600E}$ and *Pten* deletion (Scortegagna et al. 2014).

MAPK12, also called p38γ, is one isoform of the p38 MAP kinases which are strongly activated by pro-inflammatory cytokines, tumor necrosis factor α (TNFα) and environmental stress. They are involved in cellular processes like differentiation, proliferation and survival (reviewed in Nebreda & Porras 2000). In melanoma cells, p38γ is particularly implicated in cell death induced via UV radiation and cisplatin treatment (Pillaire et al. 2000). Together with its upstream kinase MAPK kinase 3 (MKK3), p38γ is strongly increased in transgenic melanoma cells overexpressing platelet-derived growth factor receptor α (PDGF-Rα). Compared to normal skin, *PDGF-Rα* gene expression was shown to be reduced in human melanoma biopsies. Overexpression of this receptor strongly impairs melanoma growth in vivo and in vitro, an effect presumably mediated through upregulation of active p38γ (Faraone et al. 2009). However, the present microarray data indicate a downregulation of *MAPK12* in melanoma cells after knockdown of *PRDX6*. In glioma (K. Yang et al. 2013) and breast cancer cells (Meng & Wu 2013), knockdown of p38γ decreases proliferation.

Interestingly, knockdown of PRDX6 reduced the expression of *PLCD1* which encodes for the phospholipase C delta 1 (PLCδ1). This enzyme hydrolyzes phosphatidylinositol-4,5-bisphosphate to produce the second messengers inositol-1,4,5-trisphosphate (IP_3) and diacylglycerol (DAG). DAG activates protein kinase C (PKC) and IP_3 promotes Ca^{2+} release from intracellular stores, which mediate several cellular processes like proliferation and motility. Surprisingly, *PLCD1* was indentified as tumor suppressor that is frequently deleted in oesophageal squamous cell carcinomas (ESCCs), and reduced expression of PLCδ1 correlates with poor prognosis in patients with acute or chronic myeloid leukaemia. In contrast, other phospholipase C enzymes were shown to play important roles in cancer cell invasion and metastasis (reviewed in Park et al. 2012). Inhibition of PLCγ2 impairs cancer cell growth

in the melanoma cell line MDA-MB-435 and in other cancer cells of the NCI60 panel of human tumor cell lines (Feng et al. 2012).

According to the microarray data, one of the genes whose expression was upregulated after reduced PRDX6 protein levels is *TOB2*. The TOB2 protein belongs to a family of anti-proliferative proteins and is the transducer of the human epidermal growth factor receptor 2 (HER2). Via inhibition of G0/G1-S-phase transition, TOB2 is involved in the regulation of cell cycle progression (Ikematsu et al. 1999). In vivo and in vitro studies from Liu and colleagues revealed that in a variety of cancer cells including melanoma, upregulation of *TOB2* is involved in the anti-proliferative action of S115, a heteroaromatic thiosemicarbazone compound which induces cell cycle arrest in the G0-G1 phase and apoptosis (M. Liu et al. 2014).

Like PRDX6, PDK1, p38γ, PLCδ1 and TOB2 display functions involved in regulating cellular proliferation. However, the precise reason for PRDX6-mediated regulation of their expression is not clear. Preliminary validation of the microarray data is presented in figure 24. MEL-HO cells revealed a downregulation of all genes after siRNA-mediated knockdown of *PRDX6*. In contrast, *PLCD1* and *PDPK1* seemed to be upregulated in the UACC-62 cells line. Here, a regulation of *MAPK12* and *TOB2* was not observed.

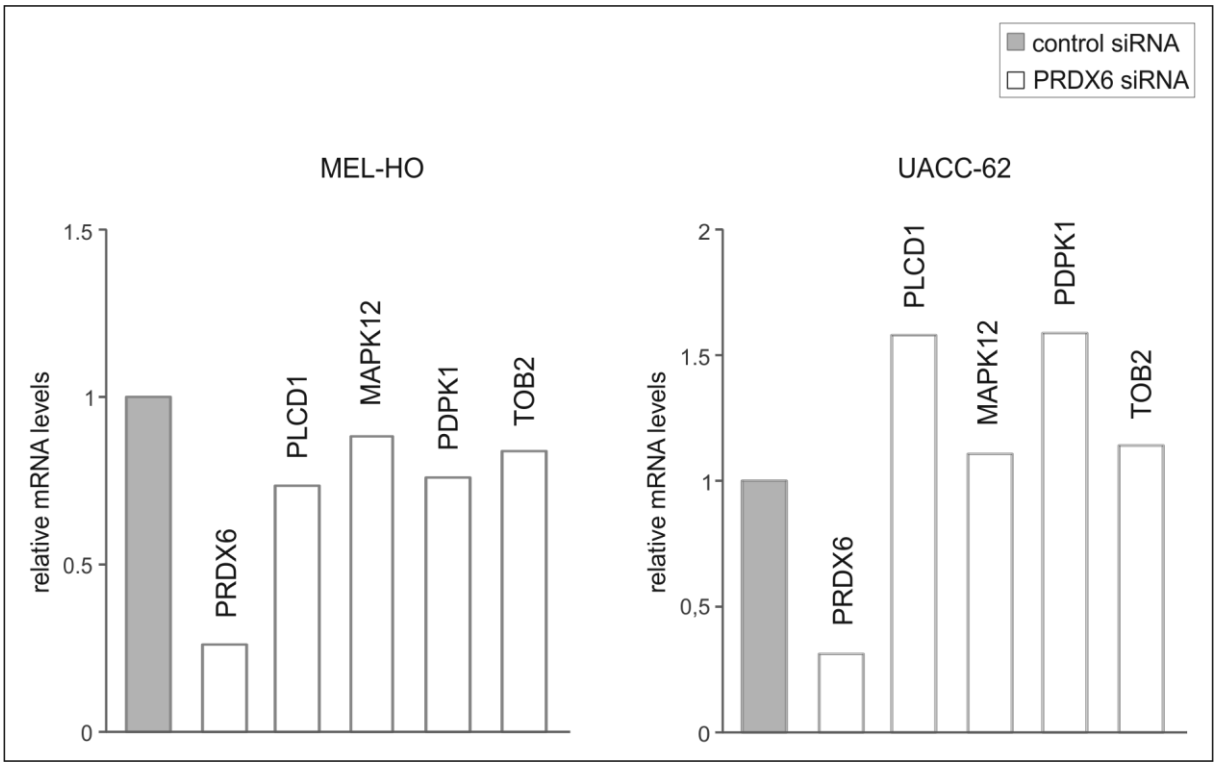

Figure 24: Validation of genes regulated by PRDX6. MEL-HO and UACC-62 cells were transfected with control and *PRDX6*-specific siRNA. Three days later cells were harvested and relative mRNA expression levels of *PRDX6*, *PLCD1*, *MAPK12*, *PDPK1* and *TOB2* were analyzed. Expression levels were normalized to RSP14. One single experiment was performed for each cell line.

8. Bibliography

Akiba, S. et al., 1998. Characterization of acidic Ca^{2+}-independent phospholipase A_2 of bovine lung. *Comparative biochemistry and physiology. Part B, Biochemistry & molecular biology*, 120(2), pp.393–404.

Ampuja, M. et al., 2013. BMP4 inhibits the proliferation of breast cancer cells and induces an MMP-dependent migratory phenotype in MDA-MB-231 cells in 3D environment. *BMC cancer*, 13(429).

Bachi, A.L.L. et al., 2009. Leukotriene B4 creates a favorable microenvironment for murine melanoma growth. *Molecular cancer research : MCR*, 7(9), pp.1417–24.

Bae, Y.S. et al., 1997. Epidermal growth factor (EGF)-induced generation of hydrogen peroxide. Role in EGF receptor-mediated tyrosine phosphorylation. *The Journal of biological chemistry*, 272(1), pp.217–21.

Becker, M.R. et al., 2009. COX-2 expression in malignant melanoma: a novel prognostic marker? *Melanoma research*, 19(1), pp.8–16.

Bennett, D.C., 2008. How to make a melanoma: what do we know of the primary clonal events? *Pigment cell & melanoma research*, 21(1), pp.27–38.

Bertolotto, C. et al., 1998. Different cis-acting elements are involved in the regulation of TRP1 and TRP2 promoter activities by cyclic AMP: pivotal role of M boxes (GTCATGTGCT) and of microphthalmia. *Molecular and cellular biology*, 18(2), pp.694–702.

Boone, B. et al., 2011. EGFR in melanoma: clinical significance and potential therapeutic target. *Journal of cutaneous pathology*, 38(6), pp.492–502.

Brar, S.S. et al., 2001. Reactive oxygen species from NAD(P)H:quinone oxidoreductase constitutively activate NF-kappaB in malignant melanoma cells. *American journal of physiology. Cell physiology*, 280(3), pp.C659–76.

Brash, a. R., 1999. Lipoxygenases: occurrence, functions, catalysis, and acquisition of substrate. *The Journal of biological chemistry*, 274(34), pp.23679–82.

Buettner, R. et al., 2008. Inhibition of Src family kinases with dasatinib blocks migration and invasion of human melanoma cells. *Molecular cancer research : MCR*, 6(11), pp.1766–74.

C.Kosswig, 1928. Über Kreuzungen zwischen den Teleostiern Xiphophorus Helleri und Platypoecilus maculatus. *Zeitschrift für Induktive Abstammungs- und Vererbungslehre*, 47(1), pp.150–158.

Cairns, R. a, Harris, I.S. & Mak, T.W., 2011. Regulation of cancer cell metabolism. *Nature reviews. Cancer*, 11(2), pp.85–95.

Carnero, A., 2010. The PKB/AKT pathway in cancer. *Current pharmaceutical design*, 16(1), pp.34–44.

Carvajal, R.D. et al., 2011. KIT as a therapeutic target in metastatic melanoma. *JAMA : the journal of the American Medical Association*, 305(22), pp.2327–34.

Chang, X.-Z. et al., 2007. Identification of the functional role of peroxiredoxin 6 in the progression of breast cancer. *Breast cancer research : BCR*, 9(6), p.R76.

Cheli, Y. et al., 2011. Mitf is the key molecular switch between mouse or human melanoma initiating cells and their differentiated progeny. *Oncogene*, 30(20), pp.2307–18.

Chen, H.-Z., Tsai, S.-Y. & Leone, G., 2009. Emerging roles of E2Fs in cancer: an exit from cell cycle control. *Nature reviews. Cancer*, 9(11), pp.785–97.

Chen, J.W. et al., 2000. 1-Cys peroxiredoxin, a bifunctional enzyme with glutathione peroxidase and phospholipase A_2 activities. *The Journal of biological chemistry*, 275(37), pp.28421–7.

Chiaverini, C. et al., 2008. Microphthalmia-associated transcription factor regulates RAB27A gene expression and controls melanosome transport. *The Journal of biological chemistry*, 283(18), pp.12635–42.

Chin, L., Garraway, L. a & Fisher, D.E., 2006. Malignant melanoma: genetics and therapeutics in the genomic era. *Genes & development*, 20(16), pp.2149–82.

Choi, H., Chang, J.-W. & Jung, Y.-K., 2011. Peroxiredoxin 6 interferes with TRAIL-induced death-inducing signaling complex formation by binding to death effector domain caspase. *Cell death and differentiation*, 18(3), pp.405–14.

Choi, H.J. et al., 1998. Crystal structure of a novel human peroxidase enzyme at 2.0 A resolution. *Nature structural biology*, 5(5), pp.400–6.

Chowdhury, I. et al., 2009. Oxidant stress stimulates expression of the human peroxiredoxin 6 gene by a transcriptional mechanism involving an antioxidant response element. *Free radical biology & medicine*, 46(2), pp.146–53.

Costin, G.-E. & Hearing, V.J., 2007. Human skin pigmentation: melanocytes modulate skin color in response to stress. *FASEB journal : official publication of the Federation of American Societies for Experimental Biology*, 21(4), pp.976–94.

Cotter, M.A. et al., 2007. N-acetylcysteine protects melanocytes against oxidative stress/damage and delays onset of ultraviolet-induced melanoma in mice. *Clinical cancer research : an official journal of the American Association for Cancer Research*, 13(19), pp.5952–8.

Cummings, B.S., 2007. Phospholipase A_2 as targets for anti-cancer drugs. *Biochemical pharmacology*, 74(7), pp.949–59.

Curtin, J. a et al., 2006. PI3-kinase subunits are infrequent somatic targets in melanoma. *The Journal of investigative dermatology*, 126(7), pp.1660–3.

Dahl, C. & Guldberg, P., 2007. The genome and epigenome of malignant melanoma. *APMIS : acta pathologica, microbiologica, et immunologica Scandinavica*, 115(10), pp.1161–76.

Dai, D.L., Martinka, M. & Li, G., 2005. Prognostic significance of activated Akt expression in melanoma: a clinicopathologic study of 292 cases. *Journal of clinical oncology : official journal of the American Society of Clinical Oncology*, 23(7), pp.1473–82.

Dankort, D. et al., 2009. Braf(V600E) cooperates with Pten loss to induce metastatic melanoma. *Nature genetics*, 41(5), pp.544–52.

Das, P. et al., 2010. Primary malignant melanoma at unusual sites: an institutional experience with review of literature. *Melanoma research*, 20(3), pp.233–9.

Davies, H. et al., 2002. Mutations of the BRAF gene in human cancer. *Nature*, 417(6892), pp.949–54.

Davies, M. a et al., 2008. A novel AKT3 mutation in melanoma tumours and cell lines. *British journal of cancer*, 99(8), pp.1265–8.

Dhomen, N. et al., 2009. Oncogenic Braf induces melanocyte senescence and melanoma in mice. *Cancer cell*, 15(4), pp.294–303.

Donnini, S. et al., 2007. EP2 prostanoid receptor promotes squamous cell carcinoma growth through epidermal growth factor receptor transactivation and iNOS and ERK1/2 pathways. *FASEB journal : official publication of the Federation of American Societies for Experimental Biology*, 21(10), pp.2418–30.

Edderkaoui, M. et al., 2011. NADPH oxidase activation in pancreatic cancer cells is mediated through Akt-dependent up-regulation of p22phox. *The Journal of biological chemistry*, 286(10), pp.7779–87.

Faraone, D. et al., 2009. Platelet-derived growth factor-receptor alpha strongly inhibits melanoma growth in vitro and in vivo. *Neoplasia (New York, N.Y.)*, 11(8), pp.732–42.

Feig, L. a, 2003. Ral-GTPases: approaching their 15 minutes of fame. *Trends in Cell Biology*, 13(8), pp.419–425.

Feng, L., Reynisdóttir, I. & Reynisson, J., 2012. The effect of PLC-γ2 inhibitors on the growth of human tumour cells. *European journal of medicinal chemistry*, 54, pp.463–9.

Ferguson, J. et al., 2013. Combination of MEK and SRC inhibition suppresses melanoma cell growth and invasion. *Oncogene*, 32(1), pp.86–96.

Fernández-Medarde, A. & Santos, E., 2011. Ras in cancer and developmental diseases. *Genes & cancer*, 2(3), pp.344–58.

Fisher, a. B. et al., 1999. Phospholipid hydroperoxides are substrates for non-selenium glutathione peroxidase. *The Journal of biological chemistry*, 274(30), pp.21326–34.

Fisher, A.B. et al., 2005. Altered lung phospholipid metabolism in mice with targeted deletion of lysosomal-type phospholipase A_2. *Journal of lipid research*, 46(6), pp.1248–56.

Fisher, A.B. et al., 2006. Lung phospholipid metabolism in transgenic mice overexpressing peroxiredoxin 6. *Biochimica et biophysica acta*, 1761(7), pp.785–92.

Fisher, A.B., 2011. Peroxiredoxin 6: a bifunctional enzyme with glutathione peroxidase and phospholipase A_2 activities. *Antioxidants & redox signaling*, 15(3), pp.831–44.

Flaherty, K.T., Hodi, F.S. & Fisher, D.E., 2012. From genes to drugs: targeted strategies for melanoma. *Nature reviews. Cancer*, 12(5), pp.349–61.

Frank, S., Munz, B. & Werner, S., 1997. The human homologue of a bovine non-selenium glutathione peroxidase is a novel keratinocyte growth factor-regulated gene. *Oncogene*, 14(8), pp.915–21.

Frey, R.S. et al., 2006. Phosphatidylinositol 3-kinase gamma signaling through protein kinase Czeta induces NADPH oxidase-mediated oxidant generation and NF-kappaB activation in endothelial cells. *The Journal of biological chemistry*, 281(23), pp.16128–38.

Friedmann, P.S. & Gilchrest, B.A., 1987. Ultraviolet radiation directly induces pigment production by cultured human melanocytes. *Journal of cellular physiology*, 133(1), pp.88–94.

Fujii, T., Fujii, J. & Taniguchi, N., 2001. Augmented expression of peroxiredoxin VI in rat lung and kidney after birth implies an antioxidative role. *European journal of biochemistry / FEBS*, 268(2), pp.218–25.

Gaggioli, C. et al., 2003. Microphthalmia-associated transcription factor (MITF) is required but is not sufficient to induce the expression of melanogenic genes. *Pigment cell research / sponsored by the European Society for Pigment Cell Research and the International Pigment Cell Society*, 16(4), pp.374–82.

Gallagher, B.M. & Phelan, S. a, 2007. Investigating transcriptional regulation of Prdx6 in mouse liver cells. *Free radical biology & medicine*, 42(8), pp.1270–7.

Garraway, L. a et al., 2005. Integrative genomic analyses identify MITF as a lineage survival oncogene amplified in malignant melanoma. *Nature*, 436(7047), pp.117–22.

Giacinti, C. & Giordano, A., 2006. RB and cell cycle progression. *Oncogene*, 25(38), pp.5220–7.

Giehl, K., 2005. Oncogenic Ras in tumour progression and metastasis. *Biological chemistry*, 386(3), pp.193–205.

Girotti, M.R. et al., 2013. Inhibiting EGF receptor or SRC family kinase signaling overcomes BRAF inhibitor resistance in melanoma. *Cancer discovery*, 3(2), pp.158–67.

Goel, V.K. et al., 2006. Examination of mutations in BRAF, NRAS, and PTEN in primary cutaneous melanoma. *The Journal of investigative dermatology*, 126(1), pp.154–60.

Gordon, M., 1927. The Genetics of a Viviparous Top-Minnow Platypoecilus; the Inheritance of Two Kinds of Melanophores. *Genetics*, 12(3), pp.253–83.

Govindarajan, B. et al., 2007. Overexpression of Akt converts radial growth melanoma to vertical growth melanoma. *The Journal of clinical investigation*, 117(3), pp.719–29.

Gray-Schopfer, V., Wellbrock, C. & Marais, R., 2007. Melanoma biology and new targeted therapy. *Nature*, 445(7130), pp.851–7.

Griffiths, B. et al., 2013. Sterol regulatory element binding protein-dependent regulation of lipid synthesis supports cell survival and tumor growth. *Cancer & metabolism*, 1(1), p.3.

Grimm, E.A. et al., 2008. Constitutive intracellular production of iNOS and NO in human melanoma: possible role in regulation of growth and resistance to apoptosis. *Nitric oxide : biology and chemistry / official journal of the Nitric Oxide Society*, 19(2), pp.133–7.

Guertin, D. a et al., 2006. Ablation in mice of the mTORC components raptor, rictor, or mLST8 reveals that mTORC2 is required for signaling to Akt-FOXO and PKCalpha, but not S6K1. *Developmental cell*, 11(6), pp.859–71.

Guo, D. et al., 2014. Targeting SREBP-1-driven lipid metabolism to treat cancer. *Current pharmaceutical design*, 20(15), pp.2619–26.

Guo, Y. et al., 2011. Identification of the orphan G protein-coupled receptor GPR31 as a receptor for 12-(S)-hydroxyeicosatetraenoic acid. *The Journal of biological chemistry*, 286(39), pp.33832–40.

Harizi, H., Corcuff, J.-B. & Gualde, N., 2008. Arachidonic-acid-derived eicosanoids: roles in biology and immunopathology. *Trends in molecular medicine*, 14(10), pp.461–9.

Hartmann, A. et al., 1999. Hypoxia-induced up-regulation of angiogenin in human malignant melanoma. *Cancer research*, 59(7), pp.1578–83.

He, C. et al., 2012. Inhibiting delta-6 desaturase activity suppresses tumor growth in mice. *PloS one*, 7(10), p.e47567.

Heinzerling, L. et al., 2013. Rare BRAF mutations in melanoma patients: implications for molecular testing in clinical practice. *British journal of cancer*, 108(10), pp.2164–71.

Hennessy, B.T. et al., 2005. Exploiting the PI3K/AKT pathway for cancer drug discovery. *Nature reviews. Drug discovery*, 4(12), pp.988–1004.

Hirai, H. et al., 1995. Novel INK4 proteins, p19 and p18, are specific inhibitors of the cyclin D-dependent kinases CDK4 and CDK6. *Molecular and cellular biology*, 15(5), pp.2672–81.

Ho, J.-N. et al., 2010. Phospholipase A_2 activity of peroxiredoxin 6 promotes invasion and metastasis of lung cancer cells. *Molecular cancer therapeutics*, 9(4), pp.825–32.

Hocker, T.L., Singh, M.K. & Tsao, H., 2008. Melanoma genetics and therapeutic approaches in the 21st century: moving from the benchside to the bedside. *The Journal of investigative dermatology*, 128(11), pp.2575–95.

Hoeflich, K.P. et al., 2006. Oncogenic BRAF is required for tumor growth and maintenance in melanoma models. *Cancer research*, 66(2), pp.999–1006.

Hofmann, B., Hecht, H. & Flohé, L., 2002. Peroxiredoxins. *Biological chemistry*, 383(3-4), pp.347–64.

Homsi, J., Cubitt, C. & Daud, A., 2007. The Src signaling pathway: a potential target in melanoma and other malignancies. *Expert opinion on therapeutic targets*, 11(1), pp.91–100.

Hoogduijn, M.J. et al., 2004. Melanin protects melanocytes and keratinocytes against H2O2-induced DNA strand breaks through its ability to bind Ca2+. *Experimental cell research*, 294(1), pp.60–7.

Hooks, S.B. & Cummings, B.S., 2008. Role of Ca2+-independent phospholipase A2 in cell growth and signaling. *Biochemical pharmacology*, 76(9), pp.1059–67.

Hoyal, C.R. et al., 2003. Modulation of p47PHOX activity by site-specific phosphorylation: Akt-dependent activation of the NADPH oxidase. *Proceedings of the National Academy of Sciences of the United States of America*, 100(9), pp.5130–5.

Hu, F., Zhang, Y. & Song, Y., 2013. Lipid Metabolism, Metabolic Syndrome, and Cancer. *Intec*, Chapter 9.

Hubbard, K.B. & Hepler, J.R., 2006. Cell signalling diversity of the Gqalpha family of heterotrimeric G proteins. *Cellular signalling*, 18(2), pp.135–50.

Hussussian, C.J. et al., 1994. Germline p16 mutations in familial melanoma. *Nature genetics*, 8(1), pp.15–21.

Ibañez, I. et al., 2011. Reactive oxygen species in the biology of melanoma. In D. Y. Tanaka, ed. *… in Melanoma Research …*. pp. 3–33.

Ikematsu, N. et al., 1999. Tob2, a novel anti-proliferative Tob/BTG1 family member, associates with a component of the CCR4 transcriptional regulatory complex capable of binding cyclin-dependent kinases. *Oncogene*, 18(52), pp.7432–41.

J. Sambrook, E.F. Fritsch, T.M., 2001. *Molecular cloning: a laboratory manual* Volume 3., Cold Spring Harbor New York.

Javelaud, D. et al., 2011. GLI2 and M-MITF transcription factors control exclusive gene expression programs and inversely regulate invasion in human melanoma cells. *Pigment cell & melanoma research*, 24(5), pp.932–43.

Jenkins, N.C. et al., 2011. The p16(INK4A) tumor suppressor regulates cellular oxidative stress. *Oncogene*, 30(3), pp.265–74.

Jiang, J.-G. et al., 2005. Cytochrome P450 2J2 promotes the neoplastic phenotype of carcinoma cells and is up-regulated in human tumors. *Cancer research*, 65(11), pp.4707–15.

Jiang, J.-G. et al., 2007. Cytochrome p450 epoxygenase promotes human cancer metastasis. *Cancer research*, 67(14), pp.6665–74.

Jo, M. et al., 2013. Lung tumor growth-promoting function of peroxiredoxin 6. *Free radical biology & medicine*, 61, pp.453–63.

Johnson, F.M. et al., 2010. Phase II study of dasatinib in patients with advanced non-small-cell lung cancer. *Journal of clinical oncology : official journal of the American Society of Clinical Oncology*, 28(30), pp.4609–15.

Jonsson, A. et al., 2010. High frequency of p16(INK4A) promoter methylation in NRAS-mutated cutaneous melanoma. *The Journal of investigative dermatology*, 130(12), pp.2809–17.

Joosse, A. et al., 2010. Reactive oxygen species and melanoma: an explanation for gender differences in survival? *Pigment cell & melanoma research*, 23(3), pp.352–64.

Kang, K.-H. et al., 2013. Enhancement role of host 12/15-lipoxygenase in melanoma progression. *European journal of cancer (Oxford, England : 1990)*, 49(12), pp.2747–59.

Kang, S.W., Baines, I.C. & Rhee, S.G., 1998. Characterization of a mammalian peroxiredoxin that contains one conserved cysteine. *The Journal of biological chemistry*, 273(11), pp.6303–11.

Kaspar, J.W., Niture, S.K. & Jaiswal, A.K., 2009. Nrf2:INrf2 (Keap1) signaling in oxidative stress. *Free radical biology & medicine*, 47(9), pp.1304–9.

Katz, M., Amit, I. & Yarden, and Y., 2007. Regulation of MAPKs by growth factors and receptor tyrosine kinases. *Biochim Biophys Acta.*, 1773(8), pp.1161–1176.

Kim, H.-S. et al., 2003. Induction of 1-cys peroxiredoxin expression by oxidative stress in lung epithelial cells. *American journal of physiology. Lung cellular and molecular physiology*, 285(2), pp.L363–9.

Kim, S.Y. et al., 2008. H2O2-dependent hyperoxidation of peroxiredoxin 6 (Prdx6) plays a role in cellular toxicity via up-regulation of iPLA2 activity. *The Journal of biological chemistry*, 283(48), pp.33563–8.

Kim, T. et al., 1997. Identification of a Human cDNA Clone for Lysosomal Type Ca^{2+}-independent Phospholipase A_2 and Properties of the Expressed Protein. *Journal of Biological Chemistry*, 272(4), pp.2542–2550.

Kim, T.S. et al., 1998. Cloning and expression of rat lung acidic Ca^{2+}-independent PLA_2 and its organ distribution. *The American journal of physiology*, 274(5 Pt 1), pp.L750–61.

Knudsen, E.S. & Knudsen, K.E., 2008. Tailoring to RB: tumour suppressor status and therapeutic response. *Nature reviews. Cancer*, 8(9), pp.714–24.

Krycer, J.R. et al., 2010. The Akt-SREBP nexus: cell signaling meets lipid metabolism. *Trends in endocrinology and metabolism: TEM*, 21(5), pp.268–76.

Kümin, A. et al., 2006. Peroxiredoxin 6 is a potent cytoprotective enzyme in the epidermis. *The American journal of pathology*, 169(4), pp.1194–205.

Lee, S.B. et al., 2009. Peroxiredoxin 6 promotes lung cancer cell invasion by inducing urokinase-type plasminogen activator via p38 kinase, phosphoinositide 3-kinase, and Akt. *Molecules and cells*, 28(6), pp.583–8.

Lee, T.H. et al., 1999. Characterization of the murine gene encoding 1-Cys peroxiredoxin and identification of highly homologous genes. *Gene*, 234(2), pp.337–44.

Lei, X. et al., 2010. Spontaneous development of endoplasmic reticulum stress that can lead to diabetes mellitus is associated with higher calcium-independent phospholipase A2 expression: a role for regulation by SREBP-1. *The Journal of biological chemistry*, 285(9), pp.6693–705.

Leikam, C. et al., 2014. Cystathionase mediates senescence evasion in melanocytes and melanoma cells. *Oncogene*, 33(6), pp.771–82.

Leikam, C. et al., 2008. Oncogene activation in melanocytes links reactive oxygen to multinucleated phenotype and senescence. *Oncogene*, 27(56), pp.7070–82.

Libra, M., Malaponte, G. & Navolanic, P., 2005. Analysis of BRAF mutation in primary and metastatic melanoma. *Cell cycle*, 4(10), pp.1382–1384.

Lieder, F. et al., 2012. Identification of UV-protective activators of nuclear factor erythroid-derived 2-related factor 2 (Nrf2) by combining a chemical library screen with computer-based virtual screening. *The Journal of biological chemistry*, 287(39), pp.33001–13.

Liu, F.-J., Wang, X.-B. & Cao, A.-G., 2014. Screening and functional analysis of a differential protein profile of human breast cancer. *Oncology letters*, 7(6), pp.1851–1856.

Liu, J.J. & Fisher, D.E., 2010. Lighting a path to pigmentation: mechanisms of MITF induction by UV. *Pigment cell & melanoma research*, 23(6), pp.741–5.

Liu, L.-Z. et al., 2006. Reactive oxygen species regulate epidermal growth factor-induced vascular endothelial growth factor and hypoxia-inducible factor-1alpha expression through activation of AKT and P70S6K1 in human ovarian cancer cells. *Free radical biology & medicine*, 41(10), pp.1521–33.

Liu, M. et al., 2014. Characterization of the anticancer effects of S115, a novel heteroaromatic thiosemicarbazone compound, in vitro and in vivo. *Acta pharmacologica Sinica*, 35(10), pp.1302–10.

Livak, K.J. & Schmittgen, T.D., 2001. Analysis of relative gene expression data using real-time quantitative PCR and the 2(-Delta Delta C(T)) Method. *Methods (San Diego, Calif.)*, 25(4), pp.402–8.

Lo, J. a. & Fisher, D.E., 2014. The melanoma revolution: from UV carcinogenesis to a new era in therapeutics. *Science (New York, N.Y.)*, 346(6212), pp.945–9.

Lokaj, K. et al., 2009. Quantitative differential proteome analysis in an animal model for human melanoma. *Journal of proteome research*, 8(4), pp.1818–27.

Lomas, J. et al., 2008. The genetics of malignant melanoma. *Frontiers in Bioscience*, 13, pp.5071–5093.

Lu, Z. et al., 2010. 3-phosphoinositide-dependent protein kinase-1 regulates proliferation and survival of cancer cells with an activated mitogen-activated protein kinase pathway. *Molecular cancer research : MCR*, 8(3), pp.421–32.

Madonna, G. et al., 2012. NF-κB as potential target in the treatment of melanoma. *Journal of translational medicine*, 10(1), p.53.

Mailand, N., Gibbs-Seymour, I. & Bekker-Jensen, S., 2013. Regulation of PCNA-protein interactions for genome stability. *Nature reviews. Molecular cell biology*, 14(5), pp.269–82.

Manevich, Y. et al., 2002. 1-Cys peroxiredoxin overexpression protects cells against phospholipid peroxidation-mediated membrane damage. *Proceedings of the National Academy of Sciences of the United States of America*, 99(18), pp.11599–604.

Manevich, Y. et al., 2009. Binding of peroxiredoxin 6 to substrate determines differential phospholipid hydroperoxide peroxidase and phospholipase A(2) activities. *Archives of biochemistry and biophysics*, 485(2), pp.139–49.

Manevich, Y. et al., 2007. Structure and phospholipase function of peroxiredoxin 6: identification of the catalytic triad and its role in phospholipid substrate binding. *Journal of lipid research*, 48(10), pp.2306–18.

Manevich, Y. & Fisher, A.B., 2005. Peroxiredoxin 6, a 1-Cys peroxiredoxin, functions in antioxidant defense and lung phospholipid metabolism. *Free radical biology & medicine*, 38(11), pp.1422–32.

Marshall, J.-C. et al., 2007. The effects of a cyclooxygenase-2 (COX-2) expression and inhibition on human uveal melanoma cell proliferation and macrophage nitric oxide production. *Journal of carcinogenesis*, 6, p.17.

McHowat, J. et al., 2011. Platelet-activating factor and metastasis: calcium-independent phospholipase $A_2\beta$ deficiency protects against breast cancer metastasis to the lung. *American journal of physiology. Cell physiology*, 300(4), pp.C825–32.

Meierjohann, S., 2014. Oxidative stress in melanocyte senescence and melanoma transformation. *European journal of cell biology*, 93(1-2), pp.36–41.

Meierjohann, S. & Schartl, M., 2006. From Mendelian to molecular genetics: the Xiphophorus melanoma model. *Trends in genetics : TIG*, 22(12), pp.654–61.

Meng, F. & Wu, G., 2013. Is p38γ MAPK a metastasis-promoting gene or an oncogenic property-maintaining gene? *Cell cycle (Georgetown, Tex.)*, 12(14), pp.2329–30.

Meyskens FL Jr, Buckmeier JA, McNulty SE, T.N., 1999. Activation of Nuclear Factor-kB in Human Metastatic Melanoma Cells and the Effect of Oxidative Stress1. *Clinical cancer research*, 5(5), pp.1197–1202.

Michaloglou, C. et al., 2005. $BRAF^{E600}$-associated senescence-like cell cycle arrest of human naevi. *Nature*, 436(7051), pp.720–724.

Miller, A.J. & Mihm, M.C., 2006. Melanoma. *The New England journal of medicine*, 355(1), pp.51–65.

Minisini, A.M. et al., 2013. Expression of thymidine phosphorylase and cyclooxygenase-2 in melanoma. *Melanoma research*, 23(2), pp.96–101.

Mirmohammadsadegh, A. et al., 2006. Epigenetic silencing of the PTEN gene in melanoma. *Cancer research*, 66(13), pp.6546–52.

Mo, Y. et al., 2003. 1-Cys peroxiredoxin knock-out mice express mRNA but not protein for a highly related intronless gene. *FEBS Letters*, 555(2), pp.192–198.

Monteiro, G. et al., 2007. Reduction of 1-Cys peroxiredoxins by ascorbate changes the thiol-specific antioxidant paradigm, revealing another function of vitamin C. *Proceedings of the National Academy of Sciences of the United States of America*, 104(12), pp.4886–91.

Naryzhny, S.N. & Lee, H., 2010. Proliferating cell nuclear antigen in the cytoplasm interacts with components of glycolysis and cancer. *FEBS letters*, 584(20), pp.4292–8.

Naryzhny, S.N. & Lee, H., 2004. The post-translational modifications of proliferating cell nuclear antigen: acetylation, not phosphorylation, plays an important role in the regulation of its function. *The Journal of biological chemistry*, 279(19), pp.20194–9.

Nebreda, A.R. & Porras, A., 2000. p38 MAP kinases: beyond the stress response. *Trends in biochemical sciences*, 25(6), pp.257–60.

Nicolussi, A. et al., 2014. PRDX1 and PRDX6 are repressed in papillary thyroid carcinomas via BRAF V600E-dependent and -independent mechanisms. *International journal of oncology*, 44(2), pp.548–56.

Omholt, K. et al., 2006. Mutations of PIK3CA are rare in cutaneous melanoma. *Melanoma research*, 16(2), pp.197–200.

Padua, R.A., Barrass, N. & Currie, G.A., 1984. A novel transforming gene in a human malignant melanoma cell line. *Nature*, 311(5987), pp.671–3.

Pak, J.H. et al., 2002. An antisense oligonucleotide to 1-cys peroxiredoxin causes lipid peroxidation and apoptosis in lung epithelial cells. *The Journal of biological chemistry*, 277(51), pp.49927–34.

Pak, J.H. et al., 2011. Peroxiredoxin 6 overexpression attenuates cisplatin-induced apoptosis in human ovarian cancer cells. *Cancer investigation*, 29(1), pp.21–8.

Panigrahy, D. et al., 2012. Epoxyeicosanoids stimulate multiorgan metastasis and tumor dormancy escape in mice. *The Journal of clinical investigation*, 122(1), pp.178–91.

Park, J.B. et al., 2012. Phospholipase signalling networks in cancer. *Nature reviews. Cancer*, 12(11), pp.782–92.

Peshenko, I. V & Shichi, H., 2001. Oxidation of active center cysteine of bovine 1-Cys peroxiredoxin to the cysteine sulfenic acid form by peroxide and peroxynitrite. *Free radical biology & medicine*, 31(3), pp.292–303.

Pillaire, M.J., Nebreda, a R. & Darbon, J.M., 2000. Cisplatin and UV radiation induce activation of the stress-activated protein kinase p38gamma in human melanoma cells. *Biochemical and biophysical research communications*, 278(3), pp.724–8.

Pollock, P.M. et al., 2003. High frequency of BRAF mutations in nevi. *Nature genetics*, 33(1), pp.19–20.

Puls, L.N., Eadens, M. & Messersmith, W., 2011. Current status of SRC inhibitors in solid tumor malignancies. *The oncologist*, 16(5), pp.566–78.

Van Raamsdonk, C.D. et al., 2009. Frequent somatic mutations of GNAQ in uveal melanoma and blue naevi. *Nature*, 457(7229), pp.599–602.

Van Raamsdonk, C.D. et al., 2010. Mutations in GNA11 in uveal melanoma. *The New England journal of medicine*, 363(23), pp.2191–9.

Ralat, L. a et al., 2008. Characterization of the complex of glutathione S-transferase pi and 1-cysteine peroxiredoxin. *Archives of biochemistry and biophysics*, 474(1), pp.109–18.

Ralat, L. a et al., 2006. Direct evidence for the formation of a complex between 1-cysteine peroxiredoxin and glutathione S-transferase pi with activity changes in both enzymes. *Biochemistry*, 45(2), pp.360–72.

Reddy, M.A. et al., 2009. Role of Src tyrosine kinase in the atherogenic effects of the 12/15-lipoxygenase pathway in vascular smooth muscle cells. *Arteriosclerosis, thrombosis, and vascular biology*, 29(3), pp.387–93.

Rhee, S.G. et al., 2001. Peroxiredoxin, a novel family of peroxidases. *IUBMB life*, 52(1-2), pp.35–41.

Robertson, G.P., 2005. Functional and therapeutic significance of Akt deregulation in malignant melanoma. *Cancer metastasis reviews*, 24(2), pp.273–85.

Rolfs, F. et al., 2013. Dual role of the antioxidant enzyme peroxiredoxin 6 in skin carcinogenesis. *Cancer research*, 73(11), pp.3460–9.

Rosenson, R.S. & Hurt-Camejo, E., 2012. Phospholipase A_2 enzymes and the risk of atherosclerosis. *European heart journal*, 33(23), pp.2899–909.

Rouzaud, F. et al., 2005. MC1R and the response of melanocytes to ultraviolet radiation. *Mutation research*, 571(1-2), pp.133–52.

Rundhaug, J.E. et al., 2011. The role of the EP receptors for prostaglandin E2 in skin and skin cancer. *Cancer metastasis reviews*, 30(3-4), pp.465–80.

Sales, K.J., Maudsley, S. & Jabbour, H.N., 2004. Elevated prostaglandin EP2 receptor in endometrial adenocarcinoma cells promotes vascular endothelial growth factor expression via cyclic 3',5'-adenosine monophosphate-mediated transactivation of the epidermal growth factor receptor and extracellular sign. *Molecular endocrinology (Baltimore, Md.)*, 18(6), pp.1533–45.

Salvucci, O. et al., 2001. Antiapoptotic role of endogenous nitric oxide in human melanoma cells. *Cancer research*, 61(1), pp.318–26.

Schaafhausen, M.K. et al., 2013. Tumor angiogenesis is caused by single melanoma cells in a manner dependent on reactive oxygen species and NF-κB. *Journal of cell science*, 126(Pt 17), pp.3862–72.

Schaloske, R.H. & Dennis, E. a, 2006. The phospholipase A2 superfamily and its group numbering system. *Biochimica et biophysica acta*, 1761(11), pp.1246–59.

Scortegagna, M. et al., 2014. Genetic inactivation or pharmacological inhibition of Pdk1 delays development and inhibits metastasis of Braf(V600E)::Pten(-/-) melanoma. *Oncogene*, 33(34), pp.4330–9.

Scott, K.F. et al., 2010. Emerging roles for phospholipase A_2 enzymes in cancer. *Biochimie*, 92(6), pp.601–10.

Scuderi, M.R. et al., 2008. Expression of Ca^{2+}-independent and Ca^{2+}-dependent phospholipases A_2 and cyclooxygenases in human melanocytes and malignant melanoma cell lines. *Biochimica et biophysica acta*, 1781(10), pp.635–42.

Sekulic, A. et al., 2008. Malignant melanoma in the 21st century: the emerging molecular landscape. *Mayo Clinic proceedings*, 83(7), pp.825–46.

Shichi, H. & Demar, J.C., 1990. Non-selenium glutathione peroxidase without glutathione S-transferase activity from bovine ciliary body. *Experimental eye research*, 50(5), pp.513–20.

Shull, A.Y. et al., 2012. Novel somatic mutations to PI3K pathway genes in metastatic melanoma. *PloS one*, 7(8), p.e43369.

Singh, T. et al., 2011. Berberine, an isoquinoline alkaloid, inhibits melanoma cancer cell migration by reducing the expressions of cyclooxygenase-2, prostaglandin E_2 and prostaglandin E_2 receptors. *Carcinogenesis*, 32(1), pp.86–92.

Singh, T. & Katiyar, S.K., 2011. Green tea catechins reduce invasive potential of human melanoma cells by targeting COX-2, PGE_2 receptors and epithelial-to-mesenchymal transition. *PloS one*, 6(10), p.e25224.

Smith, W.L., Garavito, R.M. & DeWitt, D.L., 1996. Prostaglandin endoperoxide H synthases (cyclooxygenases)-1 and -2. *The Journal of biological chemistry*, 271(52), pp.33157–60.

Sorokina, E.M. et al., 2009. Identification of the amino acid sequence that targets peroxiredoxin 6 to lysosome-like structures of lung epithelial cells. *American journal of physiology. Lung cellular and molecular physiology*, 297(5), pp.L871–80.

Sorokina, E.M. et al., 2011. Intracellular targeting of peroxiredoxin 6 to lysosomal organelles requires MAPK activity and binding to 14-3-3ε. *American journal of physiology. Cell physiology*, 300(6), pp.C1430–41.

Stahl, J.M. et al., 2004. Deregulated Akt3 Activity Promotes Development of Malignant Melanoma Deregulated Akt3 Activity Promotes Development of Malignant Melanoma. , pp.7002–7010.

Stoimenov, I. & Helleday, T., 2009. PCNA on the crossroad of cancer. *Biochemical Society transactions*, 37(Pt 3), pp.605–13.

Straume, O., Sviland, L. & Akslen, L.A., 2000. Loss of Nuclear p16 Protein Expression Correlates with Increased Tumor Cell Proliferation (Ki-67) and Poor Prognosis in Patients with Vertical Growth Phase Melanoma Loss of Nuclear p16 Protein Expression Correlates with Increased Tumor Cell Proliferatio. *Clinical cancer research*, 6(5), pp.1845–1853.

Strub, T. et al., 2011. Essential role of microphthalmia transcription factor for DNA replication, mitosis and genomic stability in melanoma. *Oncogene*, 30(20), pp.2319–32.

Sun, B. et al., 2008. Inhibition of Ca2+-independent phospholipase A2 decreases prostate cancer cell growth by p53-dependent and independent mechanisms. *The Journal of pharmacology and experimental therapeutics*, 326(1), pp.59–68.

Sun, C. et al., 2014. Reversible and adaptive resistance to BRAF(V600E) inhibition in melanoma. *Nature*, 508(7494), pp.118–22.

Szekeres, C.K. et al., 2000. Eicosanoid activation of extracellular signal-regulated kinase1/2 in human epidermoid carcinoma cells. *The Journal of biological chemistry*, 275(49), pp.38831–41.

Tabolacci, C. et al., 2010. Similar antineoplastic effects of nimesulide, a selective COX-2 inhibitor, and prostaglandin E1 on B16-F10 murine melanoma cells. *Melanoma research*, 20(4), pp.273–9.

Takeyama, K. et al., 2000. Oxidative stress causes mucin synthesis via transactivation of epidermal growth factor receptor: role of neutrophils. *Journal of immunology (Baltimore, Md. : 1950)*, 164(3), pp.1546–52.

Tennant, D. a, Durán, R. V & Gottlieb, E., 2010. Targeting metabolic transformation for cancer therapy. *Nature reviews. Cancer*, 10(4), pp.267–77.

Teutschbein, J. et al., 2010. Gene expression analysis after receptor tyrosine kinase activation reveals new potential melanoma proteins. *BMC cancer*, 10, p.386.

Toker, a., 2000. Akt/Protein Kinase B Is Regulated by Autophosphorylation at the hypothetical PDK-2 Site. *Journal of Biological Chemistry*, 275(12), pp.8271–4.

Tronnier, M. & Mitteldorf, C., 2014. Treating advanced melanoma: current insights and opportunities. *Cancer management and research*, 6(6), pp.349–56.

Tsao, H. et al., 2004. Genetic interaction between NRAS and BRAF mutations and PTEN/MMAC1 inactivation in melanoma. *The Journal of investigative dermatology*, 122(2), pp.337–41.

Tsatmali, M., Ancans, J. & Thody, a. J., 2002. Melanocyte Function and Its Control by Melanocortin Peptides. *Journal of Histochemistry & Cytochemistry*, 50(2), pp.125–133.

Tuveson, D. a, Weber, B.L. & Herlyn, M., 2003. BRAF as a potential therapeutic target in melanoma and other malignancies. *Cancer cell*, 4(2), pp.95–8.

Vaid, M., Singh, T. & Katiyar, S.K., 2011. Grape seed proanthocyanidins inhibit melanoma cell invasiveness by reduction of PGE2 synthesis and reversal of epithelial-to-mesenchymal transition. *PloS one*, 6(6), p.e21539.

Vergani, E. et al., 2011. Identification of MET and SRC activation in melanoma cell lines showing primary resistance to PLX4032. *Neoplasia (New York, N.Y.)*, 13(12), pp.1132–42.

Wang, D. & Dubois, R.N., 2010. Eicosanoids and cancer. *Nature reviews. Cancer*, 10(3), pp.181–93.

Wang, X. et al., 2003. Mice with targeted mutation of peroxiredoxin 6 develop normally but are susceptible to oxidative stress. *The Journal of biological chemistry*, 278(27), pp.25179–90.

Wang, Y. et al., 2004. Adenovirus-mediated transfer of the 1-cys peroxiredoxin gene to mouse lung protects against hyperoxic injury. *American journal of physiology. Lung cellular and molecular physiology*, 286(6), pp.L1188–93.

Wellbrock, C. et al., 2002. Activation of p59(Fyn) leads to melanocyte dedifferentiation by influencing MKP-1-regulated mitogen-activated protein kinase signaling. *The Journal of biological chemistry*, 277(8), pp.6443–54.

Willmore-Payne, C. et al., 2005. Human malignant melanoma: detection of BRAF- and c-kit-activating mutations by high-resolution amplicon melting analysis. *Human pathology*, 36(5), pp.486–93.

Wu, Y. et al., 2009. Mitogen-activated protein kinase-mediated phosphorylation of peroxiredoxin 6 regulates its phospholipase A_2 activity. *The Biochemical journal*, 419(3), pp.669–79.

Wu, Y.-Z. et al., 2006. Interaction of surfactant protein A with peroxiredoxin 6 regulates phospholipase A_2 activity. *The Journal of biological chemistry*, 281(11), pp.7515–25.

Yamaki, T. et al., 2004. Prostaglandin E2 activates Src signaling in lung adenocarcinoma cell via EP3. *Cancer letters*, 214(1), pp.115–20.

Yang, K. et al., 2013. p38γ overexpression in gliomas and its role in proliferation and apoptosis. *Scientific reports*, 3(2089), p.2089.

Yang, P. et al., 2007. Zyflamend-mediated inhibition of human prostate cancer PC3 cell proliferation: effects on 12-LOX and Rb protein phosphorylation. *Cancer biology & therapy*, 6(2), pp.228–36.

Yang, Y.-A. et al., 2002. Activation of fatty acid synthesis during neoplastic transformation: role of mitogen-activated protein kinase and phosphatidylinositol 3-kinase. *Experimental cell research*, 279(1), pp.80–90.

Yang, Z. et al., 2013. Targeting nitric oxide signaling with nNOS inhibitors as a novel strategy for the therapy and prevention of human melanoma. *Antioxidants & redox signaling*, 19(5), pp.433–47.

Yu, J.A. et al., 2012. Knockdown of secretory phospholipase A2 IIa reduces lung cancer growth in vitro and in vivo. *The Journal of thoracic and cardiovascular surgery*, 144(5), pp.1185–91.

Zeldin, D.C., 2001. Epoxygenase pathways of arachidonic acid metabolism. *The Journal of biological chemistry*, 276(39), pp.36059–62.

Zhang, X. et al., 2009. Triosephosphate isomerase and peroxiredoxin 6, two novel serum markers for human lung squamous cell carcinoma. *Cancer science*, 100(12), …..pp.2396–401.

Zhang, X.H. et al., 2006. Disruption of G1-phase phospholipid turnover by inhibition of Ca^{2+}-independent phospholipase A_2 induces a p53-dependent cell-cycle arrest in G1 phase. *Journal of cell science*, 119(Pt 6), pp.1005–15.

Zhou, S. et al., 2013. Functional interaction of glutathione S-transferase pi and peroxiredoxin 6 in intact cells. *The international journal of biochemistry & cell biology*, 45(2), pp.401–7.

Zipfel, P. a et al., 2010. Ral activation promotes melanomagenesis. *Oncogene*, 29(34), pp.4859–64.

9. Acknowledgements

First of all I would like to thank my supervisor PD Dr. Svenja Meierjohann for her constant enthusiasm, encouragement, help, support and great guidance during my thesis.

I also would like to thank Prof. Dr. Dr. Manfred Schartl for his friendly support and advice throughout my thesis.

Furthermore, I would like to thank Prof. Dr. Thomas Müller for his kind willingness to act as second reviewer for my thesis.

A big thanks goes to Dr. Werner Schmitz for performing the gas chromatographic analyses.

Furthermore, I would like to thank my former lab members (Anita, Hannes, Max, Claudia, Daniela, Katja and Johannes) for their help, practical support and for scientific discussions. In addition, I would like to thank all my colleagues of the departments PCI and EBC for the nice working atmosphere.

I also would like to thank Janine, Shannon, Heike, Barbara, Martina, Peter and Susanne for always supporting me, for great lunch times, nice coffee breaks and for becoming very good friends during the last years.

Special thanks go to my friends and family. Especially, I would like to thank Anja, Ana, Lena, and most importantly, my parents for their support, encouragement, and for always believing in me at any time.